Nanobeams for Nanoelectronic Devices; the Importance of ERL for Characterization of the Optoelectronic Device Structures

Andrei Sirenko

Department of Physics, New Jersey Institute of Technology

Newark, NJ 07102 sirenko@njit.edu

A. Kazimirov and D. H. Bilderback

Cornell High Energy Synchrotron Source

Cornell University, Ithaca, NY 14853

Z.-H. Cai and B. Lai

Advanced Photon Source, Argonne National Laboratory,

Argonne, IL 60439

ERL X-ray Science Workshop 6:

"Workshop on New Science Opportunities with Nanometer-Sized ERL X-Ray Beams"

June 23rd, 2006

Outline

- Introduction
- Nanoscale Selective Area Epitaxy
  - Advantages of monolithic integration
  - Nanoscale Growth and Nano-hetero-integration
- X-ray Diffraction with submicron spatial resolution
  - Experiments at CHESS and APS
  - Challenges to maximize $N_{ph}/(A \cdot \Delta th)$
- Future experiments with ERL nanobeams
  - HRXRD for optoelectronics
  - RSM + real space mapping; XSW
  - Nanotechnology requirements for $N_{ph}/(A \cdot \Delta th)$

ERL and High Angular Resolution XRD technique

Nanometer-Sized ERL X-Ray Beams

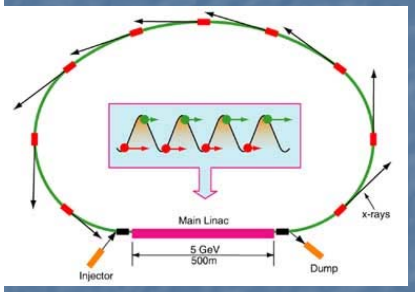

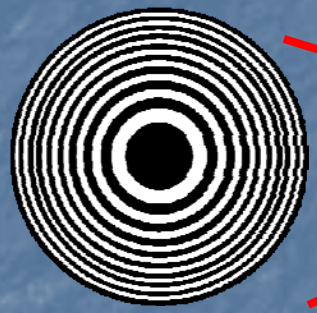

Focusing Devices

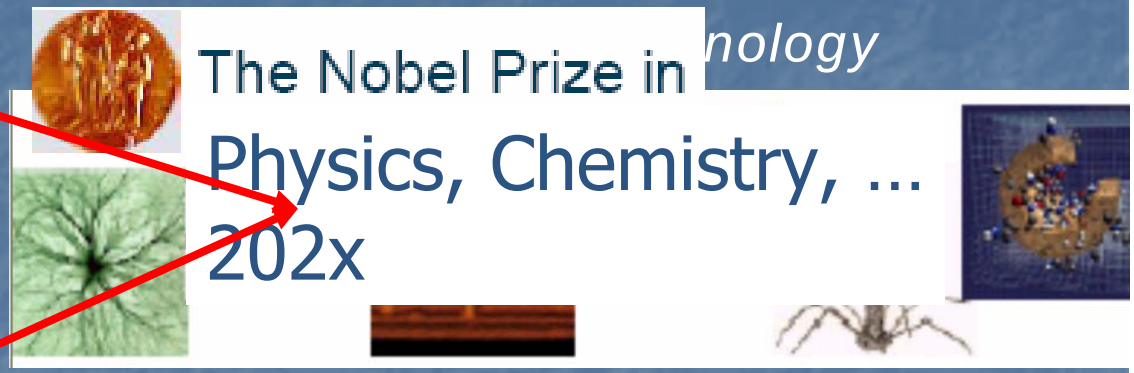

Figure of merit: N_{ph}/A

HIGH ANGULAR RESOLUTION BEAMLINE @ ERL

Figure of merit:
$N_{ph}/(A \cdot \Delta th)$

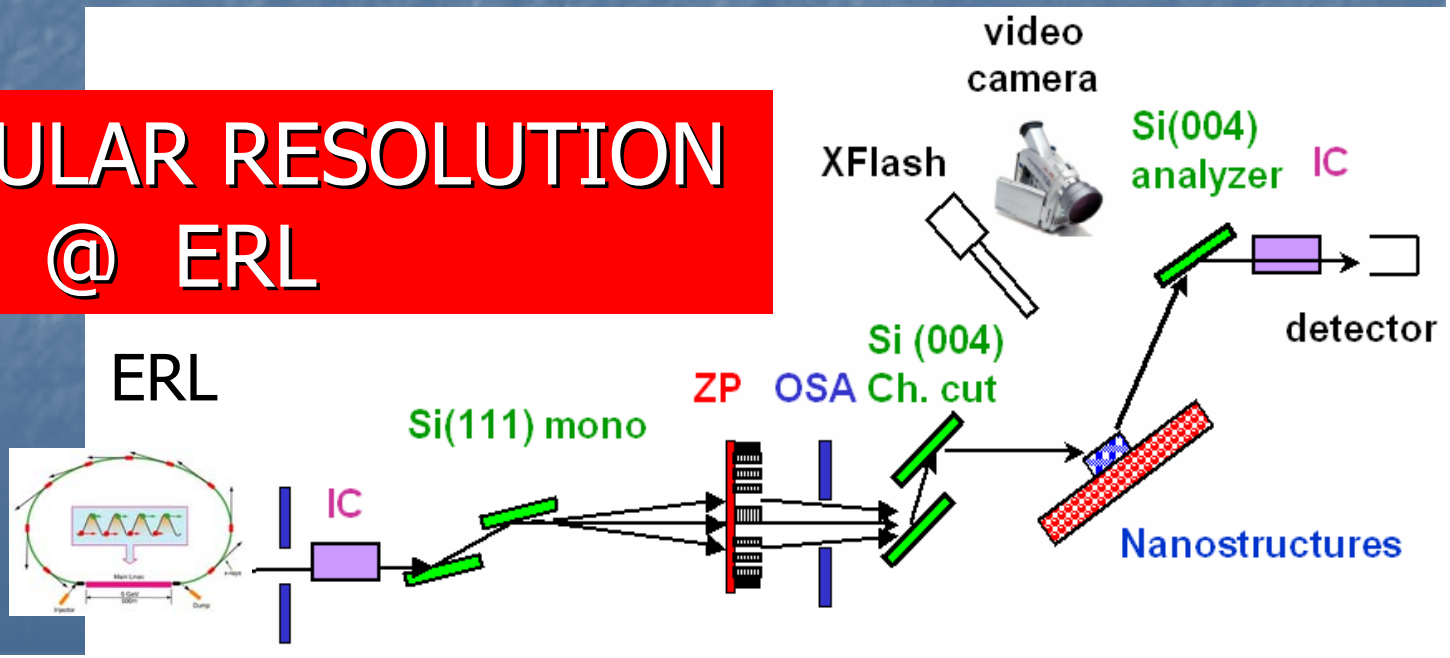

Nano science and technology

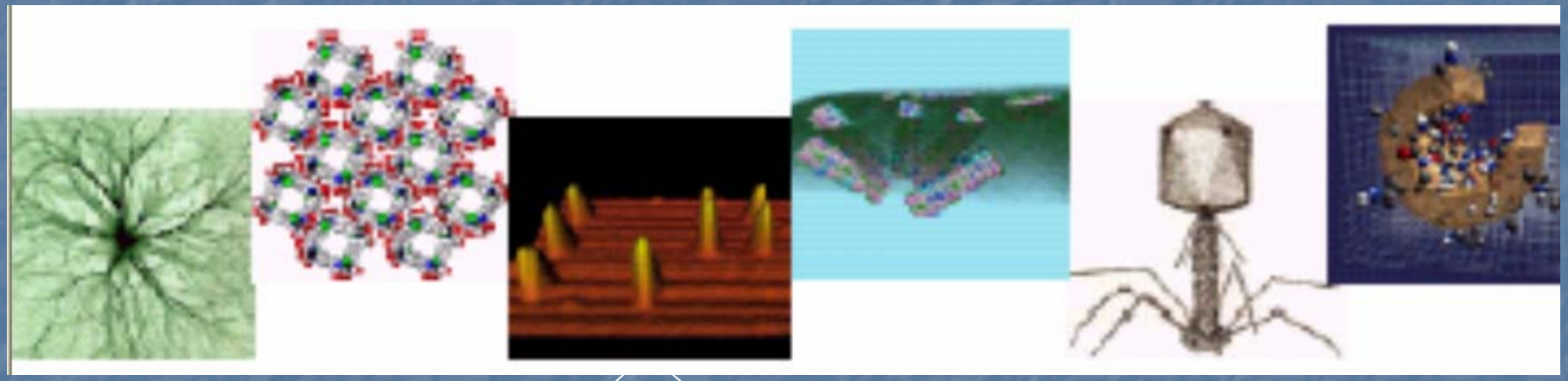

Semiconductor
Planar technology

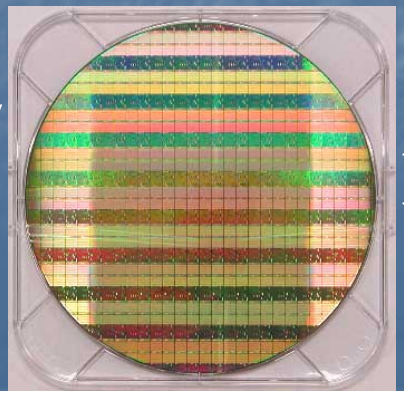

Nano-optoelectronics

High density integration in silicon technology

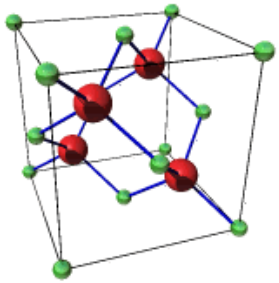

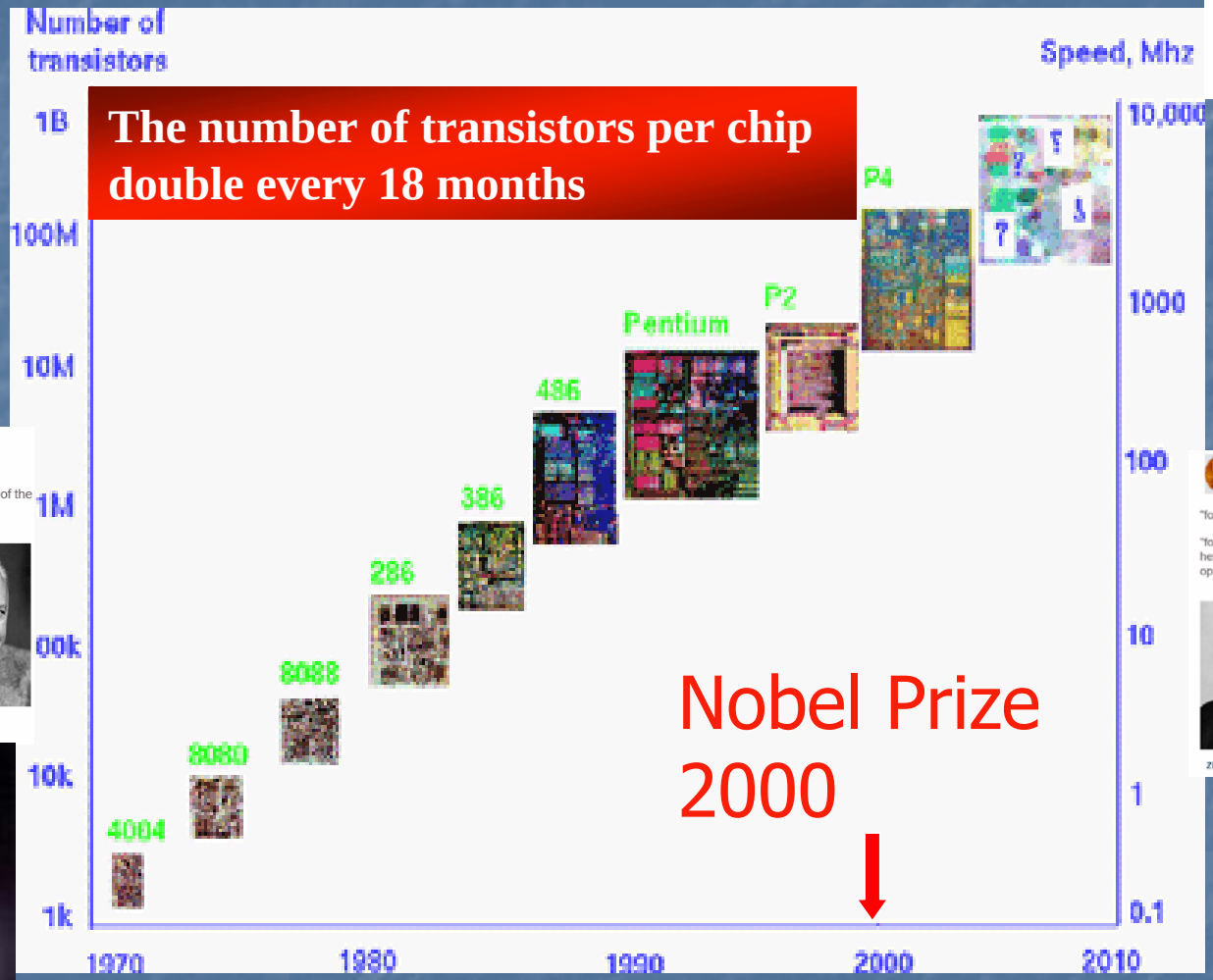

The Nobel Prize in Physics 1956

"for their researches on semiconductors and their discovery of the transistor effect"

William Bradford Shockley — John Bardeen — Walter Houser Brattain

1947

The Nobel Prize in Physics 2000

"for basic work on information and communication technology"

"for developing semiconductor heterostructures used in high-speed- and opto-electronics"

"for his part in the invention of the integrated circuit"

Zhores I. Alferov — Herbert Kroemer — Jack S. Kilby

Simulated HRXRD diffraction intensity for a 10 nm thick layer of $Si_{0.8}Ge_{0.2}$ on Si

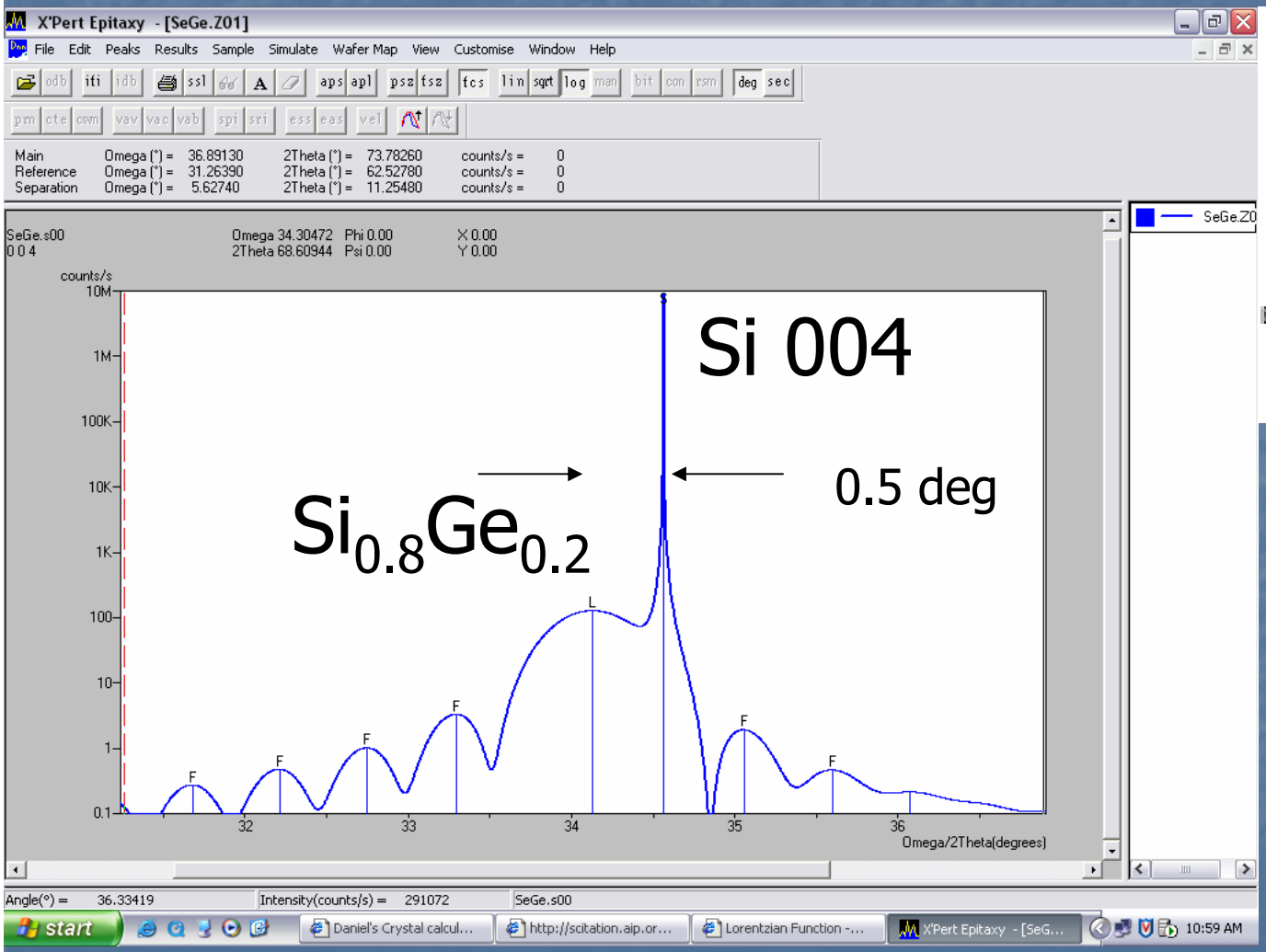

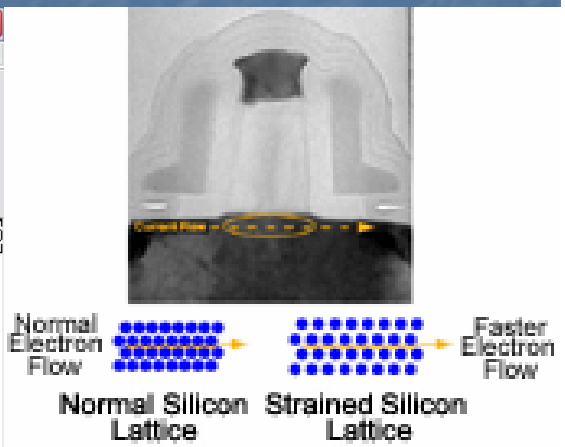

λ = 193, 130, 90,... nm

$Si_{0.8}Ge_{0.2}$

Do we really need High Angular Resolution for that ?

Future Electro-Optic Chips

No place for III-V optoelectronic components?

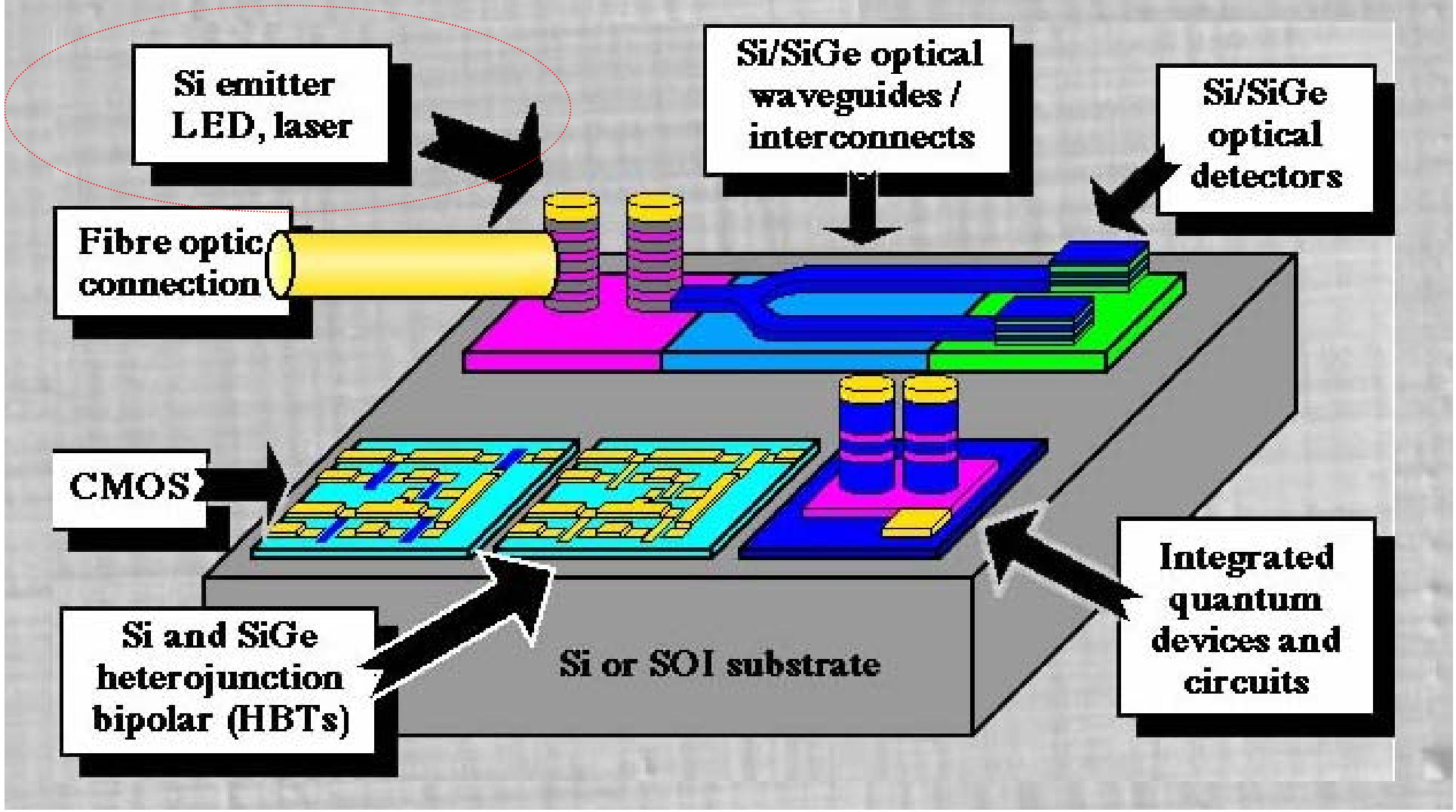

Limitations of high density integration in silicon technology

FEATURE	LIMIT	REASON
Oxide Thickness	2.3 nm	Leakage (I_{GATE})
Junction Depth	30 nm	Resistance (R_{SDE})
Channel Doping	V_T=0.25 V	Leakage (I_{OFF})
SDE Under Diffusion	15 nm	Resistance (R_{INV})
Channel Length	0.06μm	Leakage (I_{OFF})
Gate Length	0.10μm	Leakage (I_{OFF})

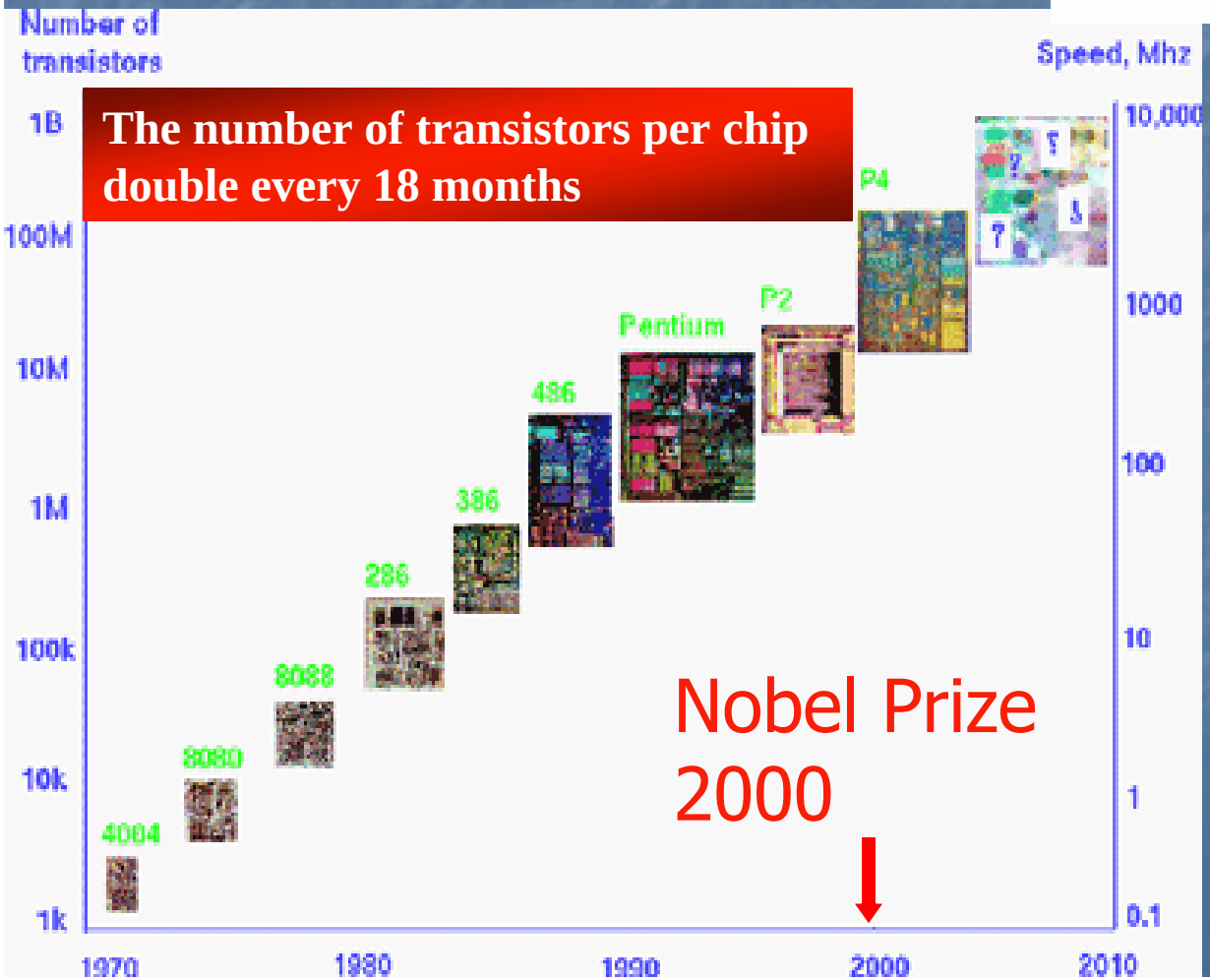

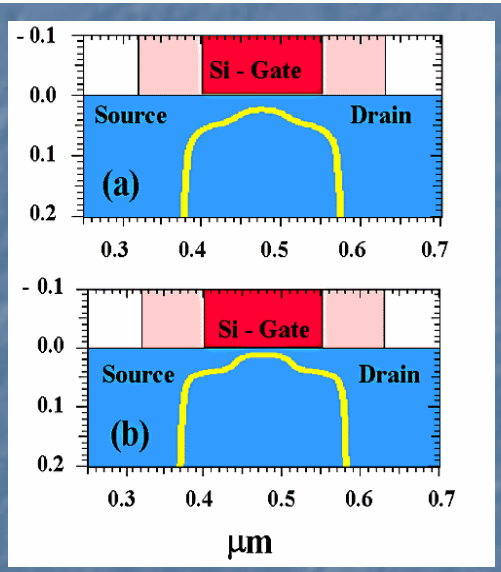

Where is optoelectronic integration on this scale?

The number of active optoelectronic devices per wafer

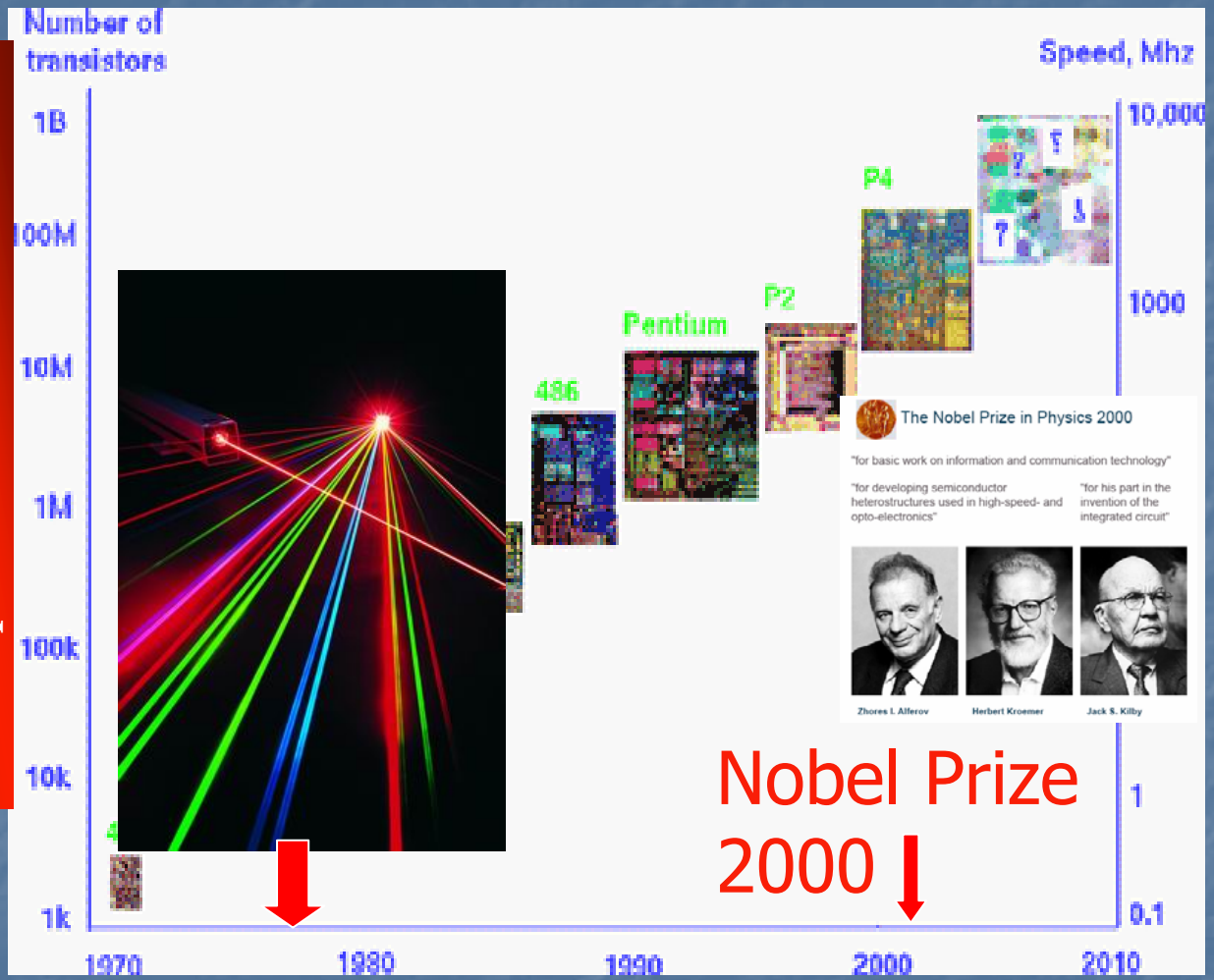

HRXRD for nano-optoelectronics

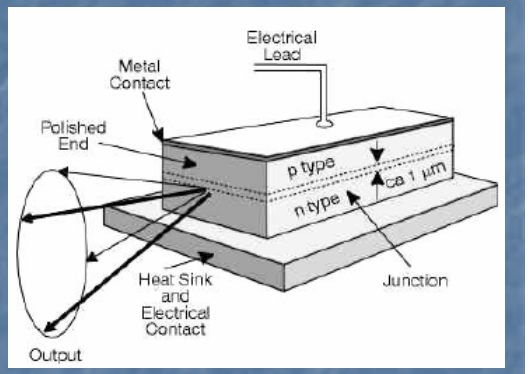

Note that active optoelectronic devices should have dimensions close to the wavelength of light

Issues with integration of Optoelectronic circuits

While electronics manufacturing has evolved from physical assembly of discrete components to high volume manufacture of multi-million-transistor devices, optical devices are generally still assembled from discrete components, a comparatively slow, laborious, costly, and low-yield process.

90% of the cost is in packaging of individual telecom components

The two approaches currently used for optical component Hybrid Integration and Monolithic Integration; both display distinct limitation

Advanced Monolithic Integration Architecture : Example

- RZ, Tandem EA Modulator

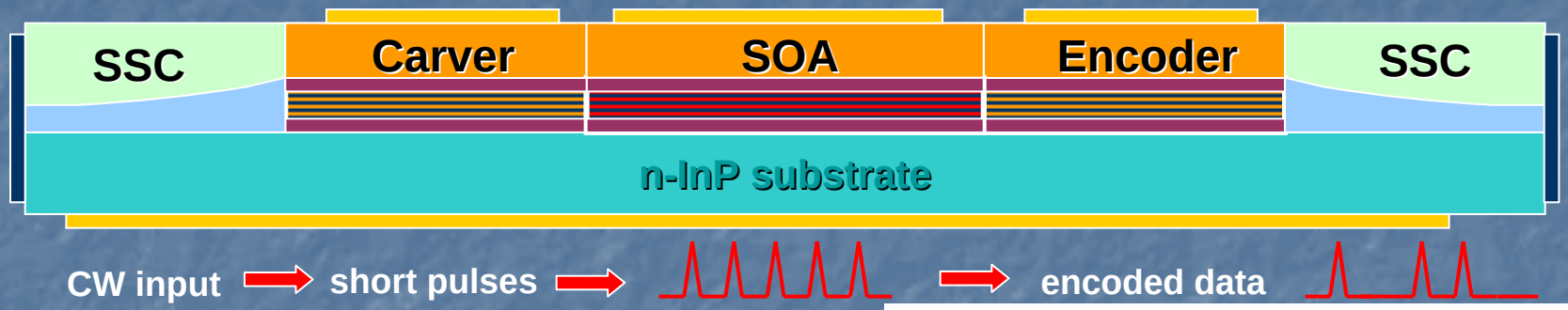

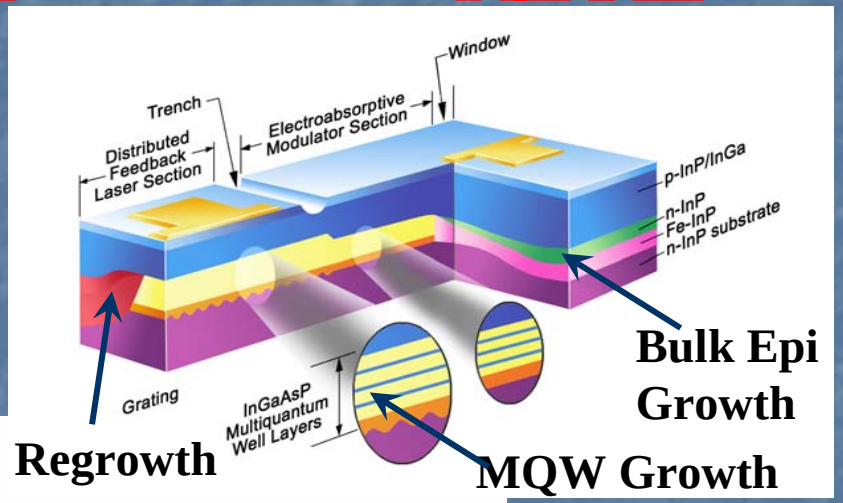

Postdeadline-OFC-2001 **PD14 - 1**

40Gb/s tandem electro-absorption modulator

A. Ougazzaden, C.W. Lentz, T.G.B. Mason, K.G. Glogovsky, C.L. Reynolds, G.J. Przybylek, R.E. Leibenguth, T. L. Kercher, J.W. Boardman, M.T. Rader, J. M. Geary, F.S. Walters, L.J. Peticolas, J.M. Freund, S.N.G. Chu, A. Sirenko, R.J. Jurchenko, M.S. Hybertsen, and L.J.P. Ketelsen

Agere Systems, 9999 Hamilton Blvd, Breinigsville, PA 18031, USA
phone: 610-391-2109, fax: 610-391-2434, email: lketelsen@agere.com

G. Raybon

Lucent Technologies, 791 Holmdel-Keyport Rd, Holmdel NJ 07733
phone: 732-888-7221, fax: 732-888-7074, email: gr@lucent.com

New substrates and integration with Si

III-V Semiconductor Optoelectronics:

GaAs: GaAlAs

InP: InGaAs, InGaAsP, InGaAlAs

GaN: B, Sb, In, Al

Alternative Substrates:

sapphire, SiC, Si, $LiNbO_3$, …

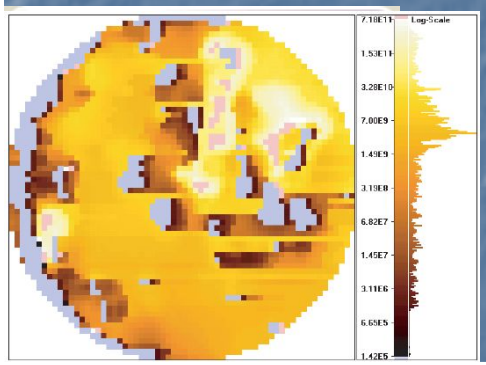

Strain $\Delta a/a$

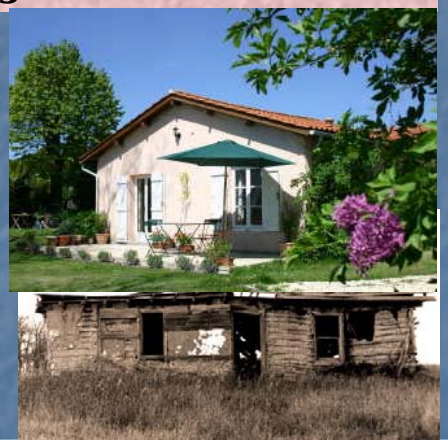

Si World:

$Si + SiO_2 + Ge$

Si or SOI platform

Nano-Hetero-Epitaxy (NHE)

Motivation: Recent results show that small diameters of the heterostructures and the absence of lateral confinement strongly enhance lateral relaxation and allow lattice and thermal expansion mismatched materials to be combined without propagation dislocations

Applications: Lattice mismatched hetero-integration of highly integrated systems combining superior proprieties of Si-based electronic and III-V based Photonic devices

Collaborations: NJIT, CHESS, Georgia Tech, Lucent, SUPELEC, Uni Metz, France

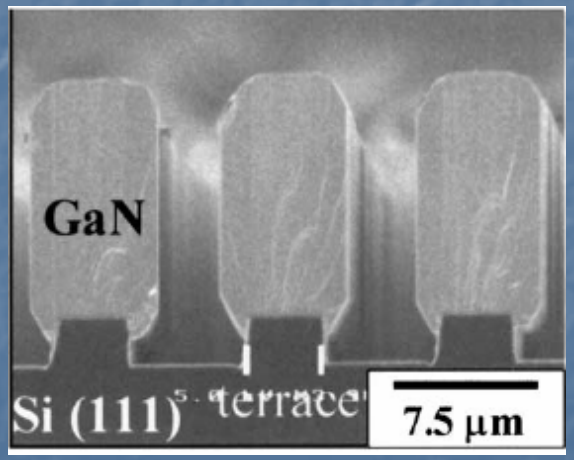

Sano et al
Maeijo Univ

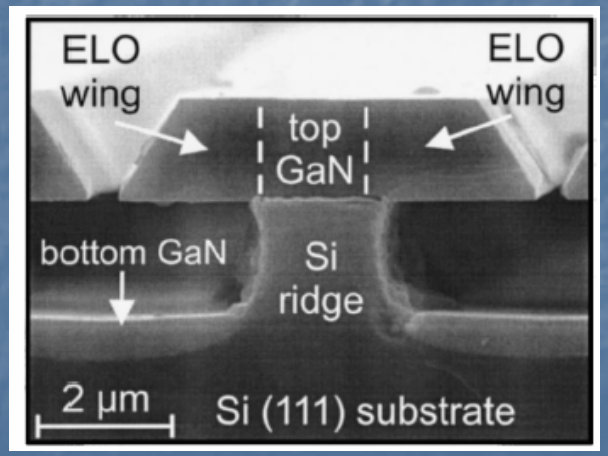

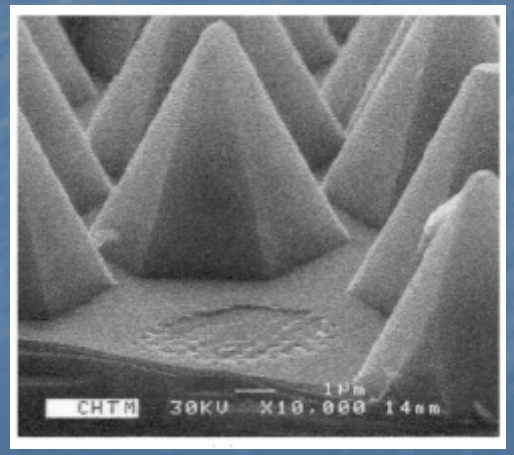

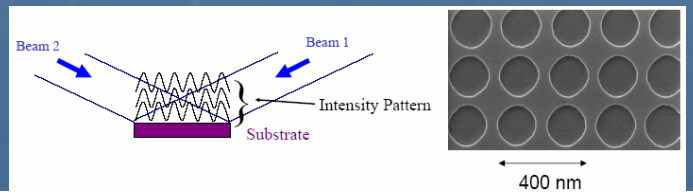

NHE (3D strain relief)

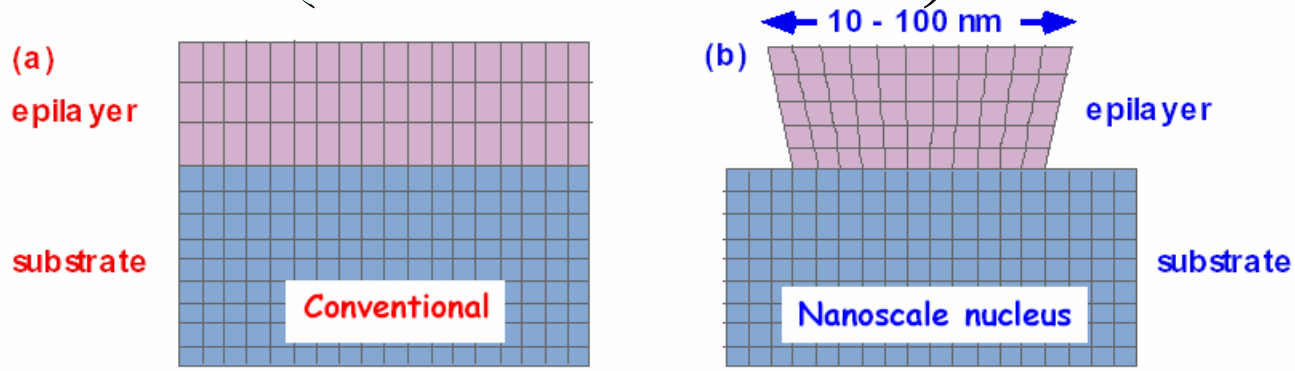

(a) Conventional Heteroepitaxy
Strain at growth interface remains constant and strain energy grows linearly with epilayer thickness. Dislocations eventually created.

(b) Stress relief in Nanosize Nucleus
3-D strain in nanosize nucleus gives exponential stress/strain decay (Luryi and Suhir, 1986). Decay length is proportional to (and of similar magnitude to) island diameter. Strain energy saturates at a maximum value.

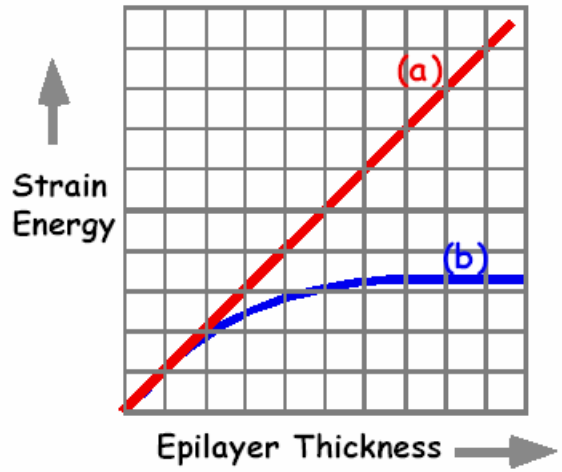

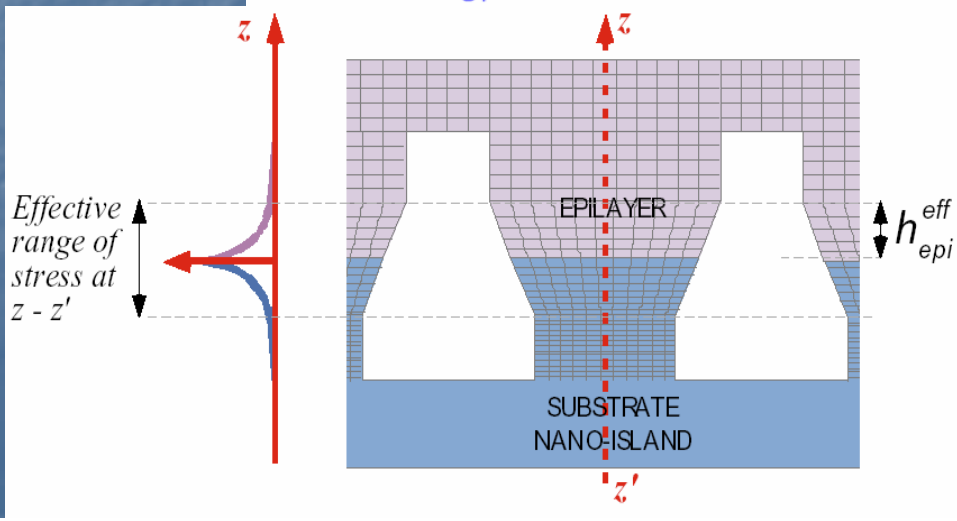

Subwavelength Optical Elements (SOEs)

Taking integrated optical-component design to the next level of density, cost, and reliability will require new optical « building blocks » with:

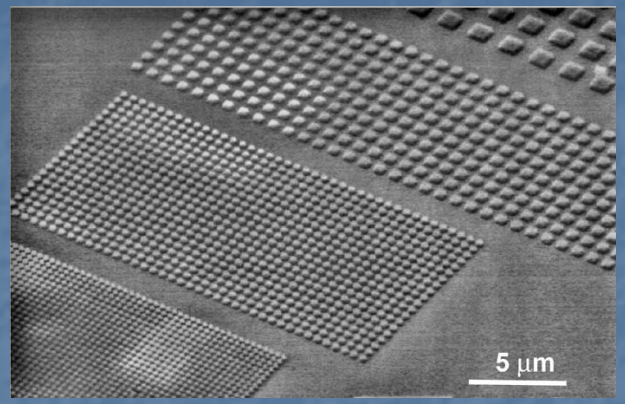

- *Broad range of optical functionality*
- *Easily integration with other optical/electronic materials*

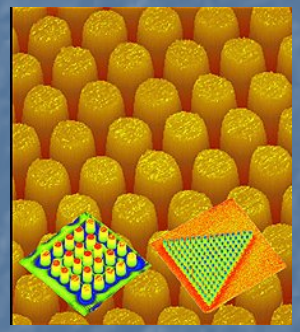

SOEs are the realization of nano-technology applied to optical elements. Through manipulation of the size, shape, type and the period of nanostructures SOEs deliver a broad range of useful optical effect and functionality.

SUMMARY for the INTRODUCTION

- NHE is one of the key technologies for Monolithic Integration of Optical Devices
- Progress in NHE depends on Submicron and nano characterizations

MOVPE: Nanoscale Selective Growth

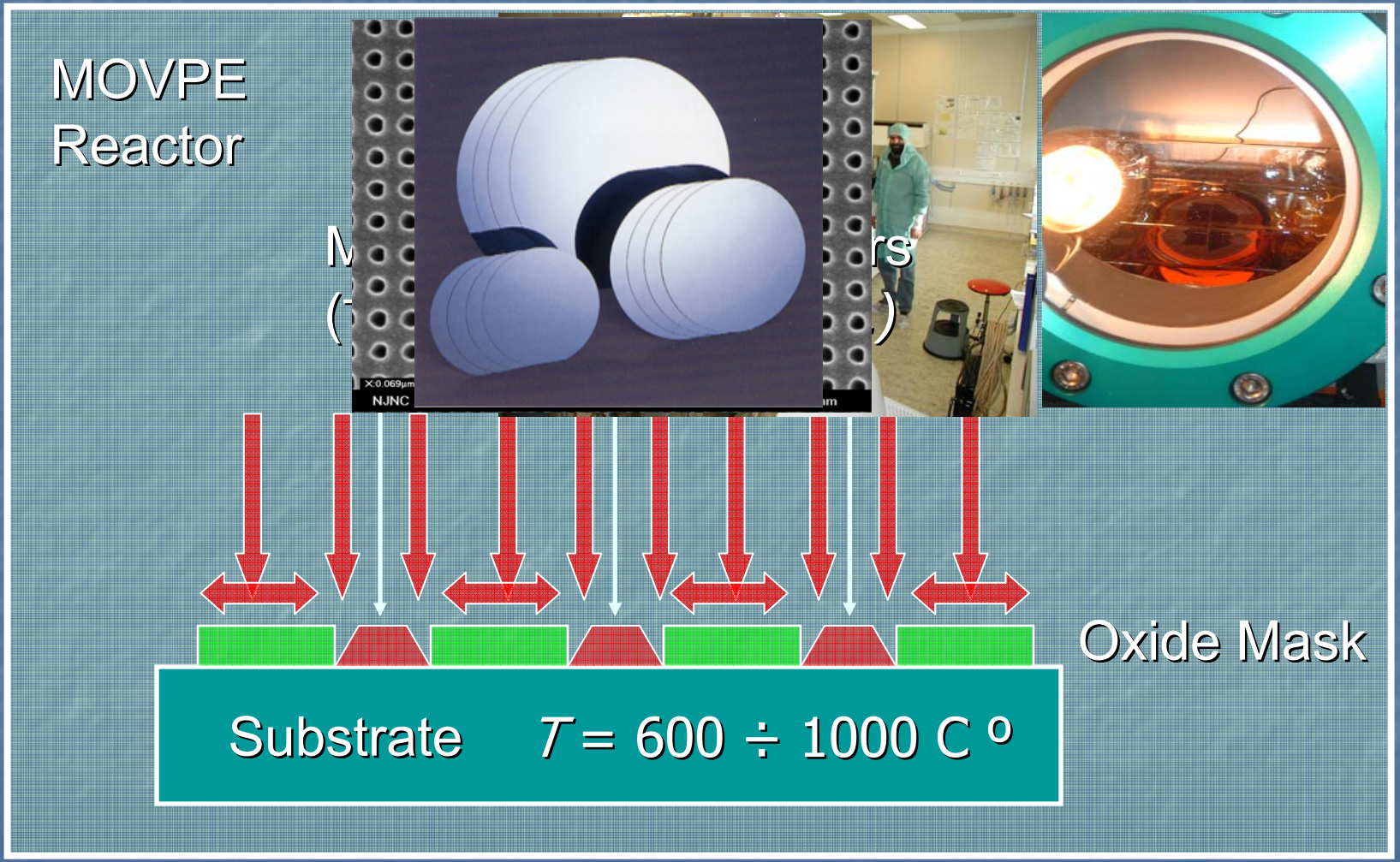

Selective Growth on Nanoscale

(Simplified Picture)

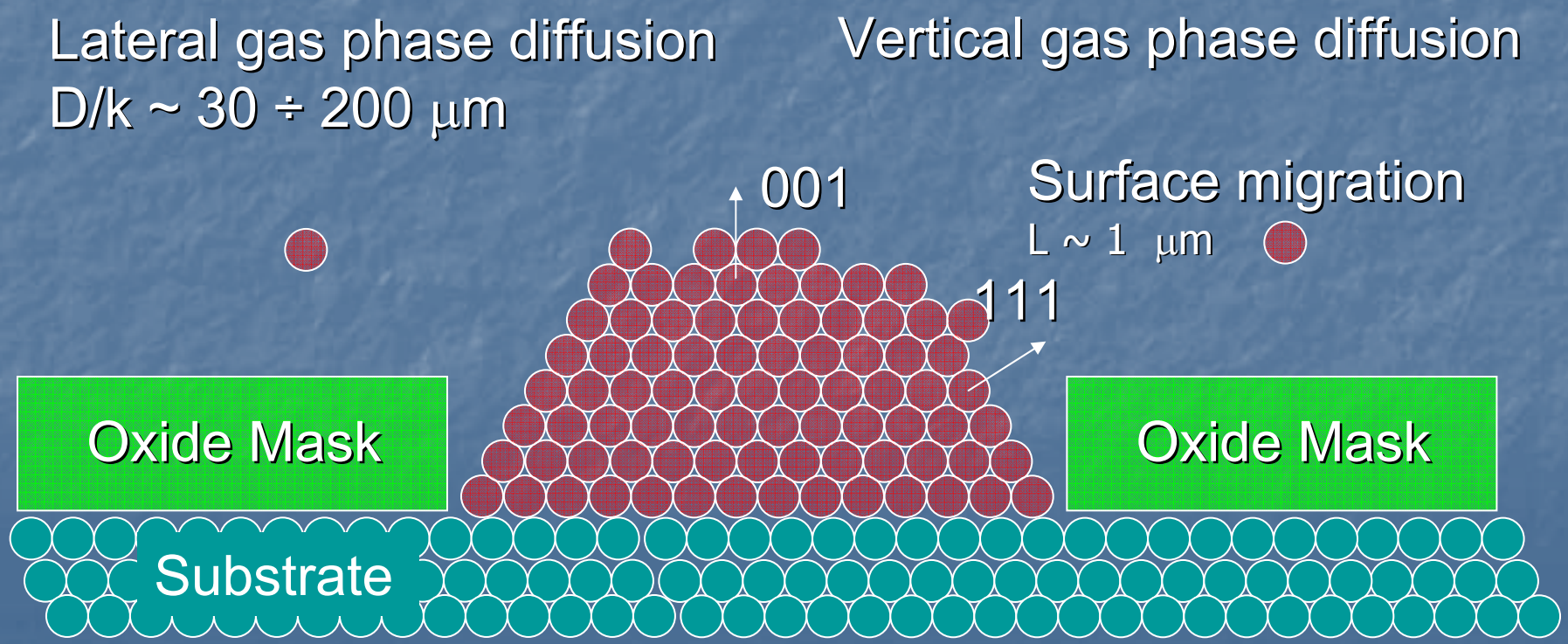

Characterization of the Nanoscale Selectively Grown structures

SEM

IMAGING TECHNIQUES

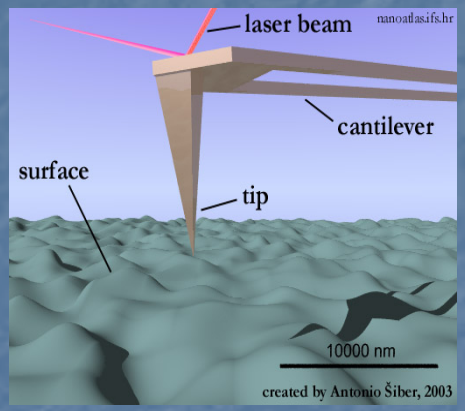

AFM

Nanostructures ?

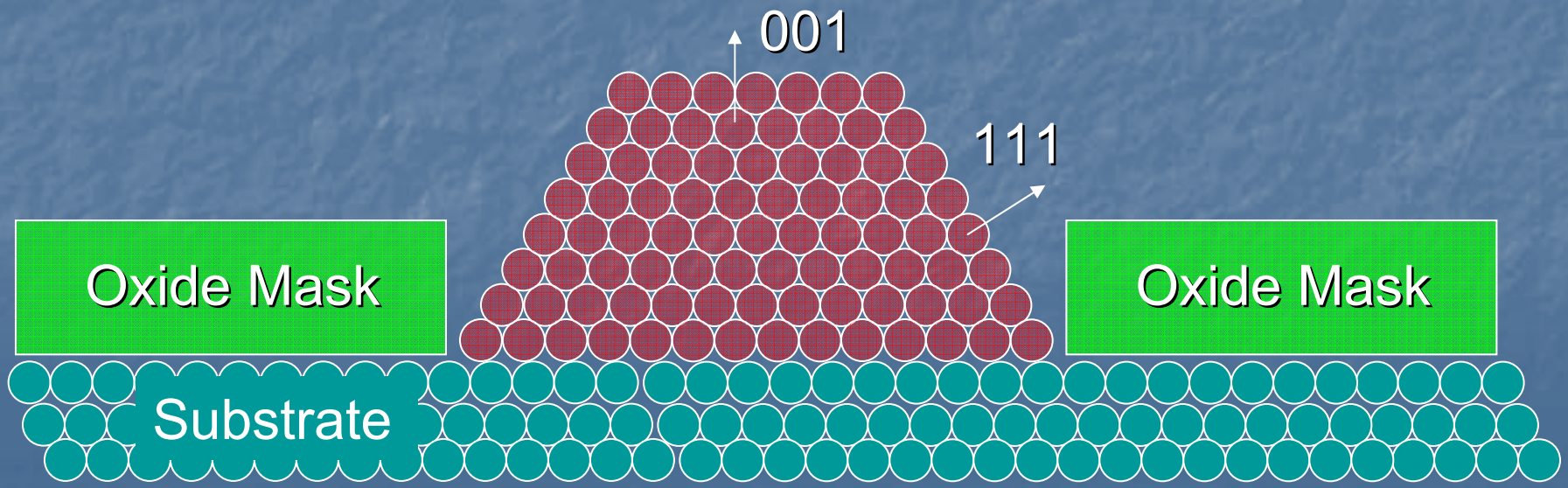

Selective Growth on Nanoscale

Sufficient surface migration

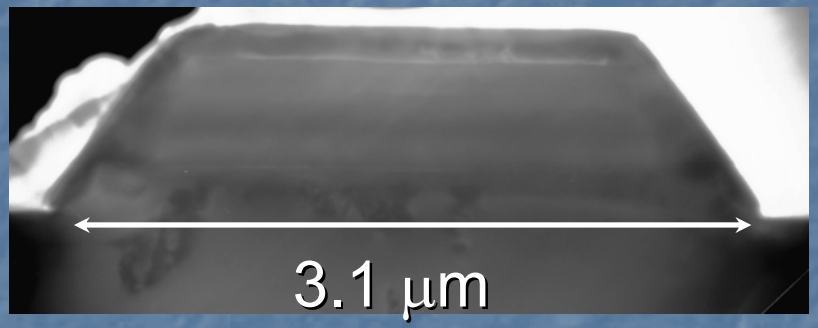

InGaAlAs-based MQW's

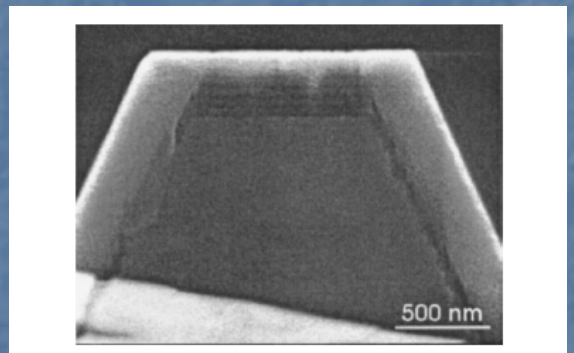

FIG. 3. SEM photograph of a stripe in ⟨1$\bar{1}$00⟩ direction with trapezoidal cross section. The Mg-doped GaN cover layer results in a brighter SEM contrast. The five QWs are resolved only on the top facet.

InGaN/GaN-based MQW's

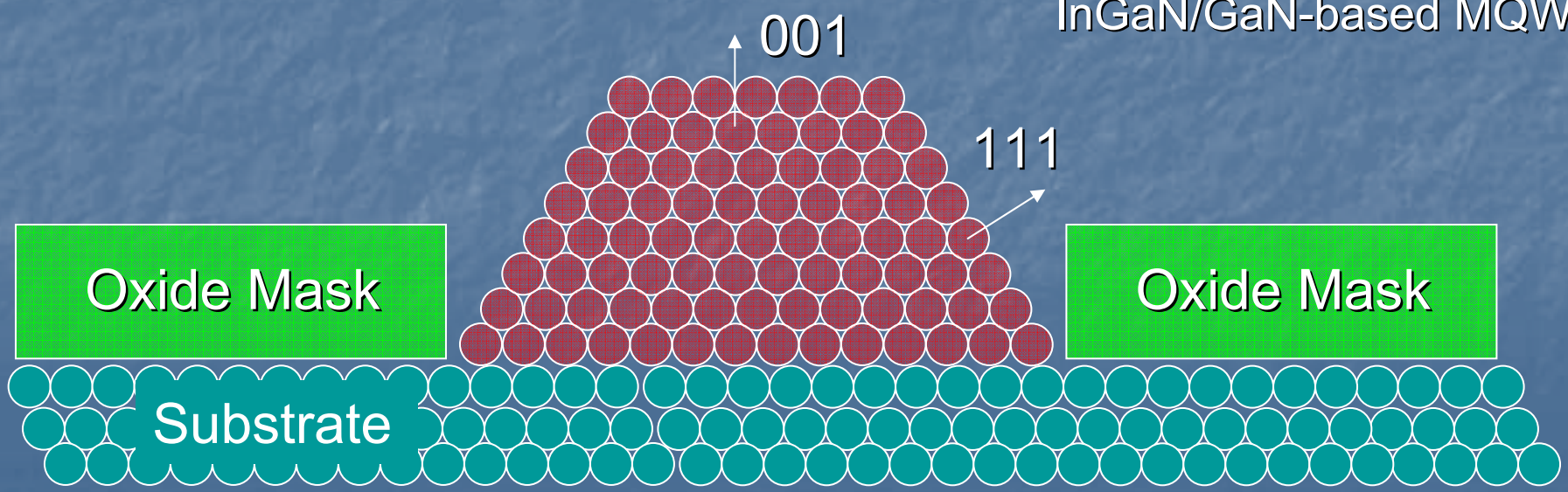

Selective Growth on Nanoscale

Insufficient surface migration

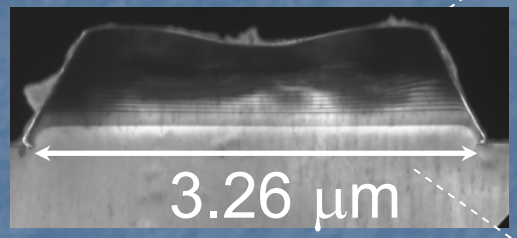

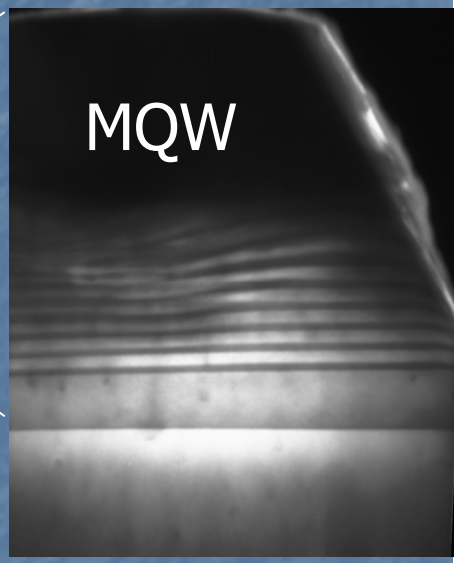

InGaAsP-based MQW's

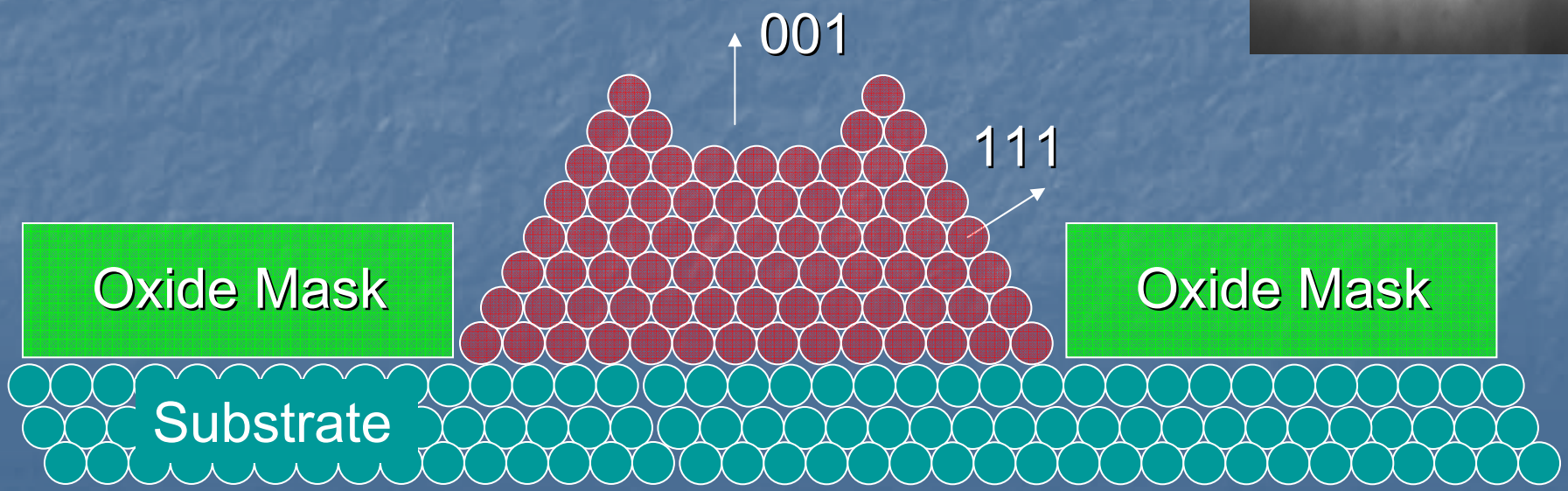

Analytical Characterization

HRXRD
RSM
XSW

Composition change
Strain $\Delta d/d$
Relaxation Effects
Sidewall and interface quality
Impurity incorporation and activation

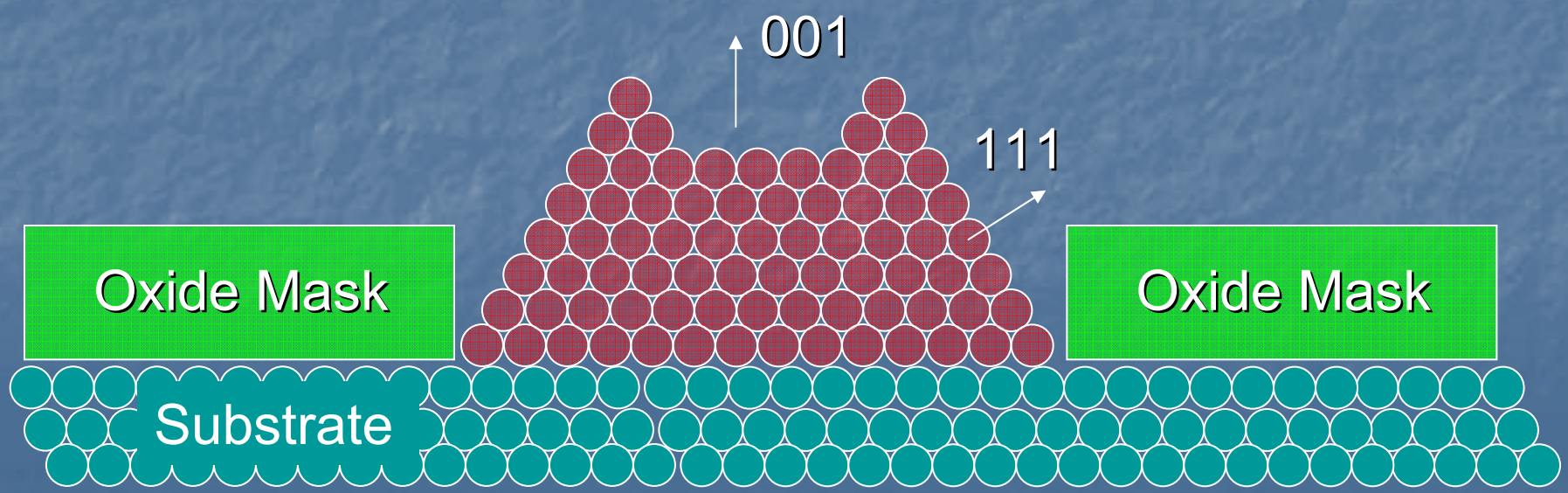

Traditional Materials Characterization in the Industrial Production Line
Example: X and Y measurement for $In_{1-x}Ga_xAs_yP_{1-y}$

2 inch wafer

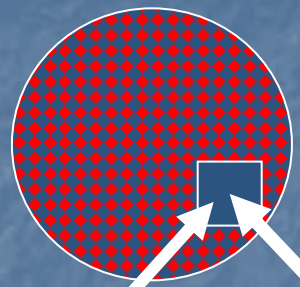

1000 devices
"Control Square"
5 x 5 mm

1.5 µm

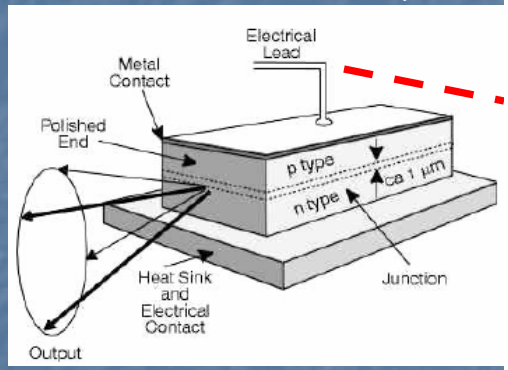

Photoluminescence

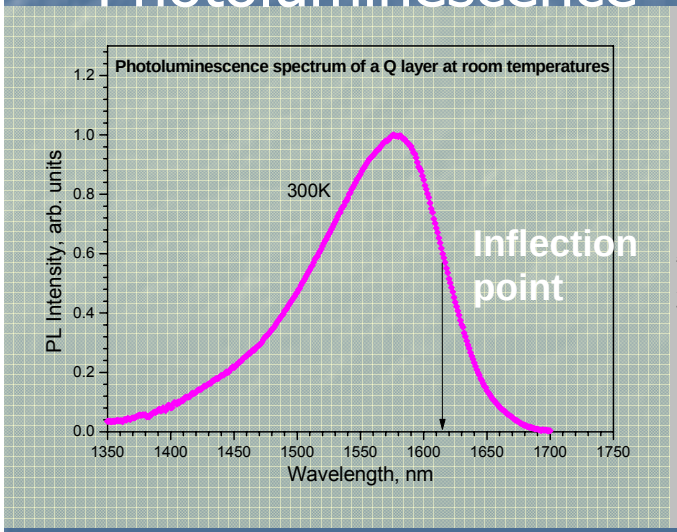

XRD

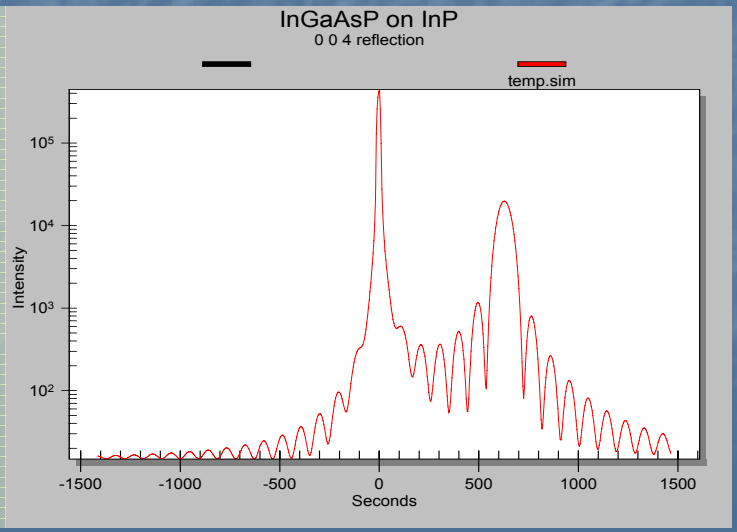

2000:
XRD with the beam size < 1 µm and angular resolution: < 20 arc sec

2010 – 2020
???

{ PL , Strain } ⟷ { X , Y }

What is "high angular resolution" XRD?

$\Delta\theta$

$\Delta\lambda$

Beam conditioner

X-rays

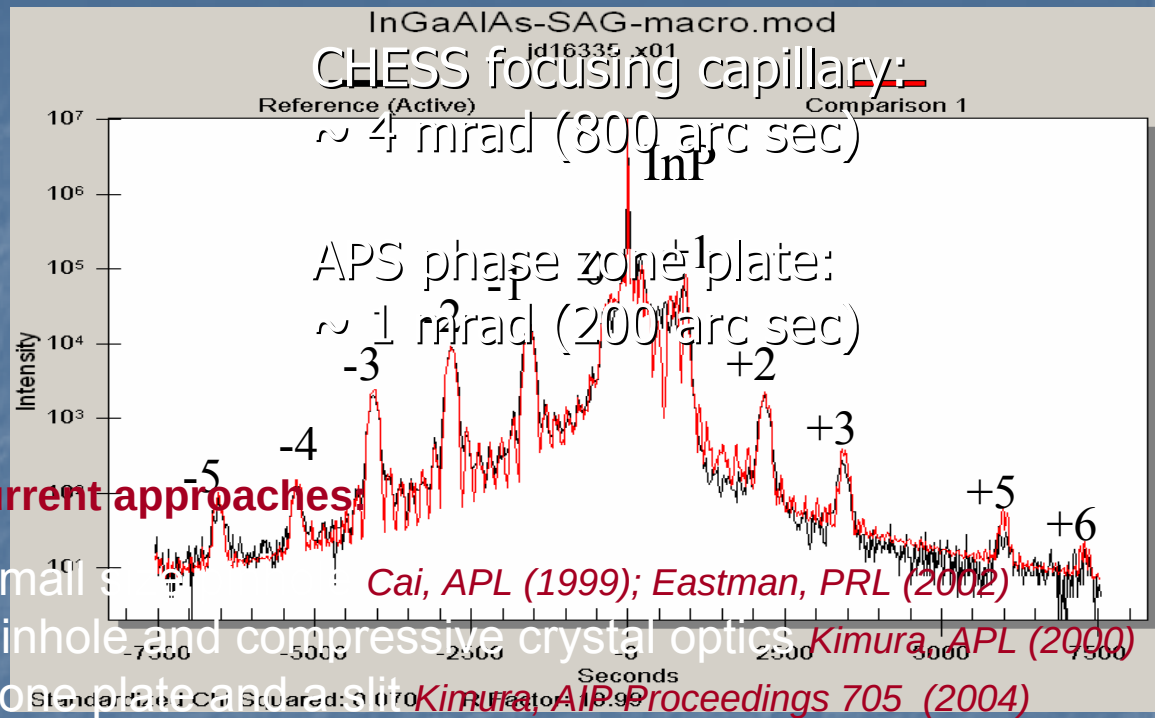

CHESS focusing capillary:
~ 4 mrad (800 arc sec)

APS phase zone plate:
~ 1 mrad (200 arc sec)

current approaches:

- small s
- pinhole and compressive crystal optics *Kimura, APL (2000)*
- zone plate and a slit *Kimura, AIP Proceedings 705 (2004)*

Cai, APL (1999); Eastman, PRL (2002)

1 μm pinhole ↔ 25 arc sec

We want to combine it with high spatial resolution Δx

High angular resolution
but low spatial resolution

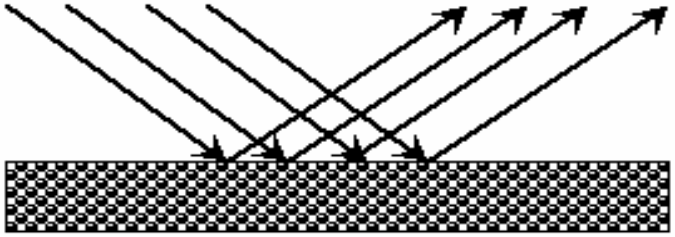

High spatial resolution
but low angular resolution

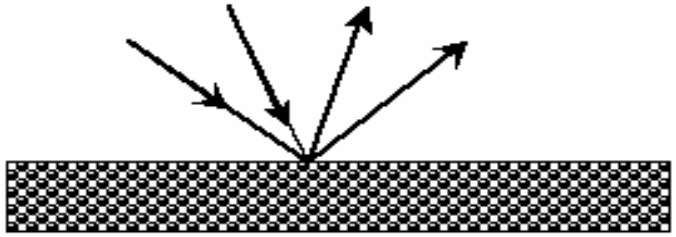

Approach developed by Alex Kazimirov *et al.*, at CHESS

post focusing crystals in non-dispersive arrangement

intensity lost: $$\frac{\Delta\theta}{NA} \approx \frac{10^{-5}}{10^{-3}} = 1\%$$

advantages:

- using 100% focusing in non-diffraction plane
- may use expanded bandwidth (e.g., multilayer optics)
- flexible control over resolution

microbeam XSW

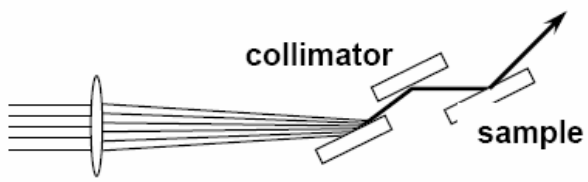

J. Physics D, 37 (2004)

microbeam HRXRD

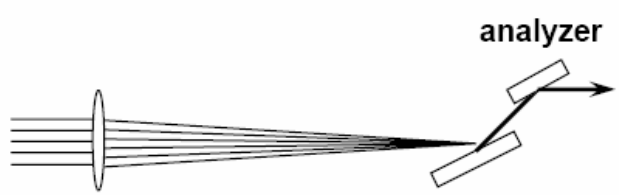

J. Appl. Phys. 97 (2005)

microbeam reciprocal space mapping

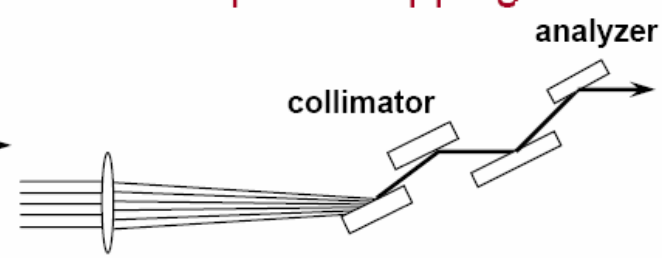

(under preparation)

angular resolution is determined by the intrinsic rocking curve width of the collimator / analyzer crystal: e.g., Si(004) – 2 arc sec at 12 keV

High resolution optics for microbeam XRD

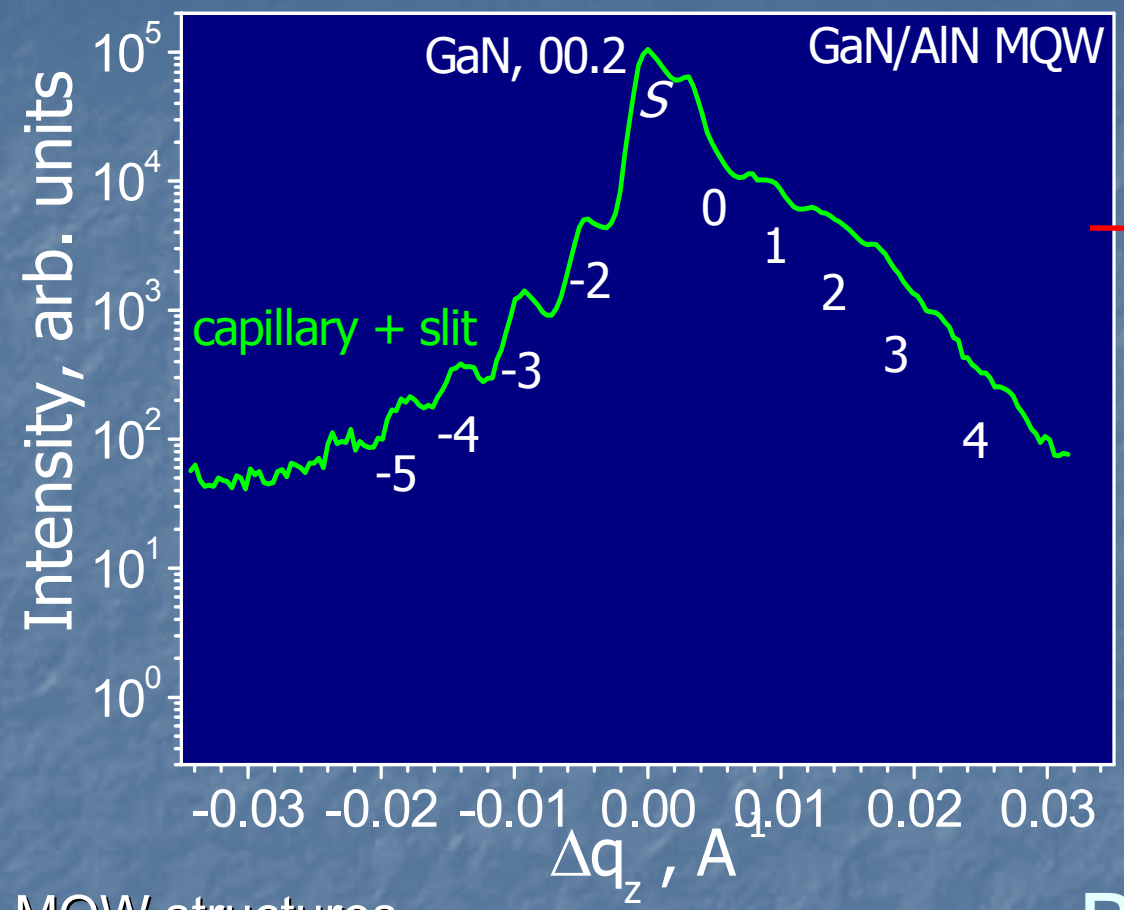

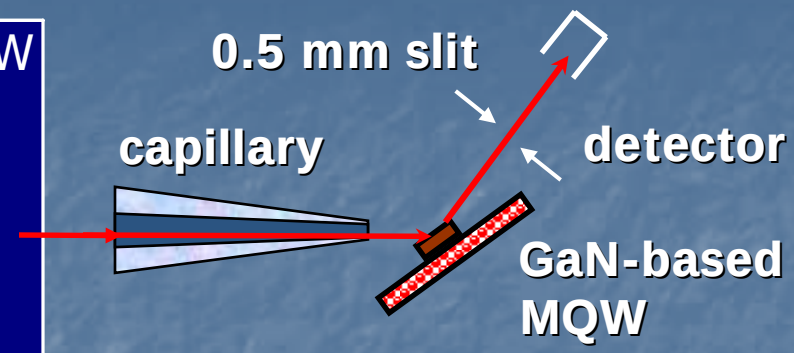

MQW structures

16.8 nm GaN
4.4 nm AlN

Beamsize: 10 μm

High resolution optics for microbeam XRD

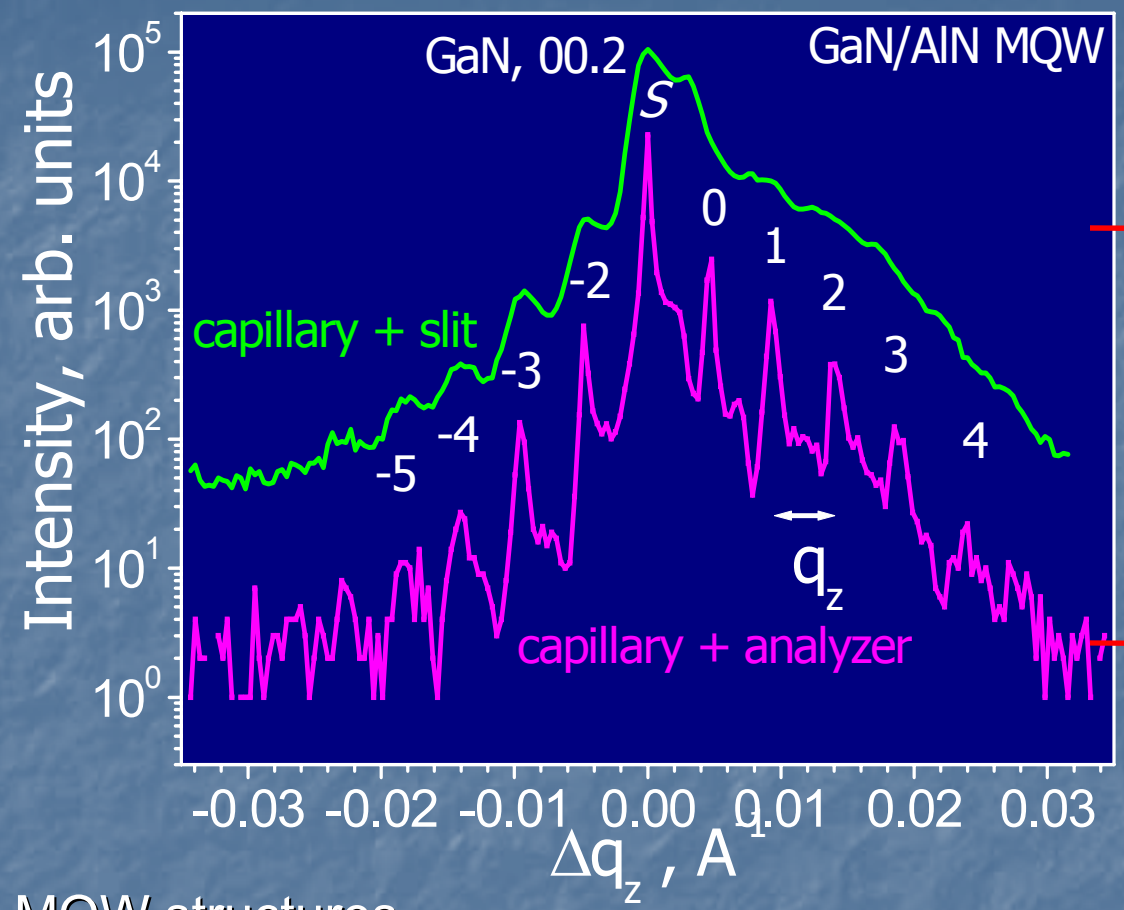

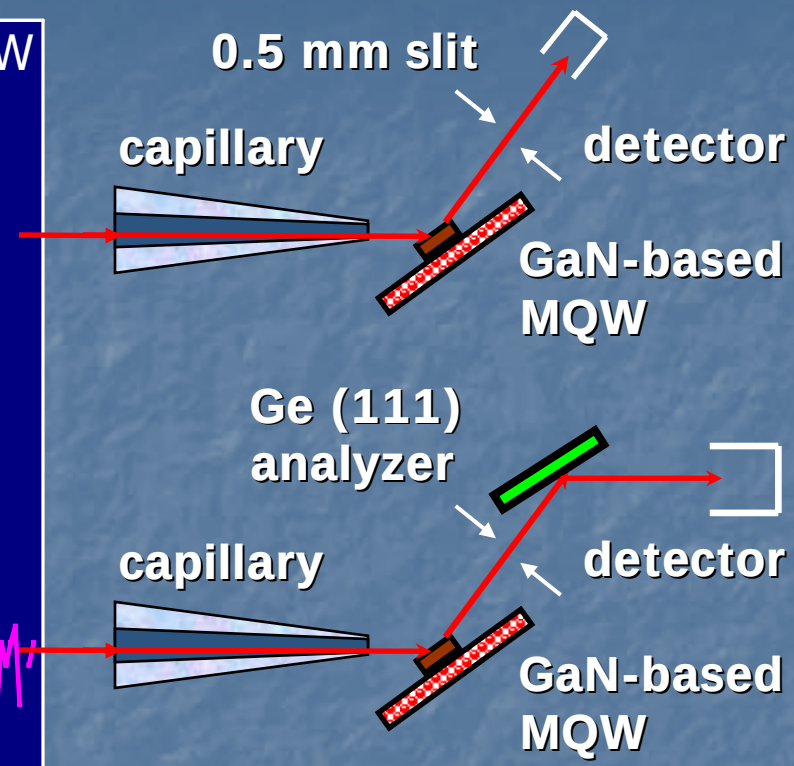

MQW structures

16.8 nm GaN
4.4 nm AlN

High resolution optics for microbeam XRD

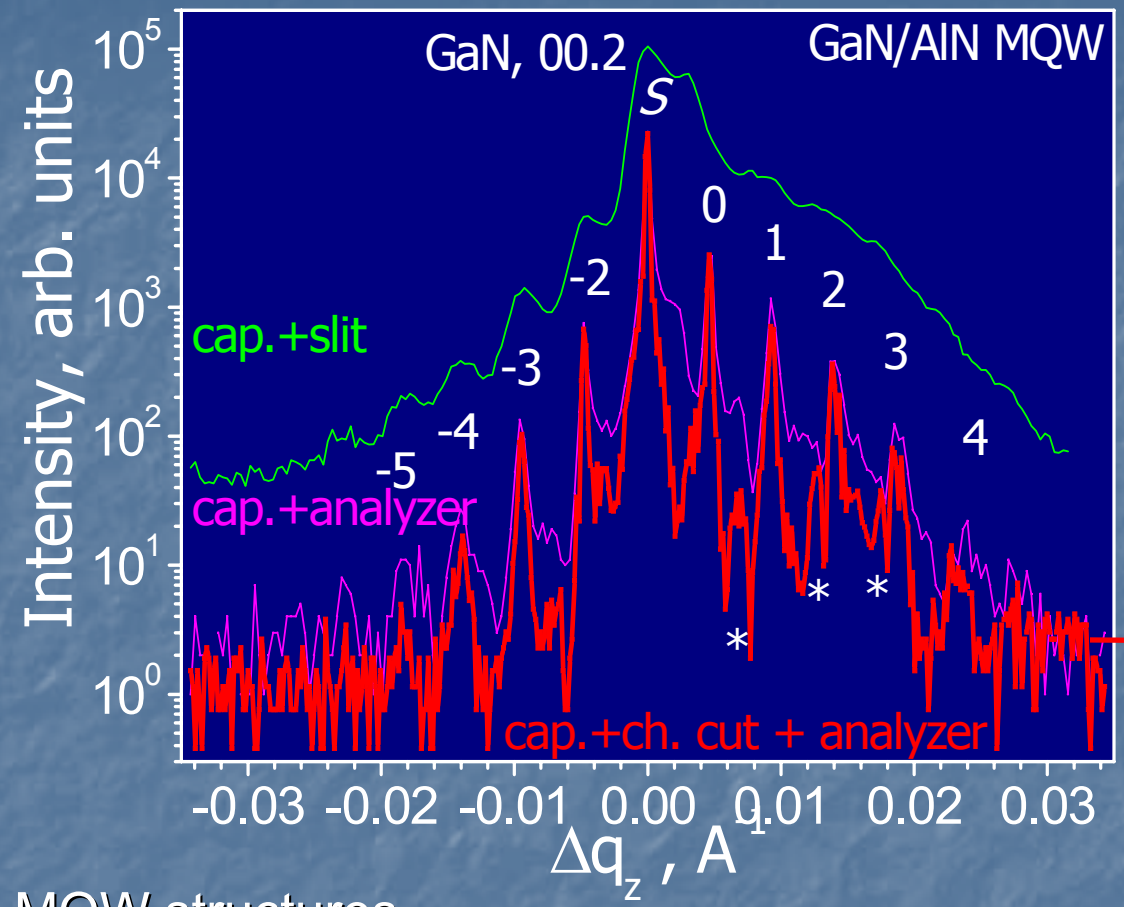

Experimental setup developed by Alex Kazimirov

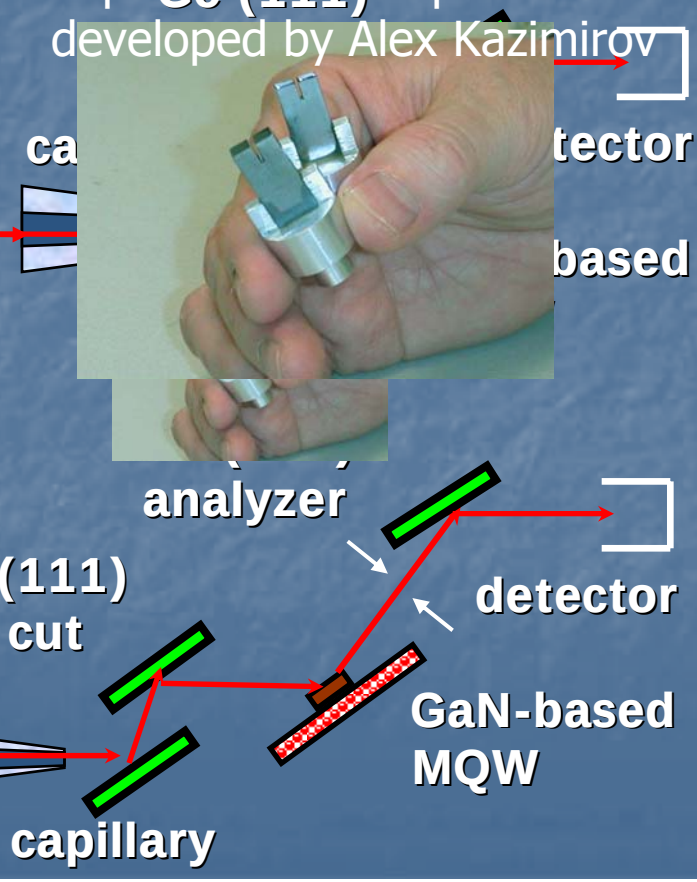

MQW structures

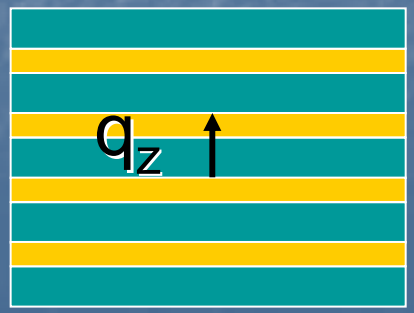

16.8 nm GaN
4.4 nm AlN

High resolution optics for microbeam XRD

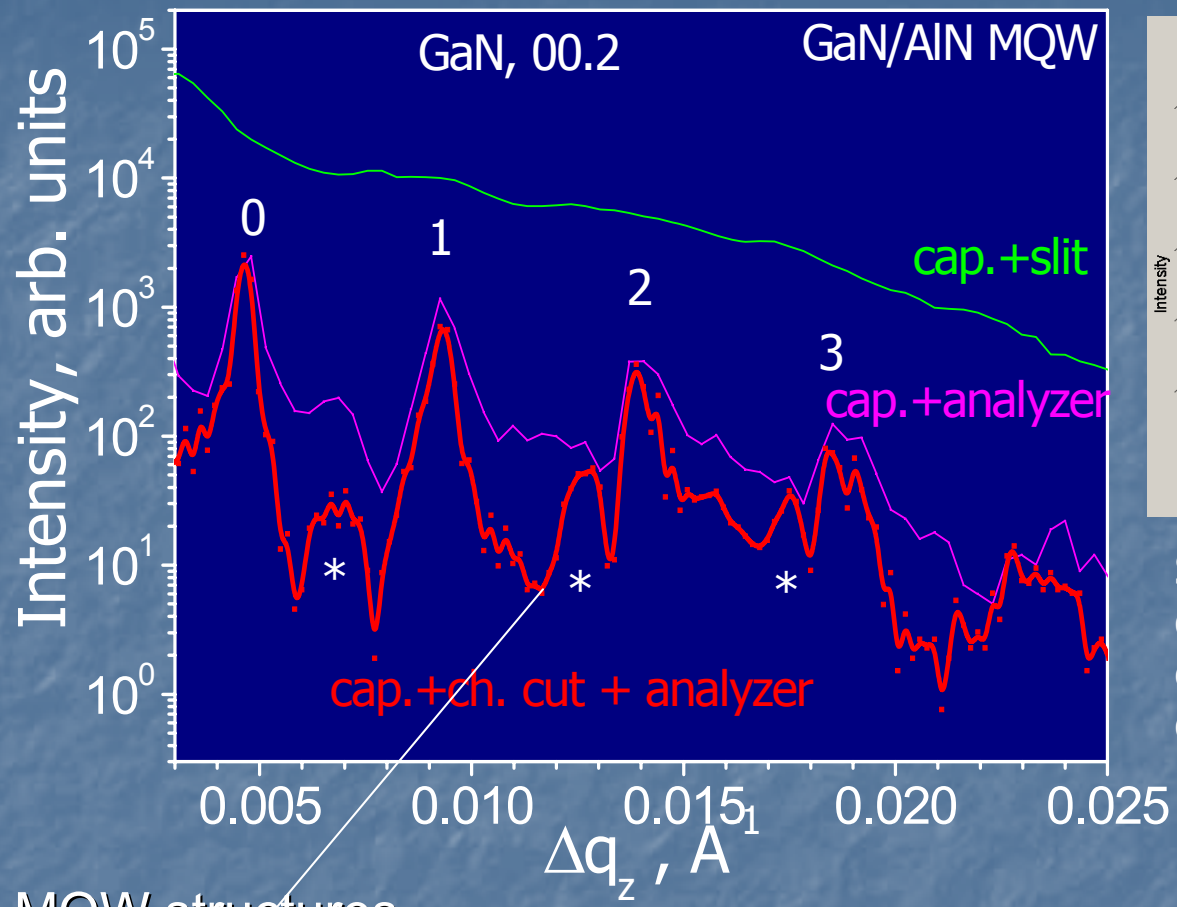

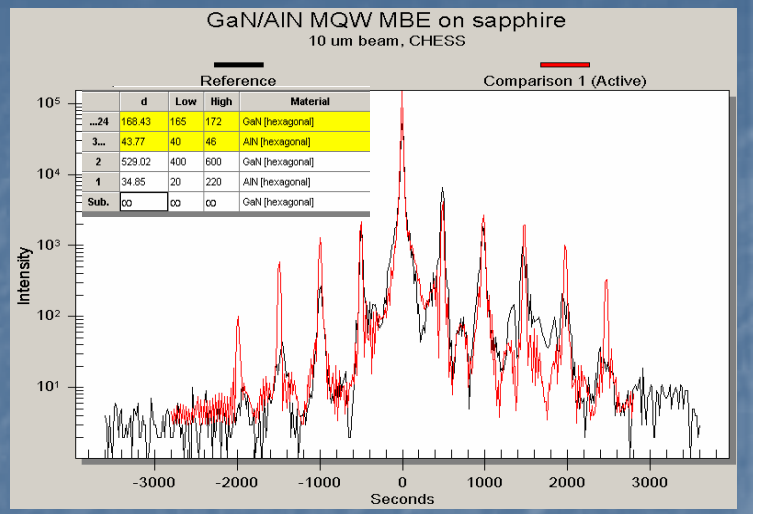

Simulation of experimental diffraction curves using computational algorithms based on dynamical diffraction theory

MQW structures

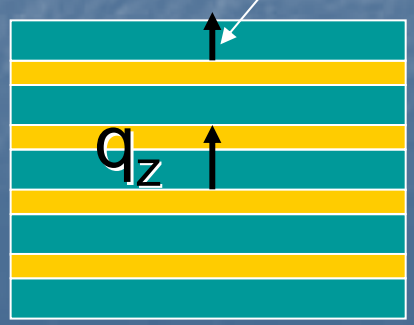

16.8 nm GaN
4.4 nm AlN

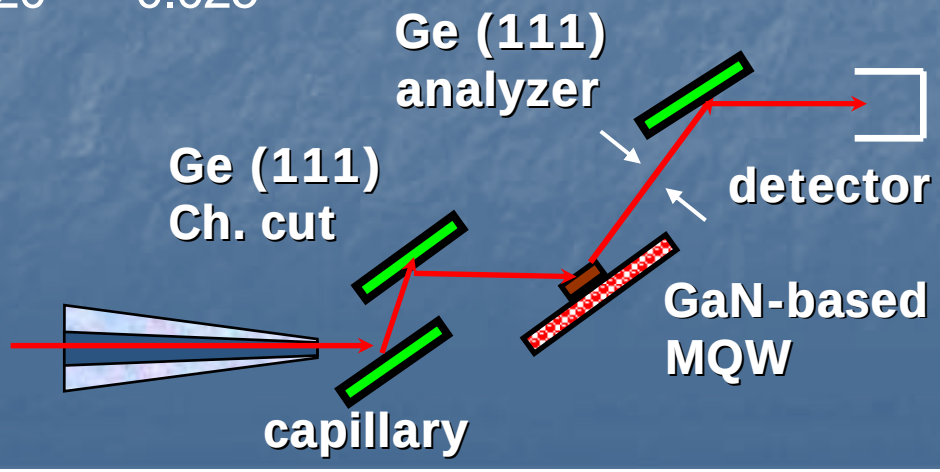

High resolution optics for microbeam XRD

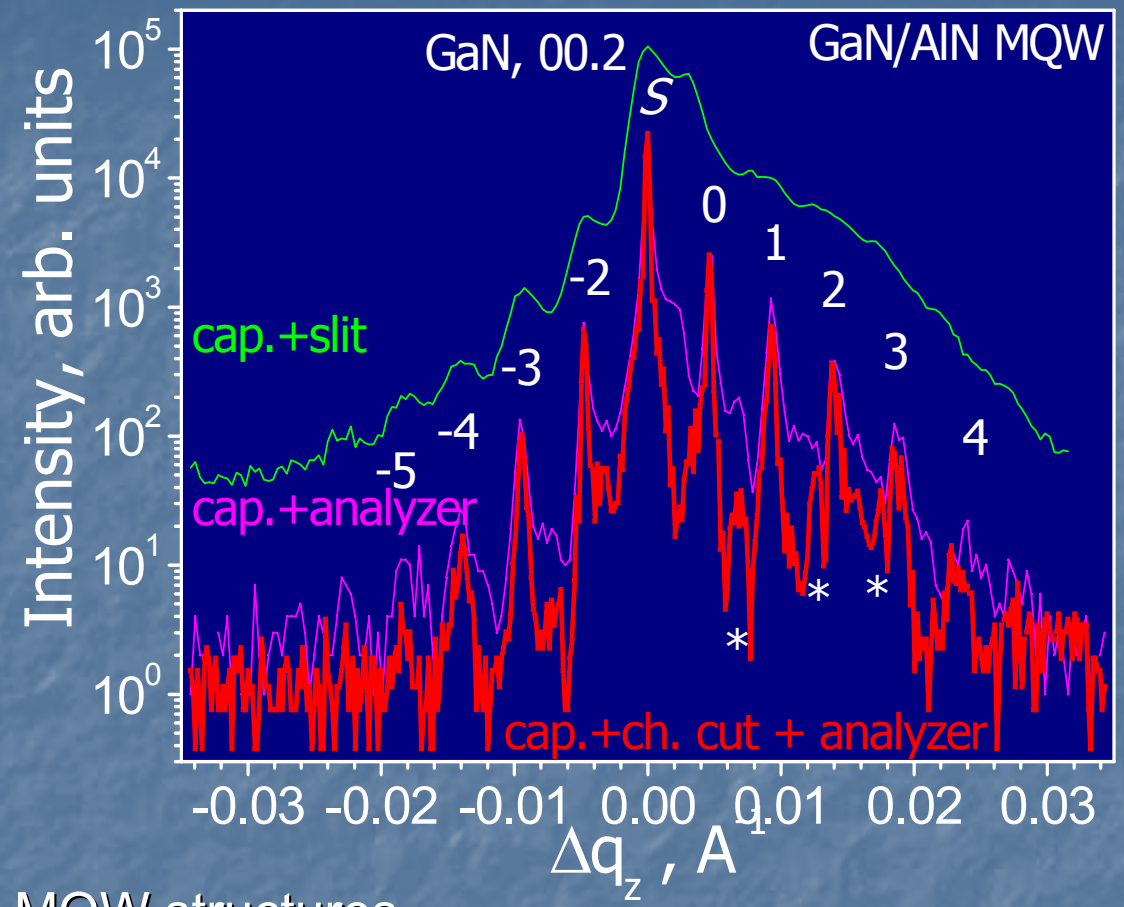

MQW structures

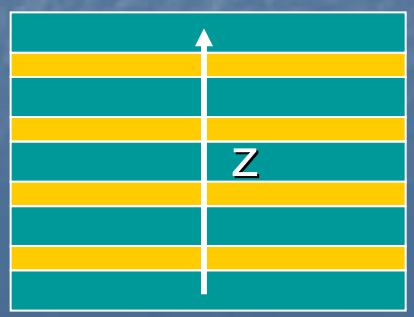

16.8 nm GaN
4.4 nm AlN

Application for RSM

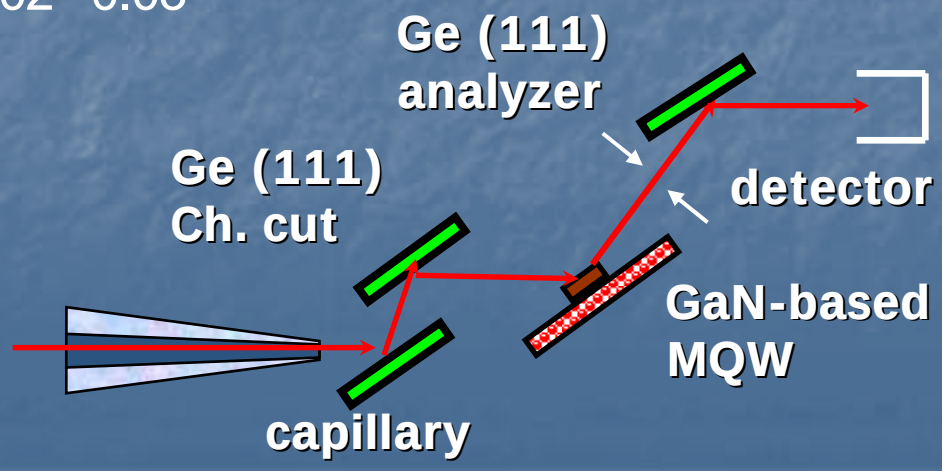

X-ray optics for microbeam RSM

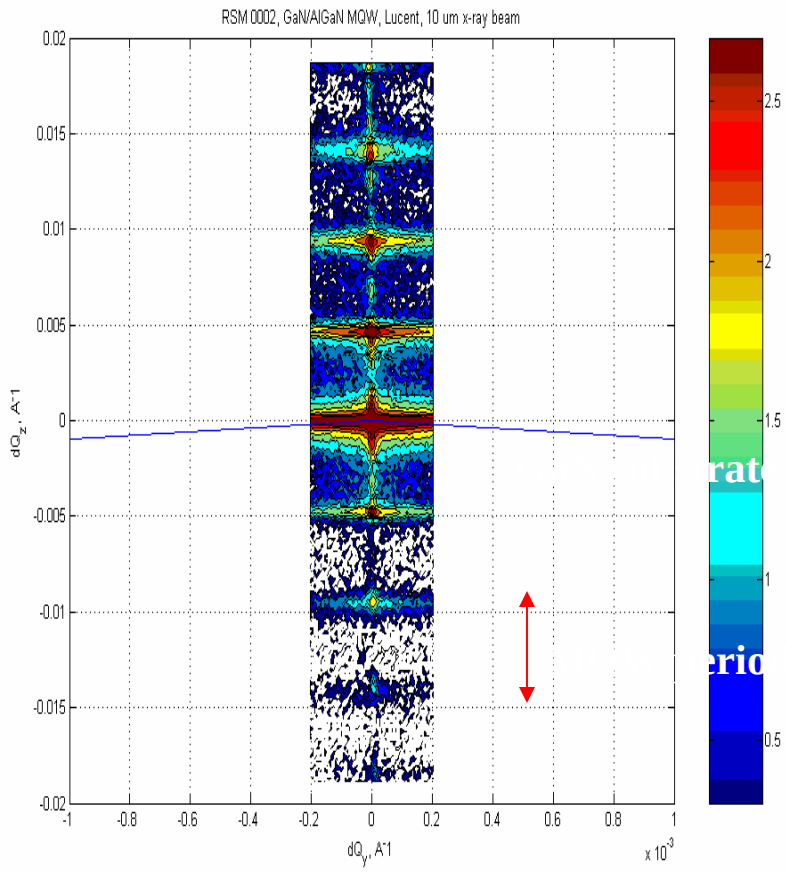

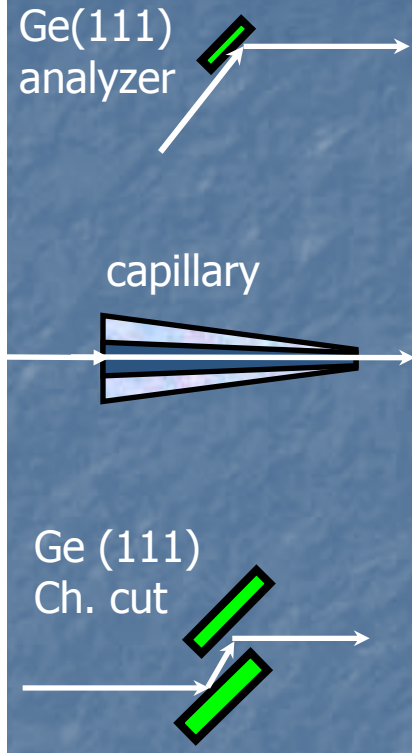

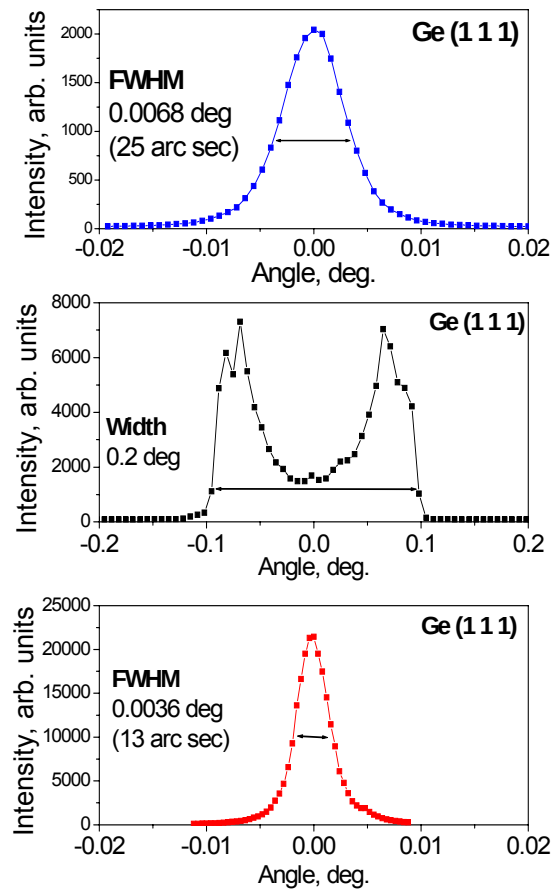

Takes ~ 15 hours to measure this Map

Max intensity: 50,000 cps

Satellites: 300 cps

MQW peaks

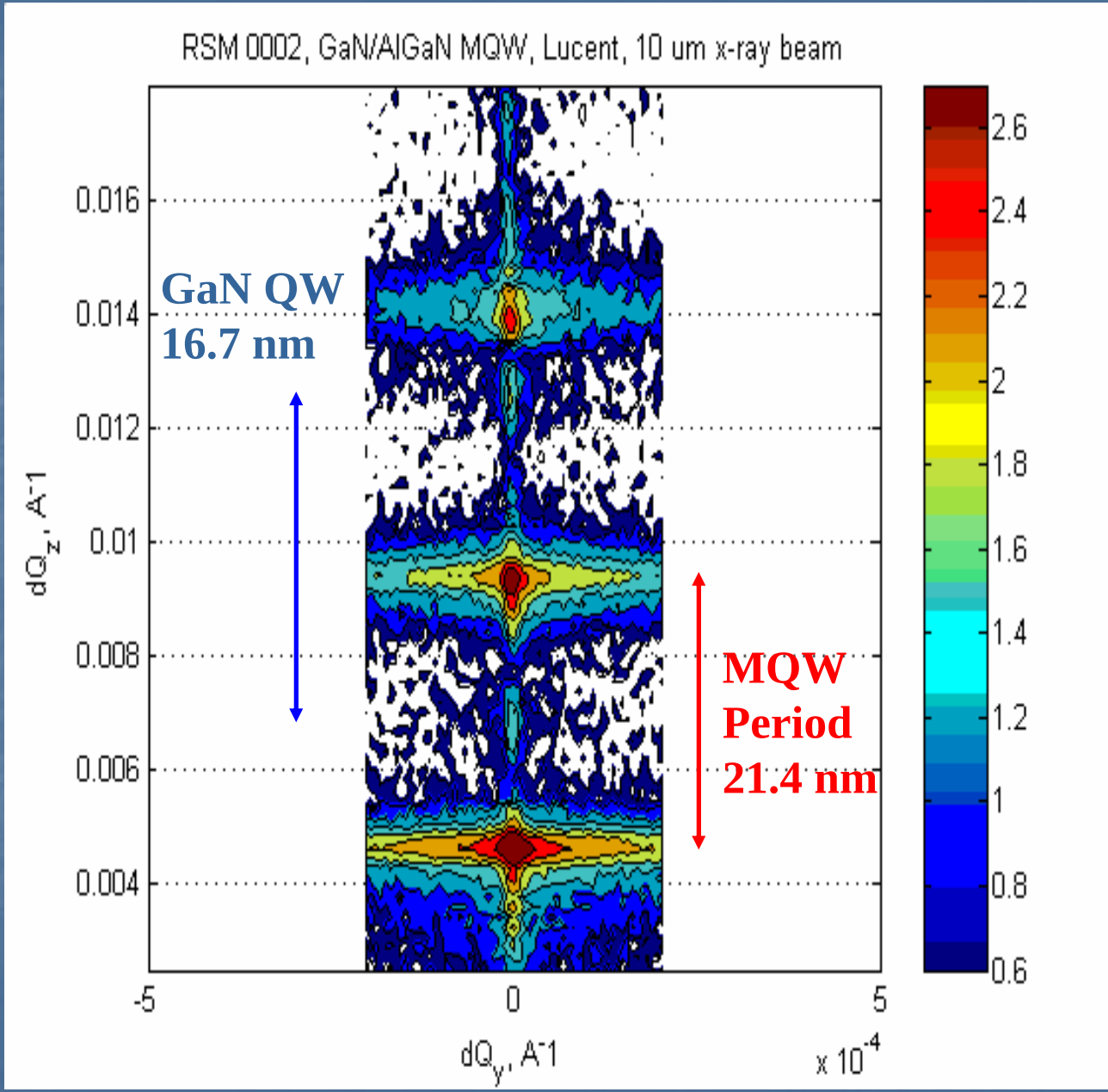
RSM 0002, GaN/AlGaN MQW, Lucent, 10 um x-ray beam
GaN QW
16.7 nm
MQW
Period
21.4 nm
0.016
0.014
0.012
0.01
0.008
0.006
0.004
dQz, A-1
-5
0
5
dQy, A-1
x 10-4
2.6
2.4
2.2
2
1.8
1.6
1.4
1.2
1
0.8
0.6

CHESS microbeam setup: HRXRD and RSM

CHESS
Cornell High Energy Synchrotron Source

A2 beamline

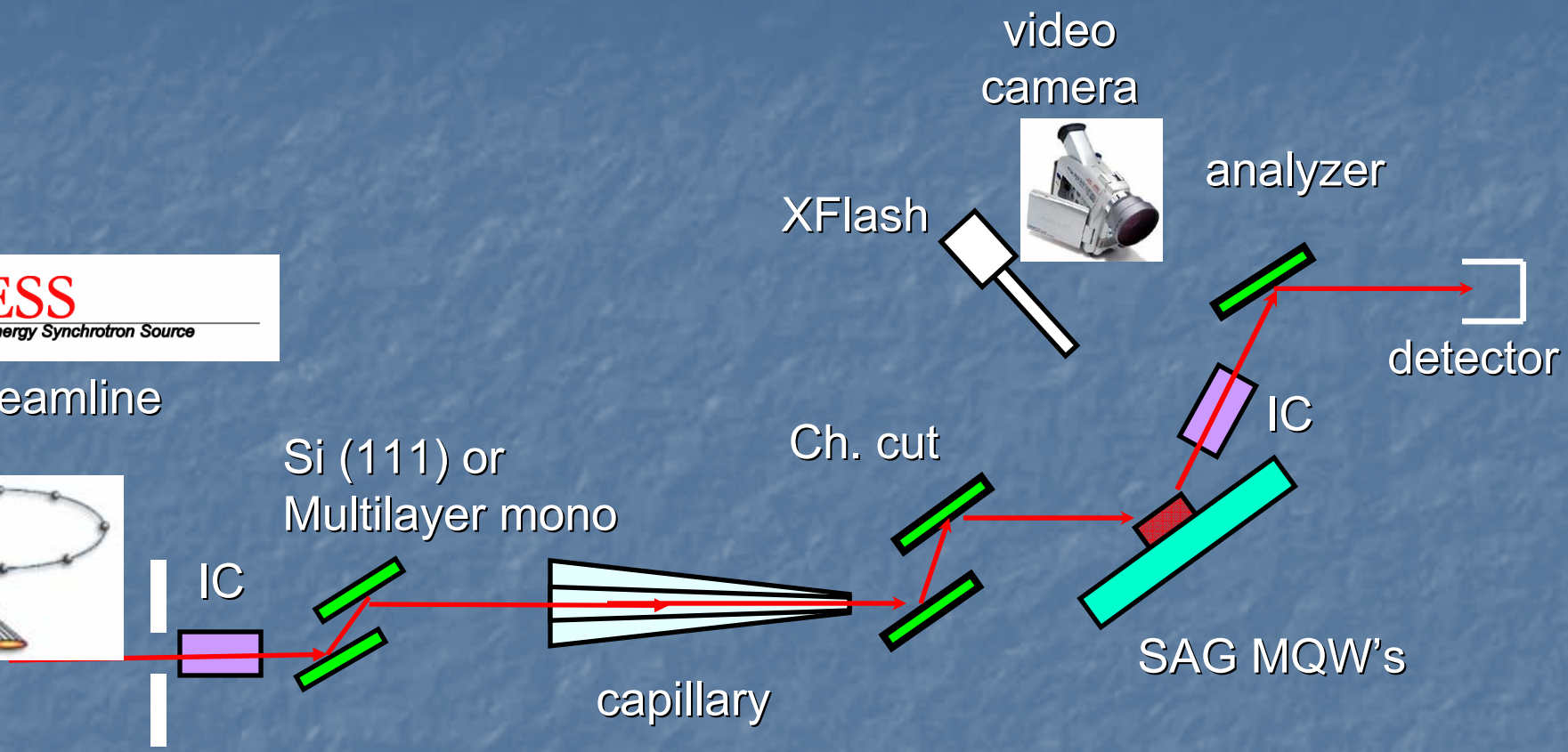

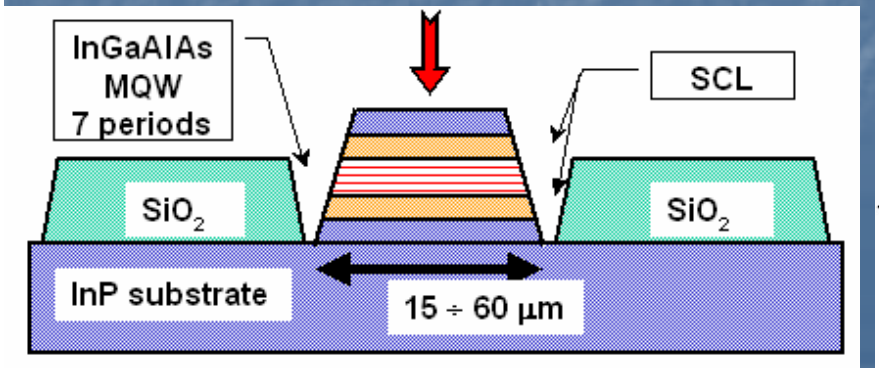

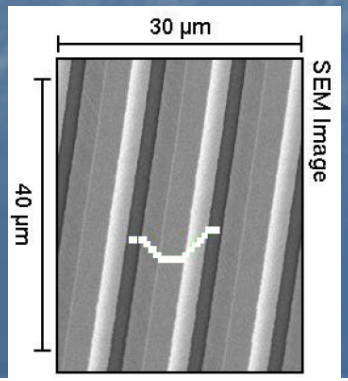

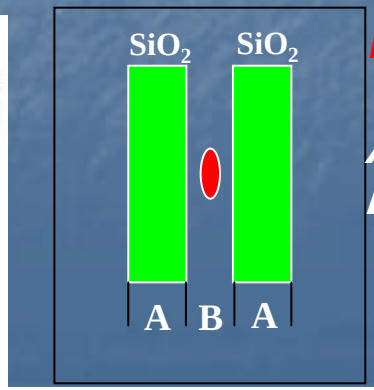

Beam: 10 µm

A = 15 ÷ 140 µm
B = 15 ÷ 60 µm

CHESS microbeam setup: RSM

strain relaxation in Selective Area Growth

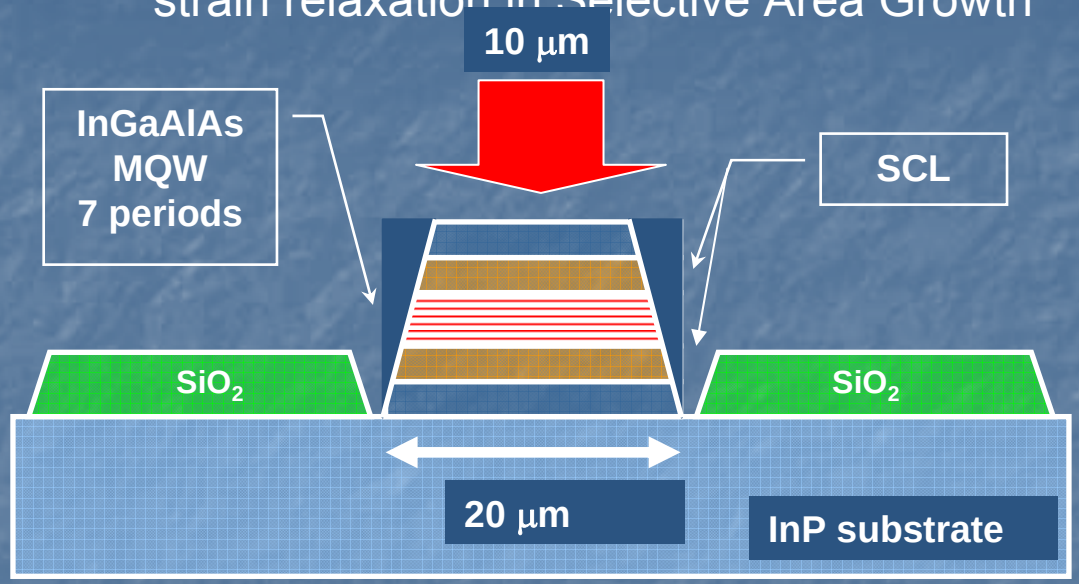

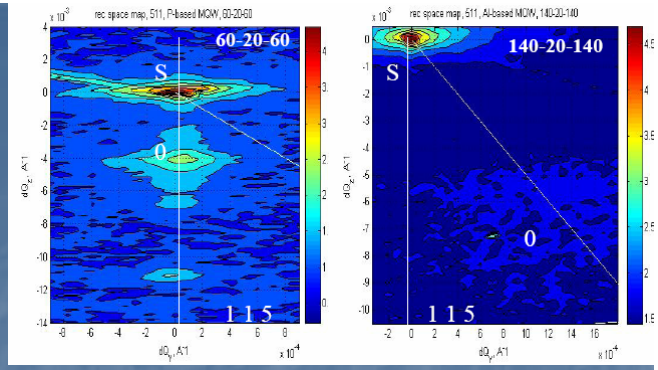

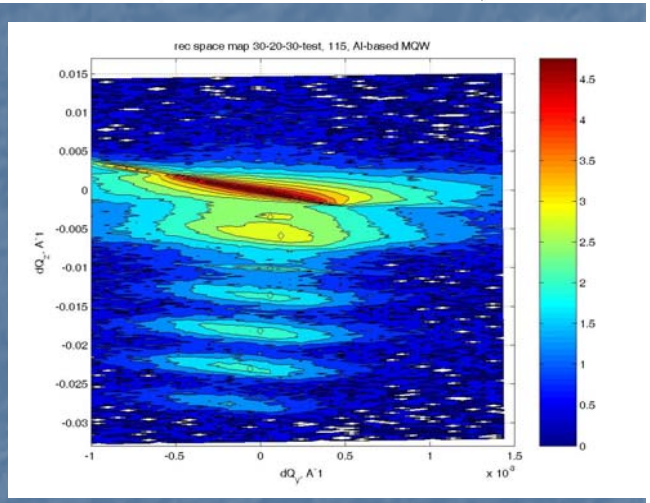

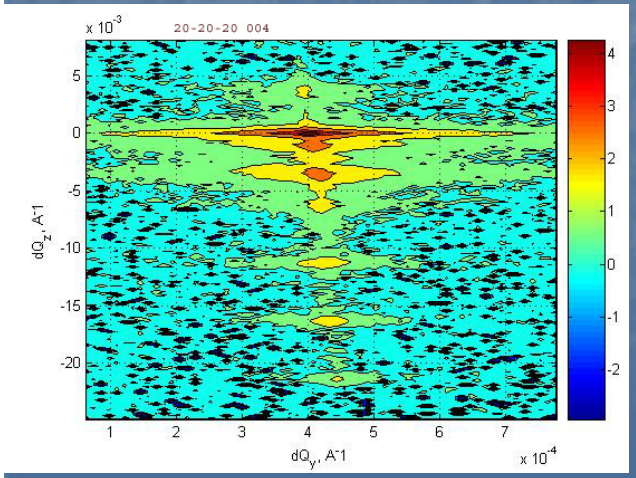

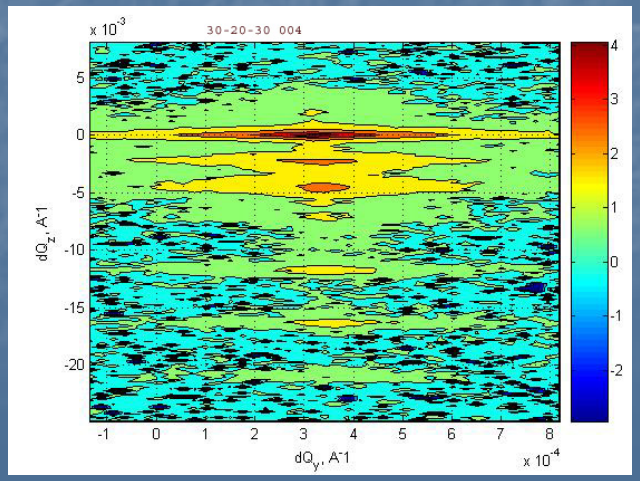

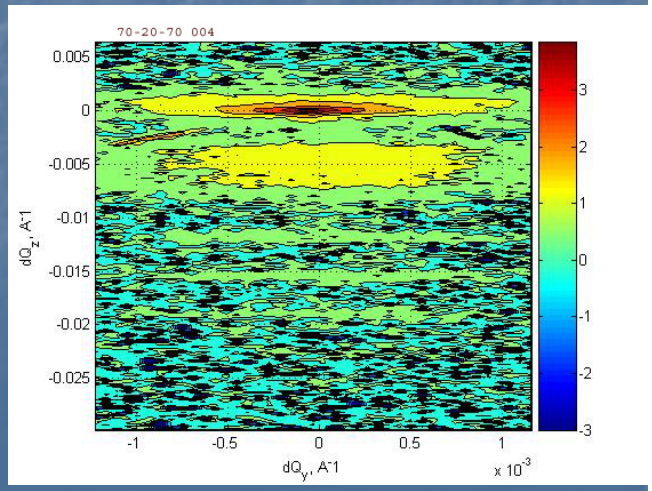

CHESS microbeam setup: HRXRD and RSM

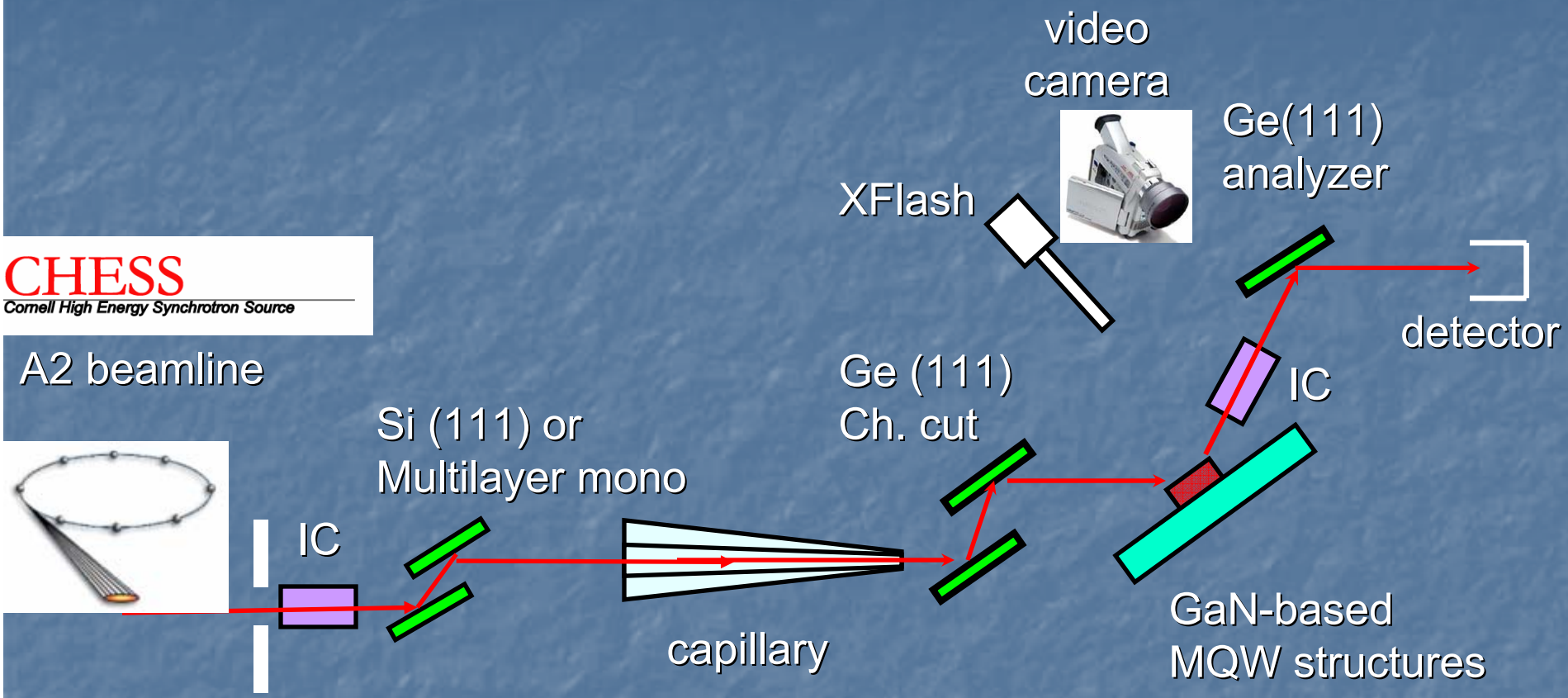

Experimental setup for the microbeam high resolution diffraction and RSM measurements at CHESS based on one-bounce imaging capillary with the working distance of ***30 mm*** *and the beam size at the focal spot of* ***10 μm****. Ge (1 1 1) channel cut crystal is embedded between the capillary optics and the investigated structures providing higher angular resolution of* ***13 arcsec****. Single-bounce Ge crystal analyzer provides high angular resolution in the detection arm.* ***Wavelength: 0.1 nm****.*

APS 2ID-D setup

- *Sirenko et al, APL **88** (2006)*
- *Kazimirov et al, J. Phys. D: Appl. Phys. **38** (2006)*

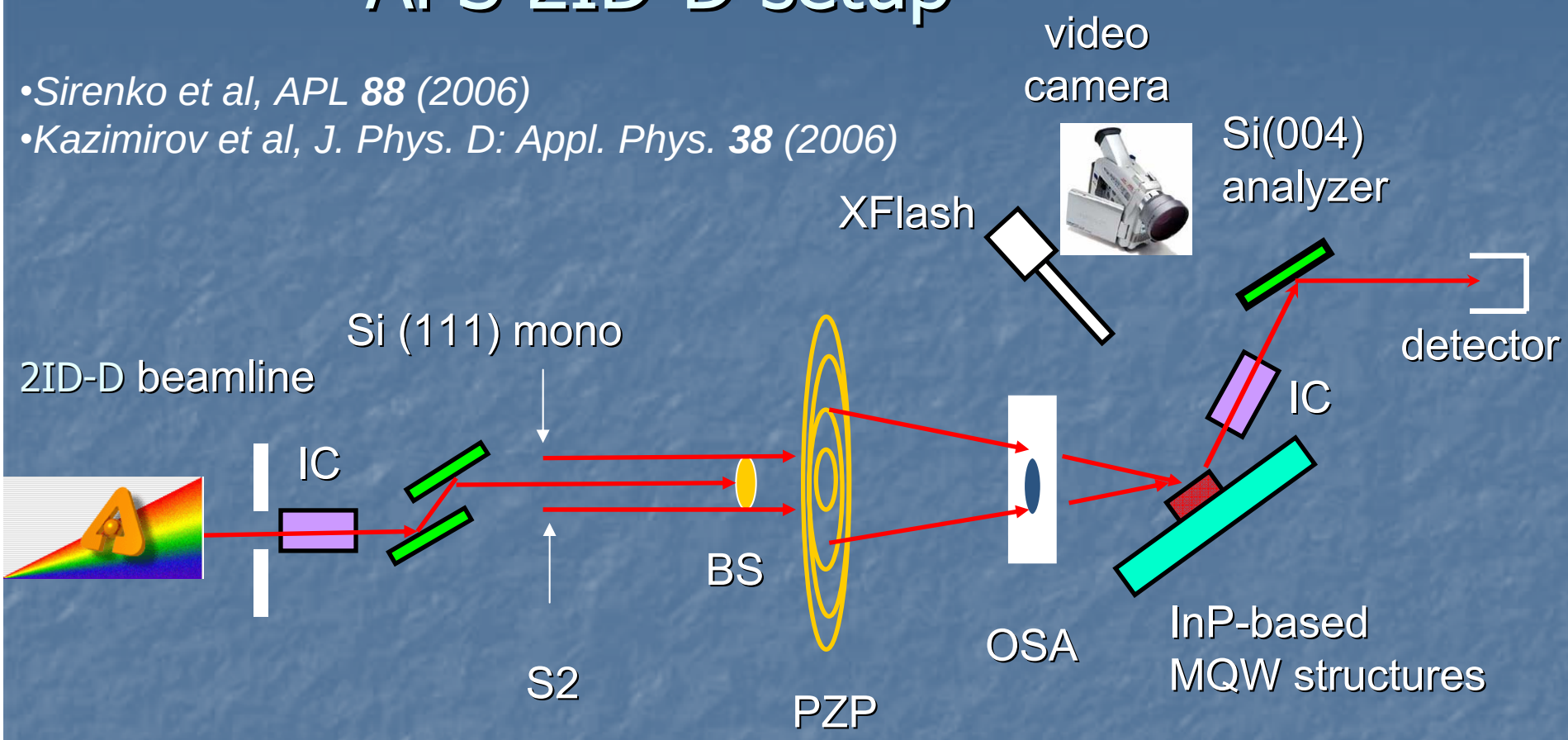

Zone plate: outer zone 0.12 μm; focal distance 149 mm

beam size: 0.35 μm (vert.) x 0.24 μm (hor.)

analyzer: Si(004) perfect crystal

angular resolution is determined by Si(004) rocking curve: 2.2 arc sec

$\Delta\theta/\Delta 2\theta$ scans: $\Delta 2\theta = 2\,\Delta\theta$

flux $\approx 7\cdot 10^6$ ph/sec

Samples: multiple quantum well waveguides grown by MOCVD selective area growth technique

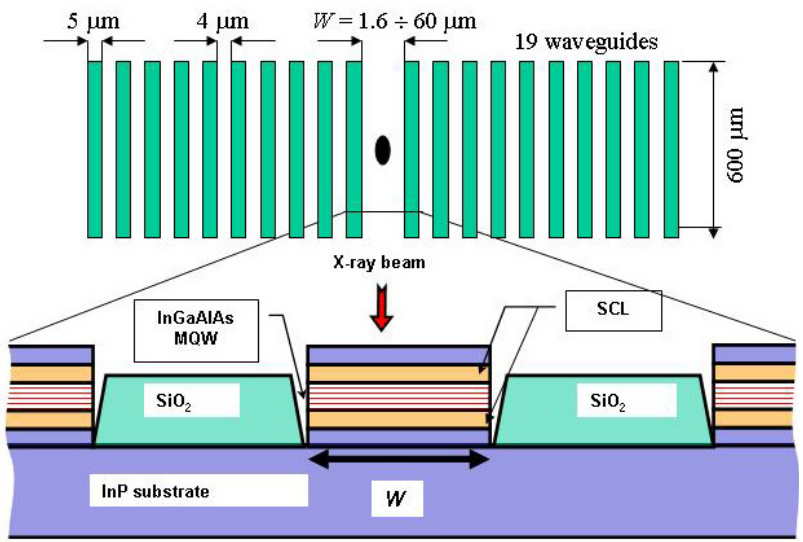

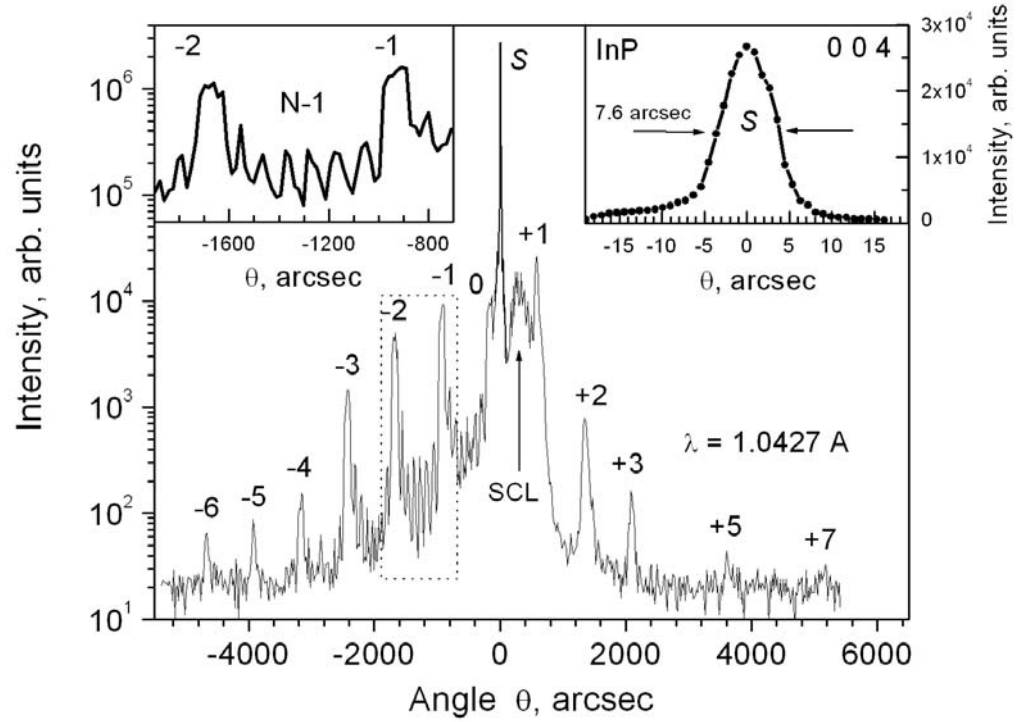

InGaAsP
InGaAlAs
} identical masks

TABLE I. Parameters of the investigated samples.

	$In_xGa_yAl_{1-x-y}As$		$In_xGa_{1-x}As_yP_{1-y}$	
	Open wafer	Ridge	Open wafer	Ridge
Well width (nm)	5.0	6.5	7.0	8.9
Barrier width (nm)	10.3	12.9	9.9	13.2
Global strain (%)	0.22	1.15	0.49	0.75
Well composition	$x=0.65$		$x=0.85$	
	$y=0.19$		$y=0.57$	
Barrier composition	$x=0.48$		$x=0.87$	
	$y=0.19$		$y=0.29$	

goal:

determine MQW composition and thickness variations:

1) across the ridge
2) as a function of ridge width (mask geometry)

Comparison of P-based and Al- based structures

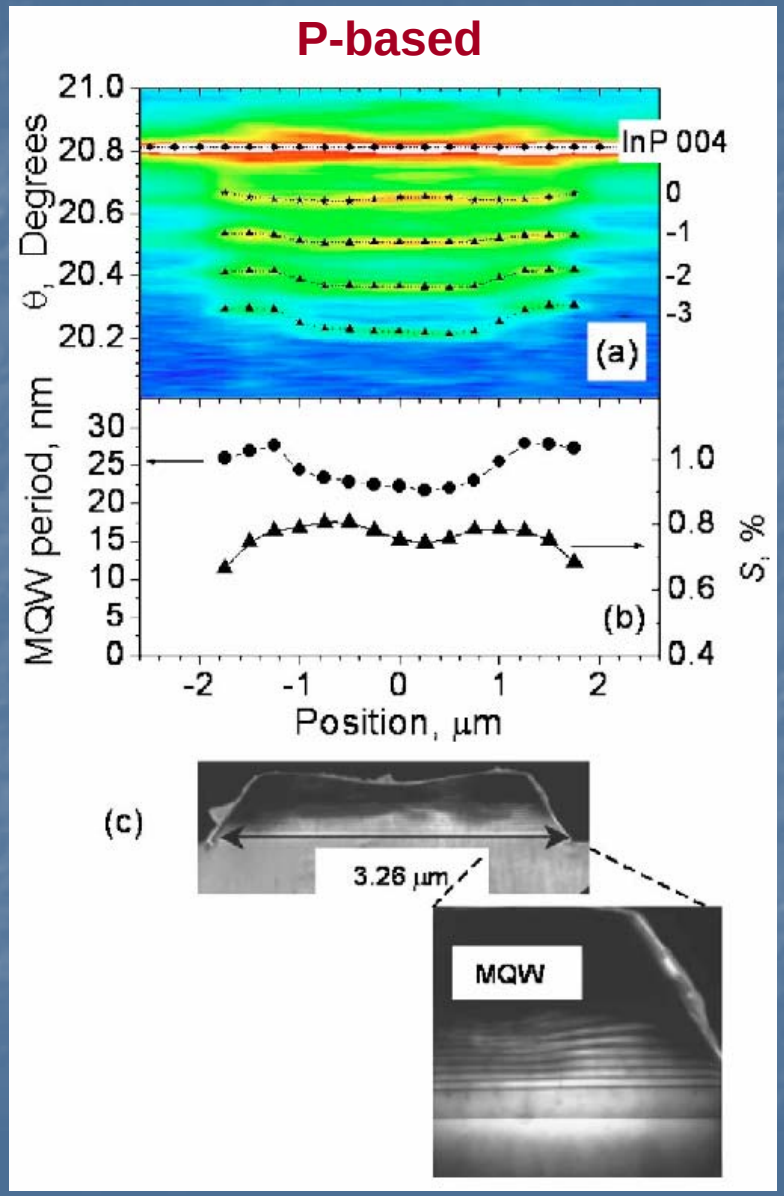

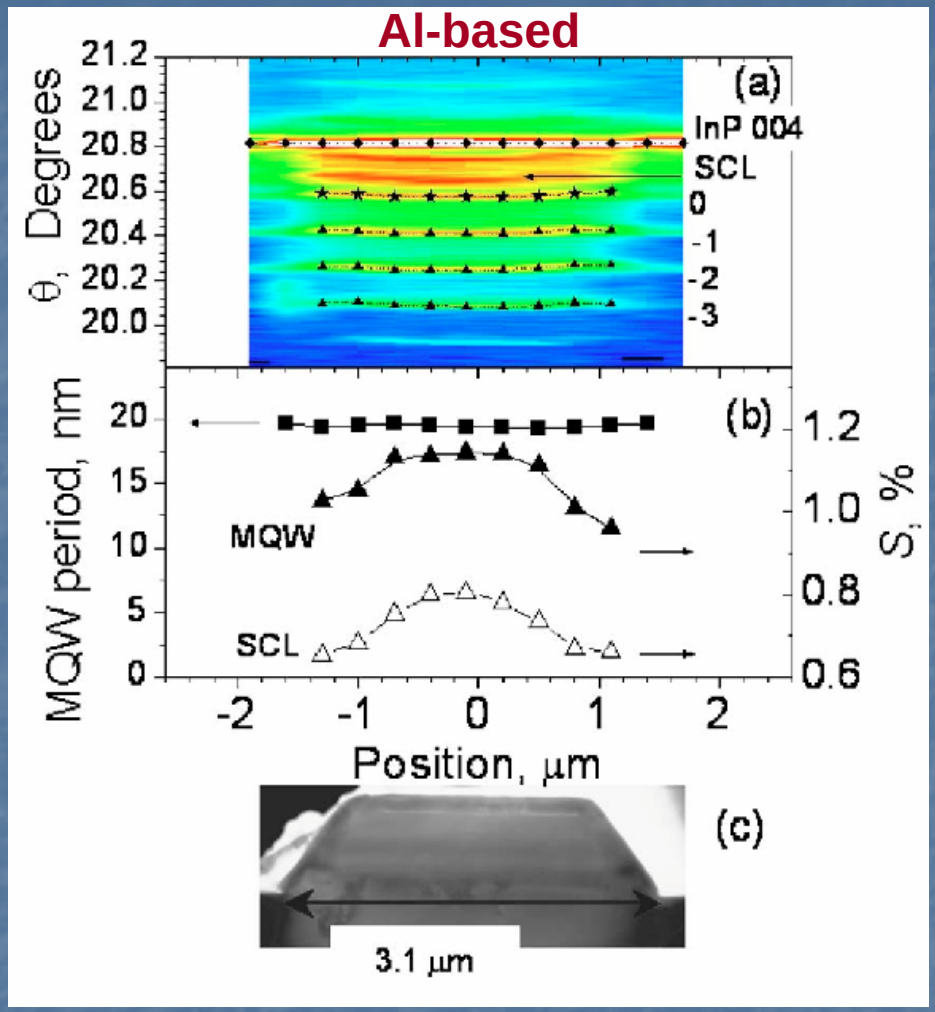

conclusion:

Al-based SAG MQW is superior in uniformity compared to traditional P-based devices

Conclusions
for submicrobeam studies of InP-based SAG

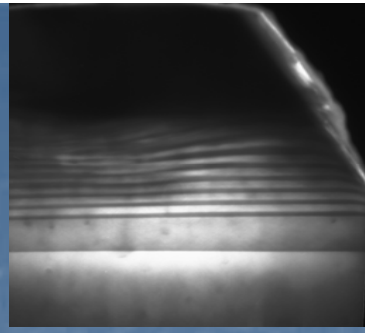

- microbeam diffraction with arc sec angular resolution and lateral 0.24 μm resolution has been demonstrated by using a combination of phase zone plate and perfect analyzer crystal
- post-focusing perfect crystal optics is an efficient way to condition microbeam for a variety of high angular resolution microbeam diffraction applications
- this setup has been applied to study compositional and thickness variations in multiple quantum well waveguides grown by MOCVD in selective area growth regime
- Al-based SAG MQW is much more superior in uniformity compared to traditional P-based devices which is promising for development of one-growth-step SAG technology

MQW 0th peak

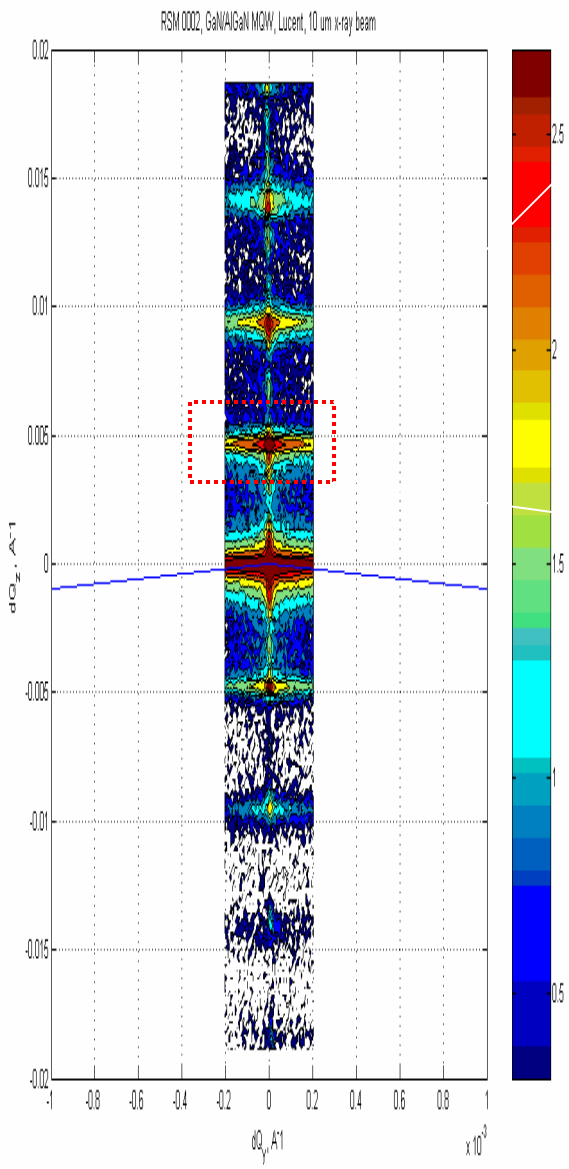
RSM 0002, GaN/AlGaN MQW, Lucent, 10 um x-ray beam
dQz, A^-1
dQy, A^-1
x 10^-3

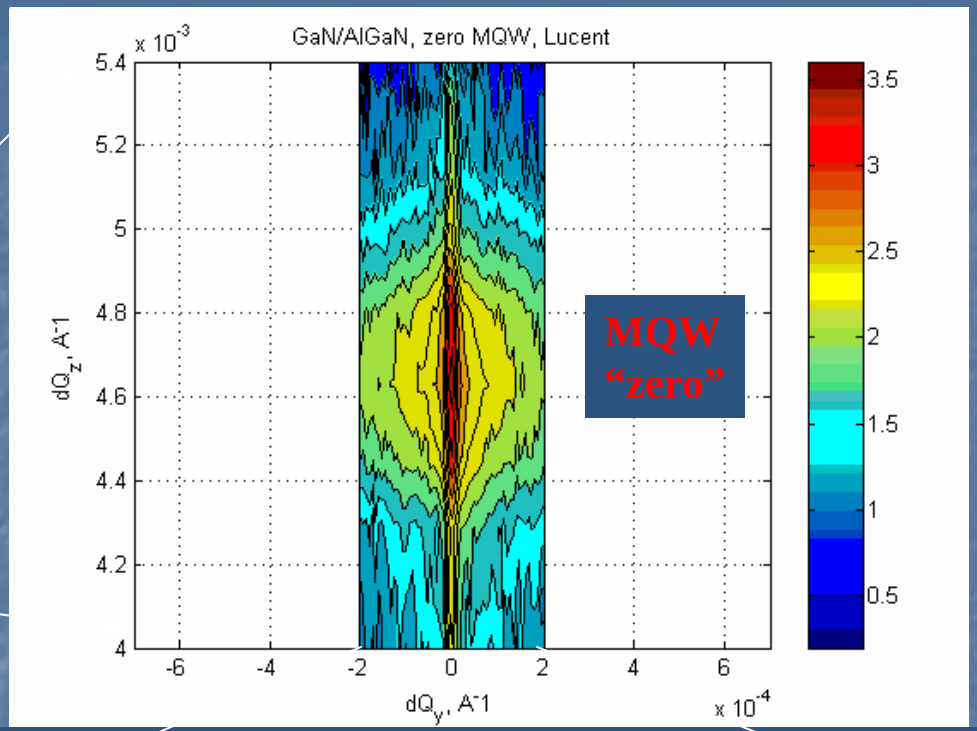
GaN/AlGaN, zero MQW, Lucent
x 10^-3
dQz, A^-1
dQy, A^-1
x 10^-4
MQW
"zero"

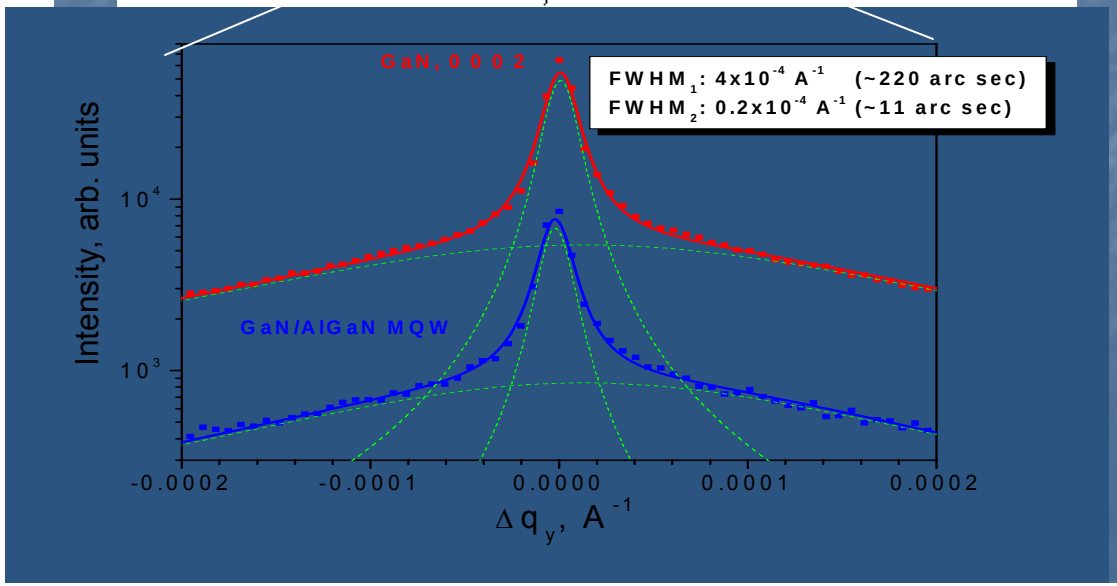
GaN, 0 0 0 2
FWHM1: 4x10^-4 A^-1 (~220 arc sec)
FWHM2: 0.2x10^-4 A^-1 (~11 arc sec)
GaN/AlGaN MQW
Intensity, arb. units
Δq_y, A^-1

GaN/InGaN MQW SAG structures

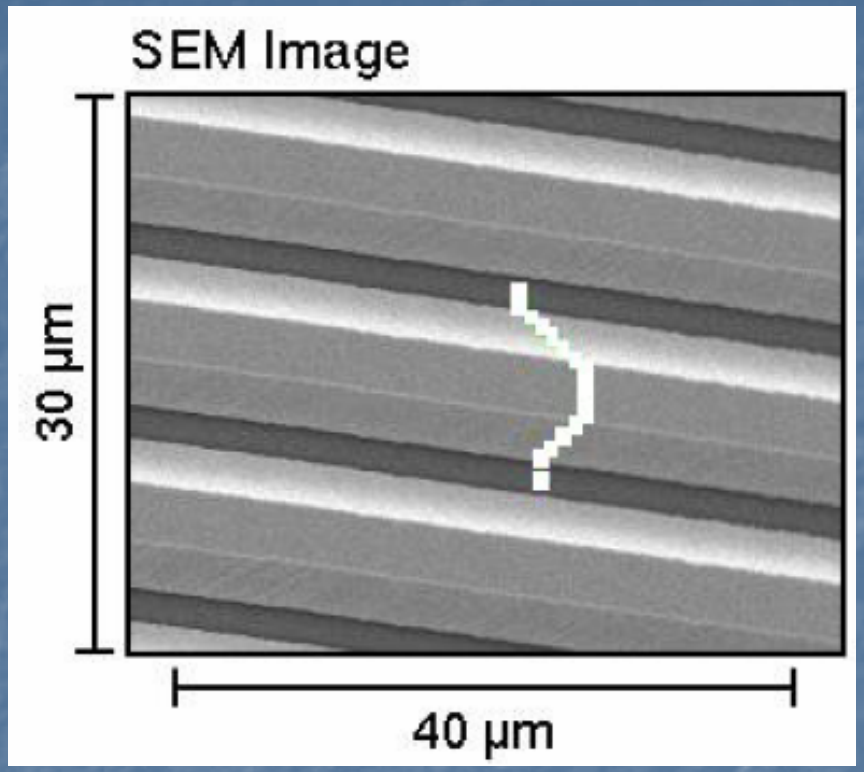

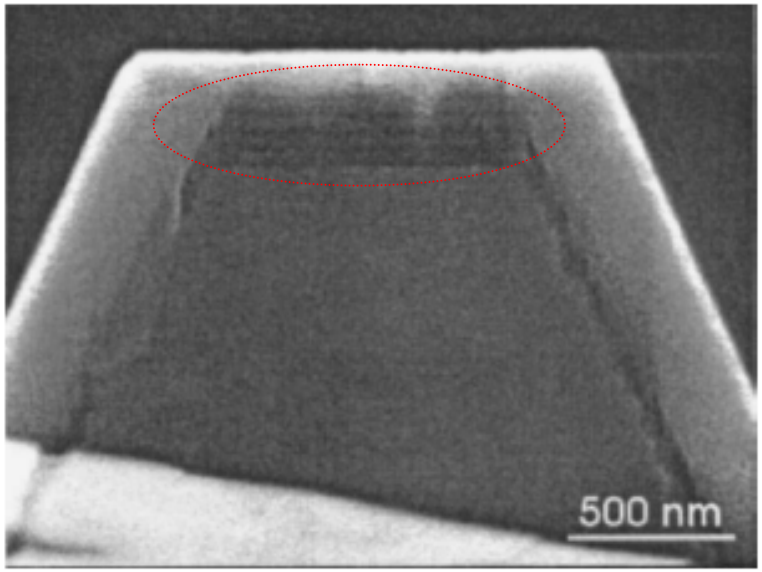

FIG. 3. SEM photograph of a stripe in $\langle 1\bar{1}00 \rangle$ direction with trapezoidal cross section. The Mg-doped GaN cover layer results in a brighter SEM contrast. The five QWs are resolved only on the top facet.

APPLIED PHYSICS LETTERS **87**, 182111 (2005)

GaInN quantum wells grown on facets of selectively grown GaN stripes

Barbara Neubert,[a] Peter Brückner, Frank Habel,[b] and Ferdinand Scholz
Optoelectronics Department, University of Ulm, 89081 Ulm, Germany

Till Riemann and Jürgen Christen
Otto-von-Guericke-University of Magdeburg, 39106 Magdeburg, Germany

Martin Beer and Joseph Zweck
University of Regensburg, 93040 Regensburg, Germany

Positioning of the SAG structures in the X-ray beam

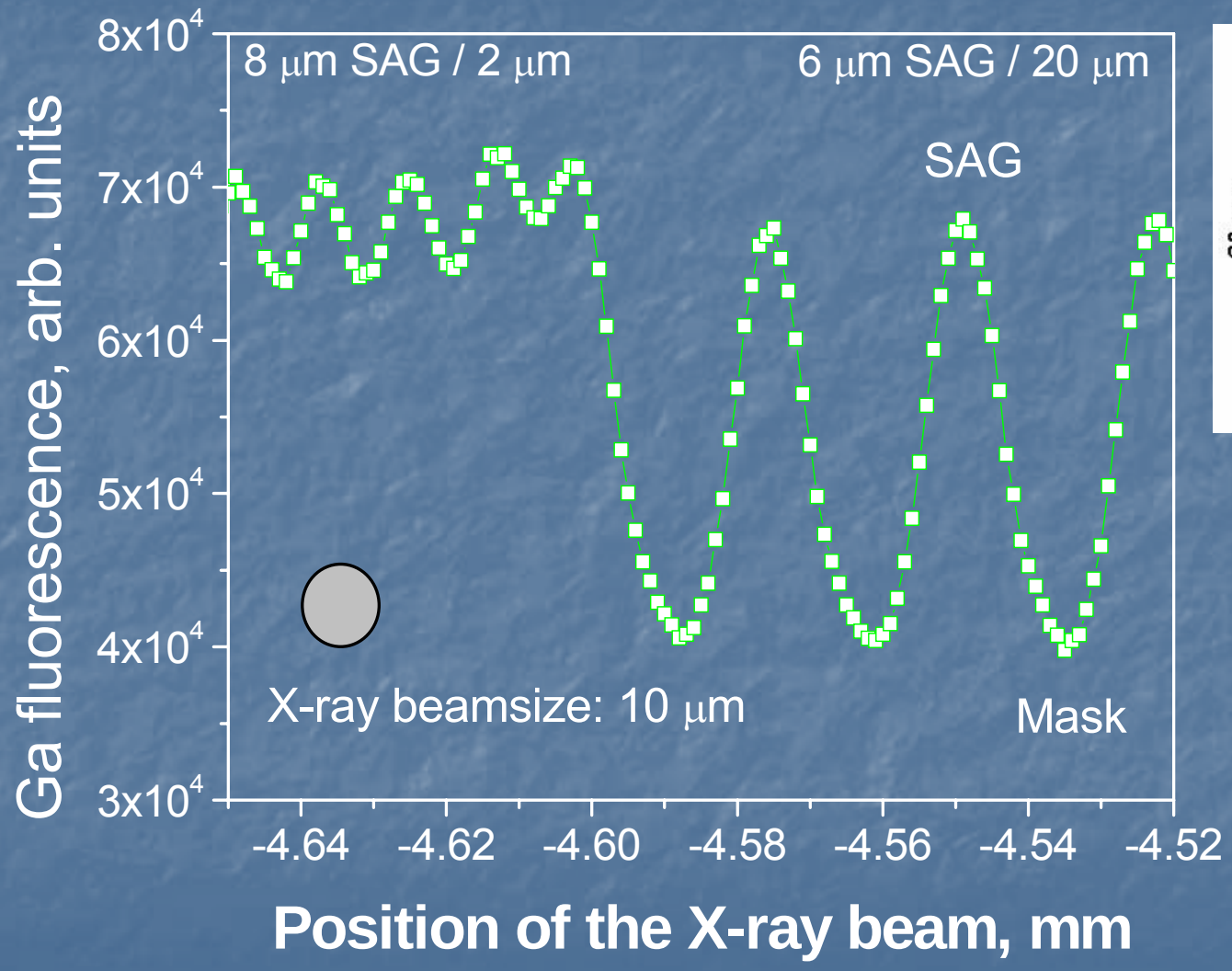

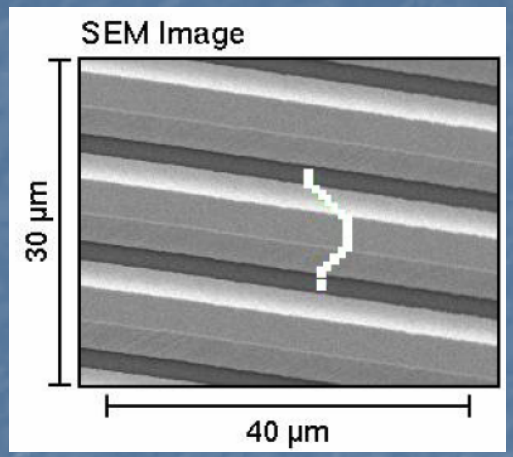

HRXRD in InGaN/GaN MQW SAG structures

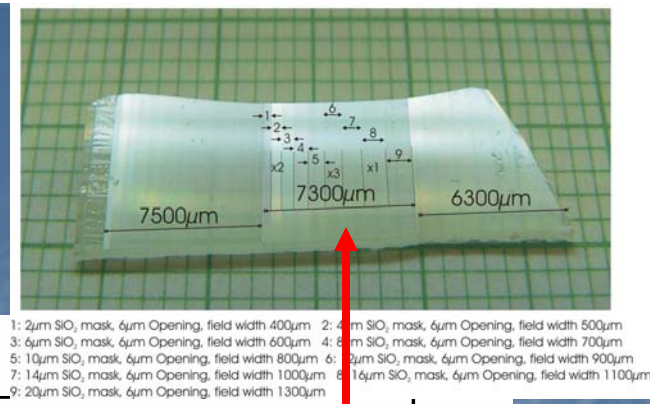

1: 2μm SiO_2 mask, 6μm Opening, field width 400μm 2: 4μm SiO_2 mask, 6μm Opening, field width 500μm
3: 6μm SiO_2 mask, 6μm Opening, field width 600μm 4: 8μm SiO_2 mask, 6μm Opening, field width 700μm
5: 10μm SiO_2 mask, 6μm Opening, field width 800μm 6: 12μm SiO_2 mask, 6μm Opening, field width 900μm
7: 14μm SiO_2 mask, 6μm Opening, field width 1000μm 8: 16μm SiO_2 mask, 6μm Opening, field width 1100μm
9: 20μm SiO_2 mask, 6μm Opening, field width 1300μm

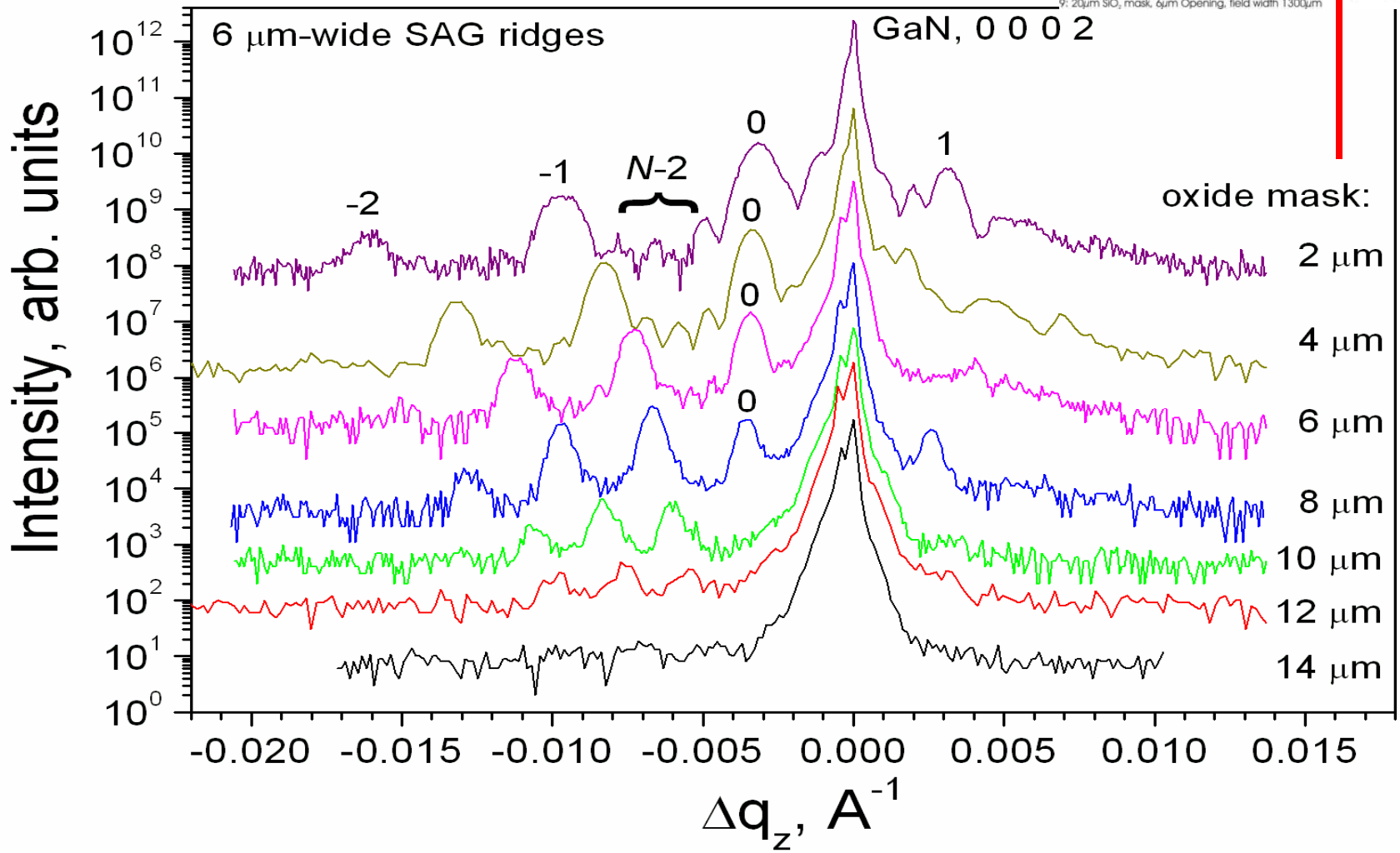

Simulations using RadsMercury BEDE dynamic diffraction model

	d	Low	High	Material	X	Low	High
17	1524	1000	5000	Ga(x)In(1-x)N [hexagonal]	0.9965	0.985	1
16	1269.36	1000	5000	Ga(x)In(1-x)N [hexagonal]	0.9986	0.985	1
15	3672.72	1000	5000	Ga(x)In(1-x)N [hexagonal]	0.9980	0.985	1
14	2708.83	1000	5000	Ga(x)In(1-x)N [hexagonal]	0.9897	0.985	1
13	2270.44	1000	5000	Ga(x)In(1-x)N [hexagonal]	1.0000	1	1
12	229.83	100	300	Al(x)Ga(1-x)N [hexagonal]	0.2228	0.21	0.23
11	125	125	125	GaN [hexagonal]	0.0000	0	0
...10	80.41	77	82	Ga(x)In(1-x)N [hexagonal]	0.8723	0.85	0.89
1...	121.17	119	125	GaN [hexagonal]	0.0000	0	0
Sub.	∞	∞	∞	GaN [hexagonal]	0	0	0

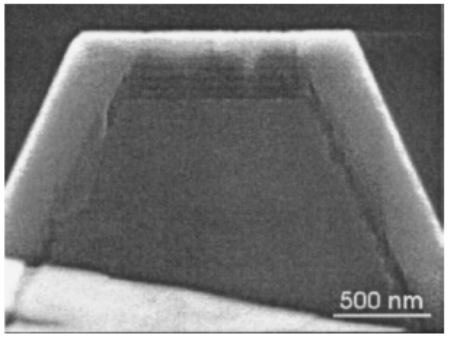

FIG. 3. SEM photograph of a stripe in ⟨1$\bar{1}$00⟩ direction with trapezoidal cross section. The Mg-doped GaN cover layer results in a brighter SEM contrast. The five QWs are resolved only on the top facet.

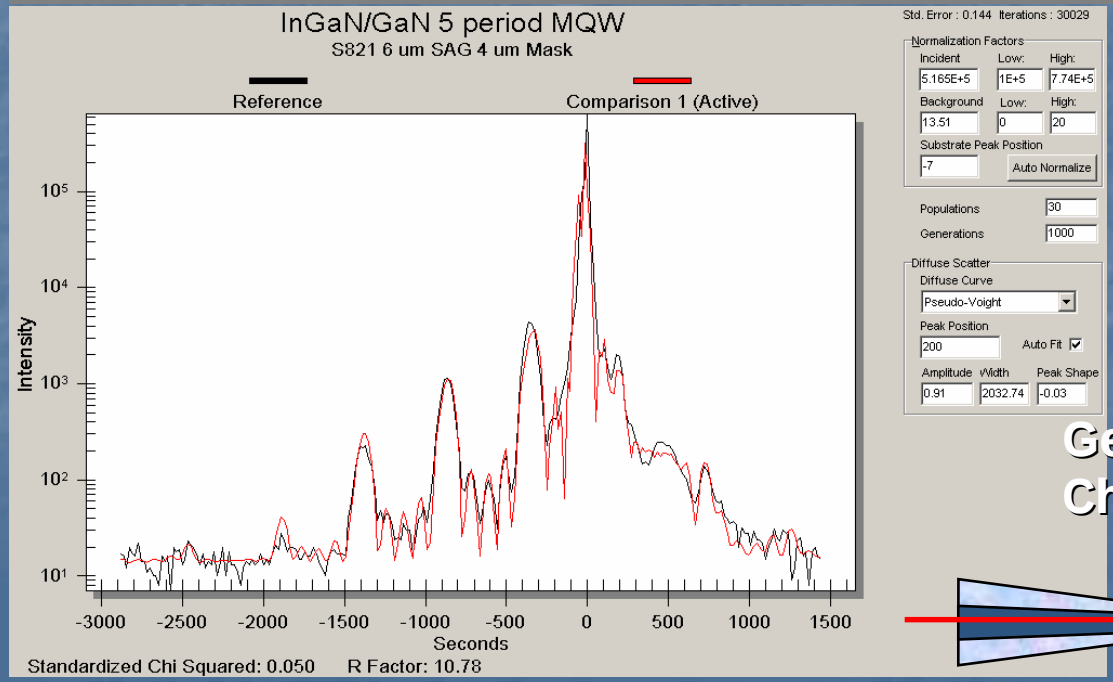

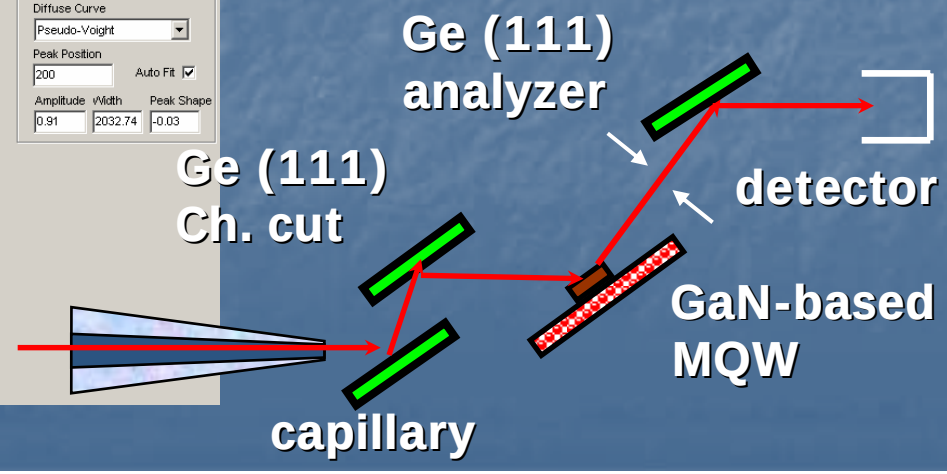

Simulations using RadsMercury BEDE dynamic diffraction model

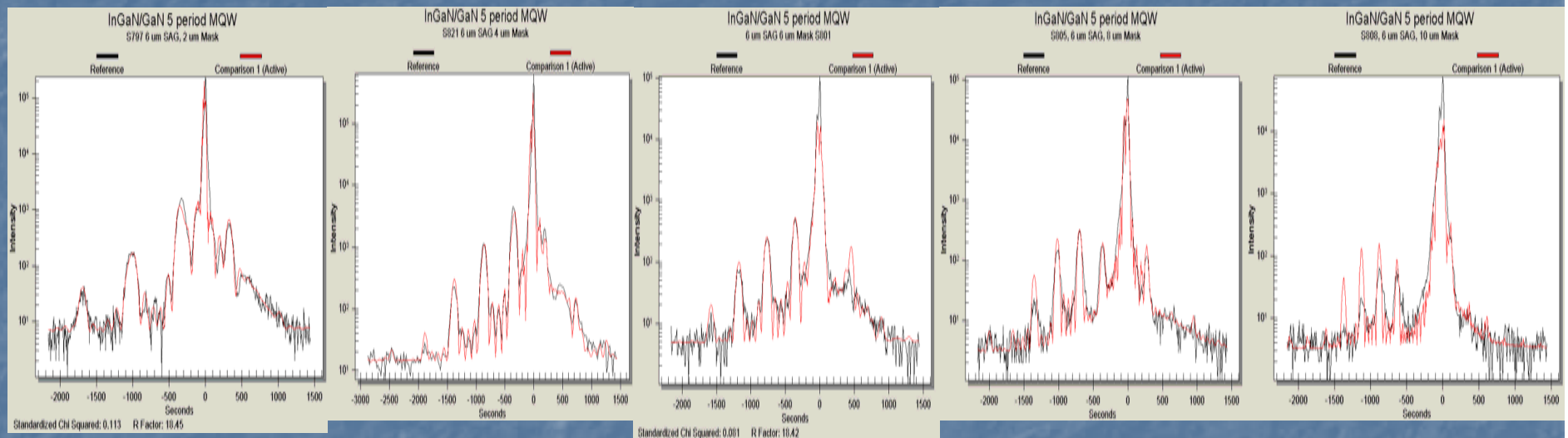

SAG: 6 μm

Mask: 2 μm

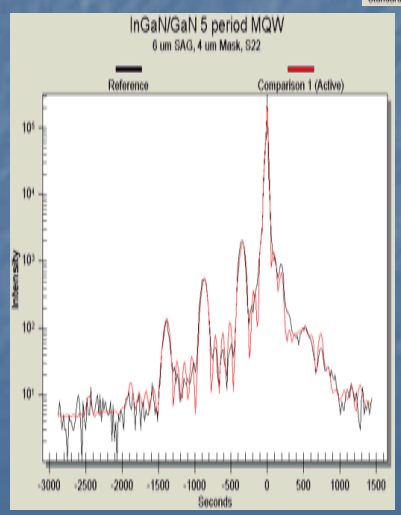

6 μm

8 μm

10 μm

Parameters of InGaN/GaN MQW structures

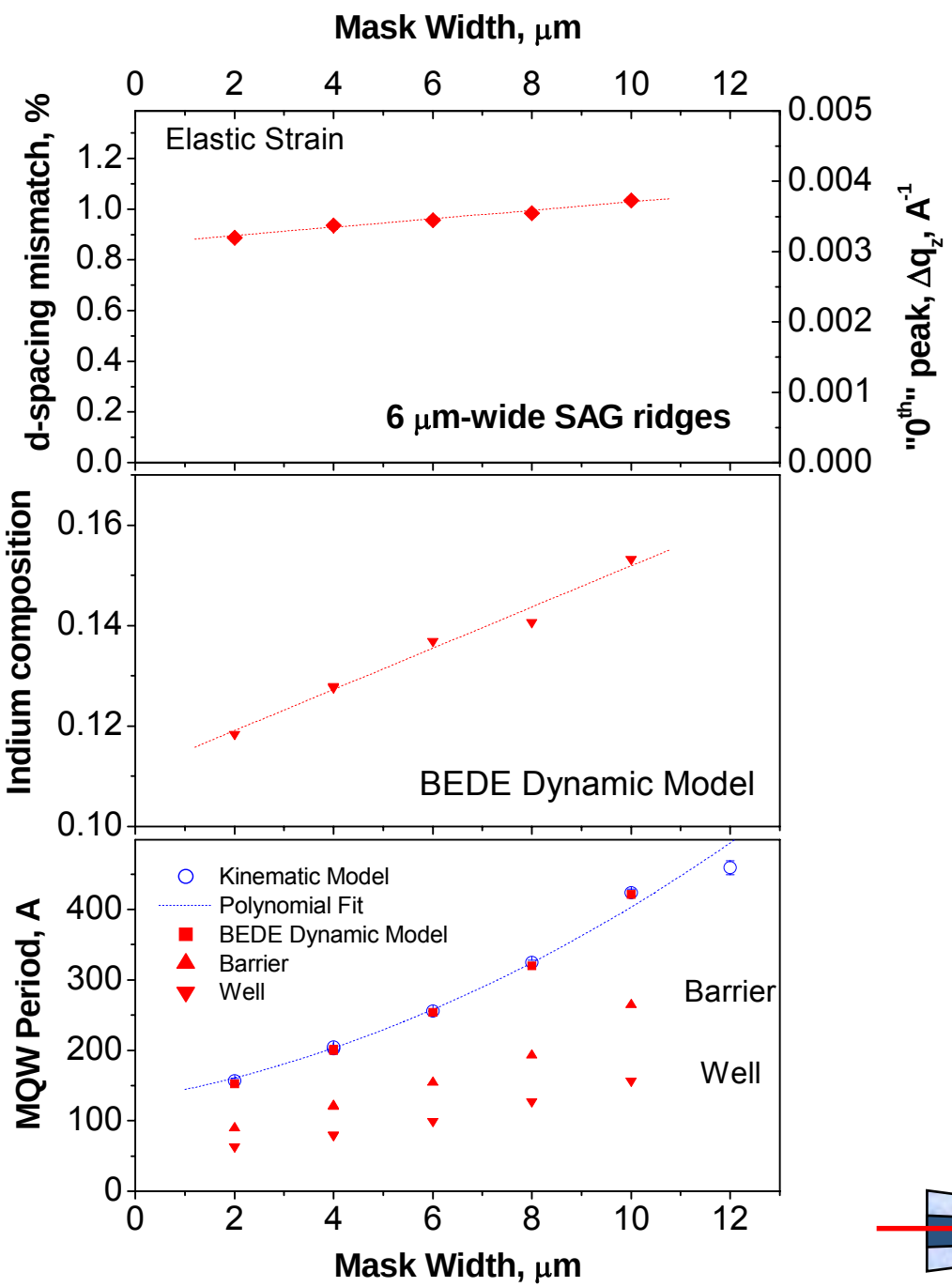

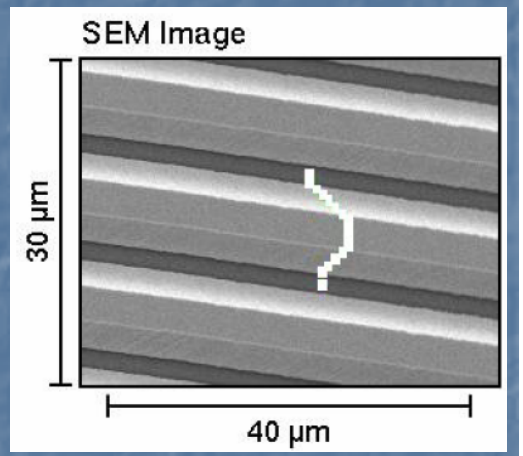

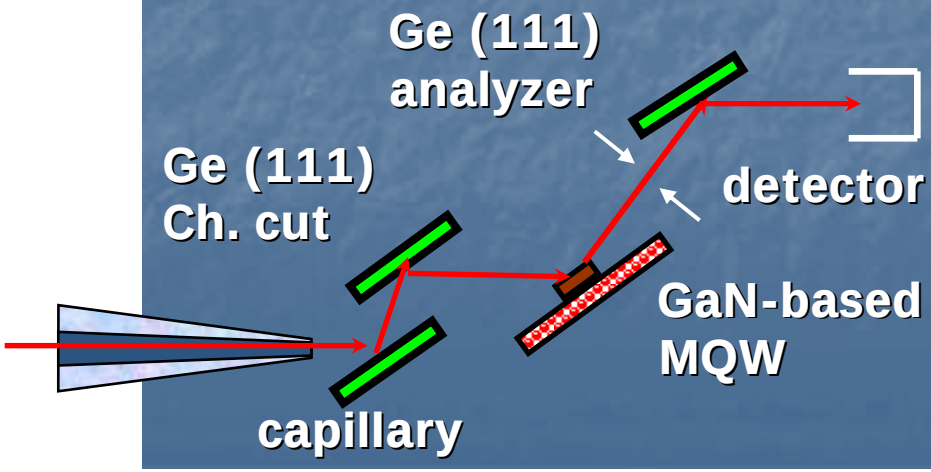

Reciprocal Space Map of GaN @CHESS

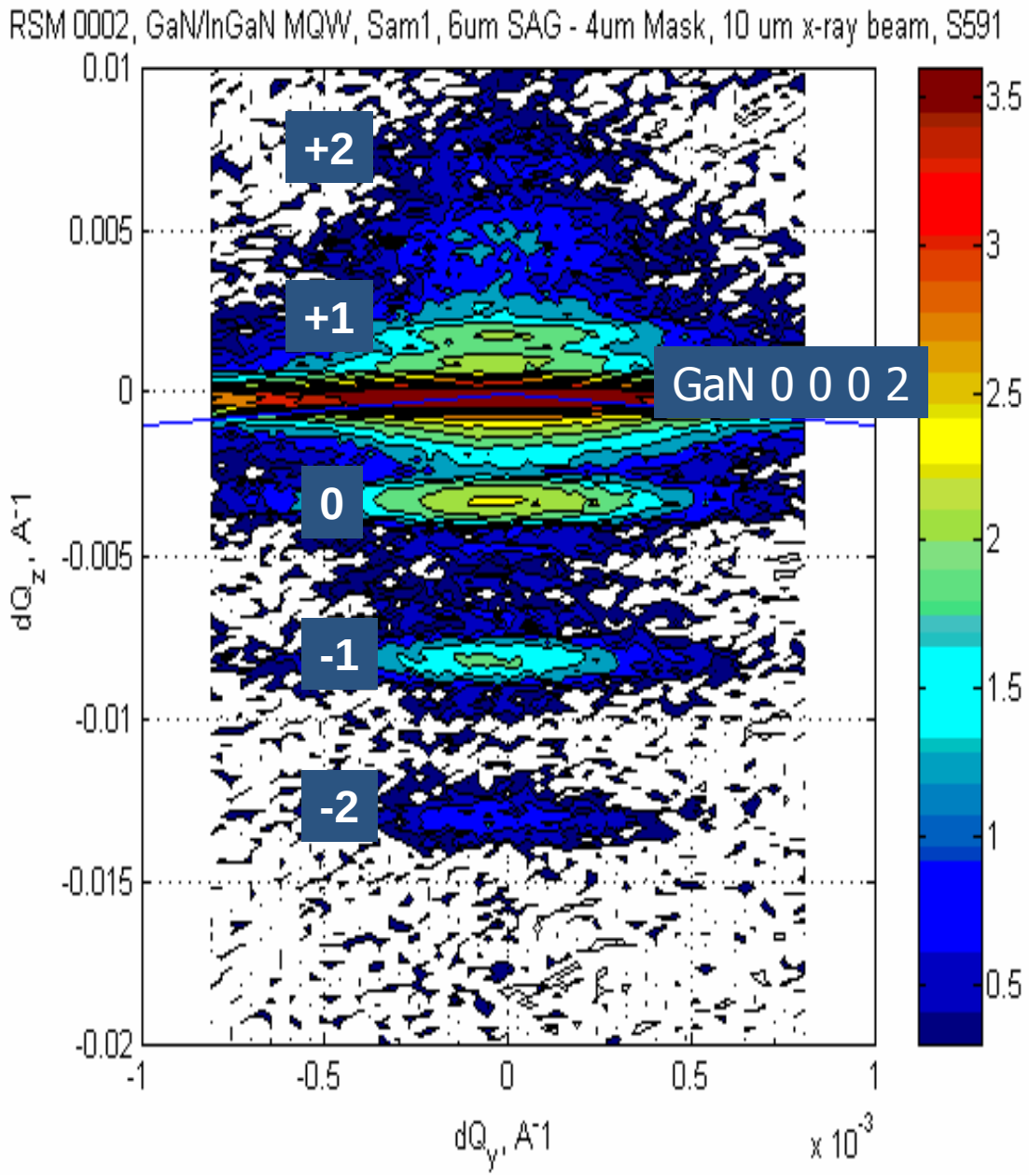

Total time for these measurements: 15 hours

SAG: 6 μm
Mask: 4 μm

MQW:
Period 20 nm,
Strain: 0.9 %

Reciprocal Space Maps 0 0 0 2 reflection of GaN @CHESS

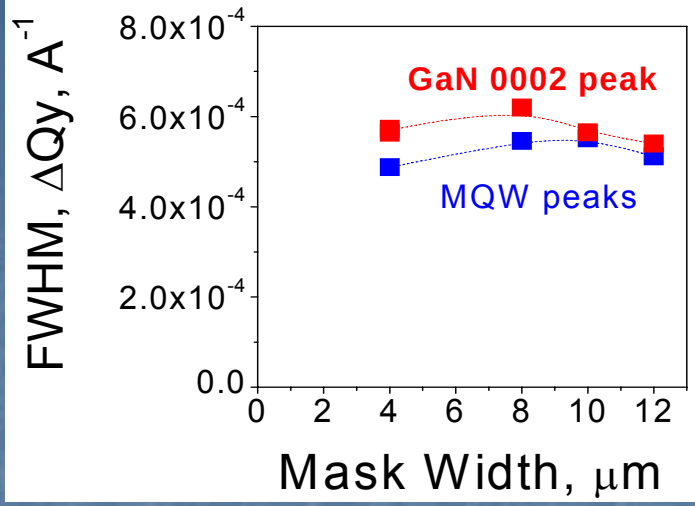

SAG: 6 μm

Mask: 4 μm 8 μm 10 μm 12 μm

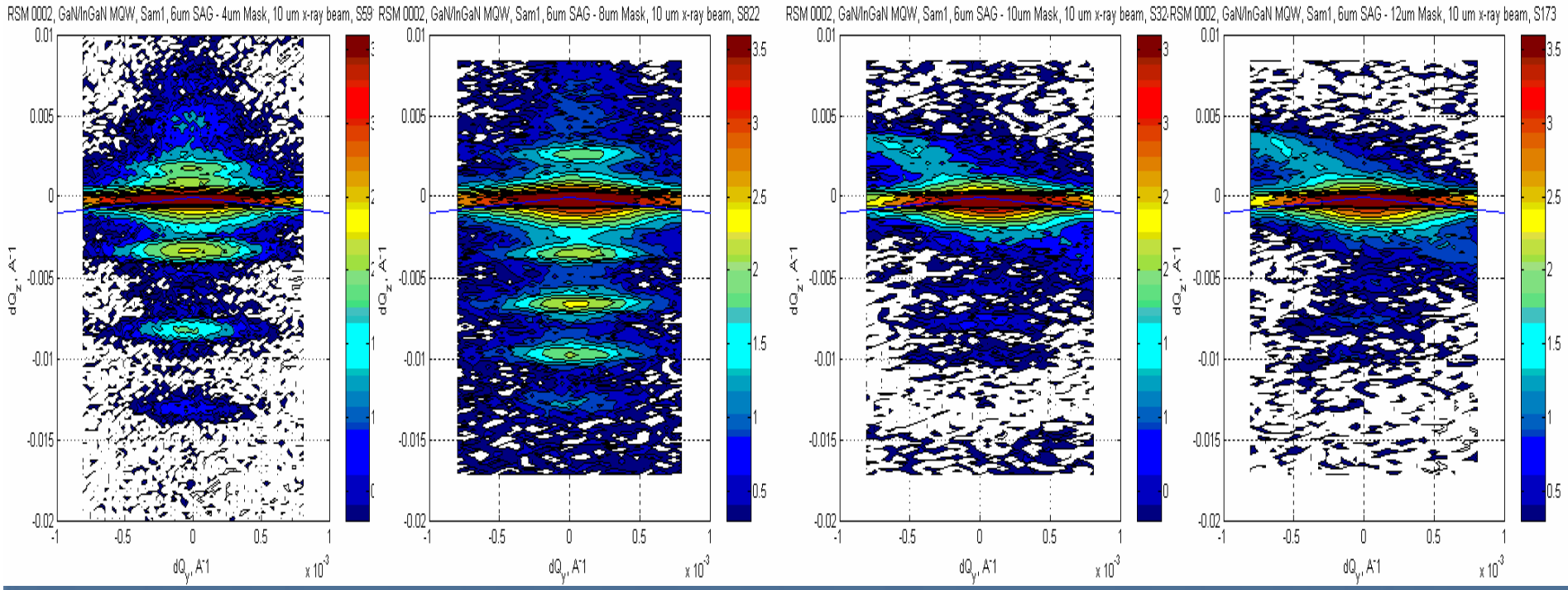

Total time for this project: 7 days

Conclusions for microbeam studies of GaN-based SAG structures

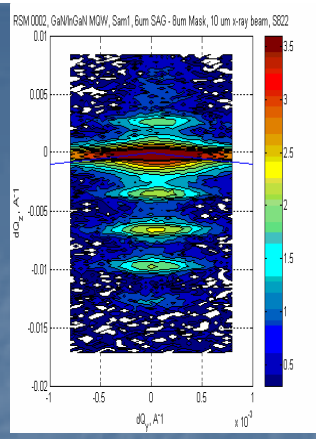

- Micro-beam HRXRD setup developed for RSM studies of nitride-based MQW's
- Accurately measured global strain and the thickness in the SAG structures
- Well/barrier thicknesses are determined from the fit using RadsMercury simulation software
- Mosaic structure in MQW is the same as that for the GaN substrate layer

Nondestructive approach to investigate Zn incorporation in InP using X-ray Standing Wave Technique (XSW)

Andrei Sirenko, Abdallah Ougazzaden, and **Alexander Kazimirov**

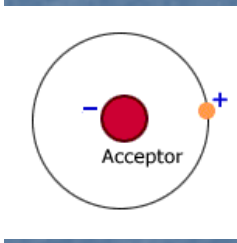

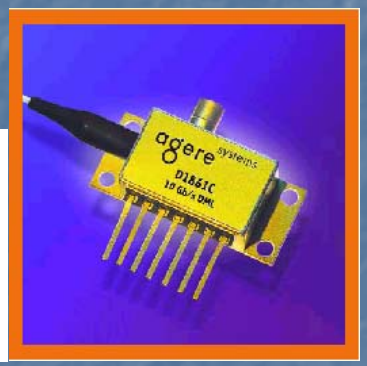

$$Zn^{(i)+} + V_{In}^{-} \rightarrow Zn^{(s)-} + 2h$$

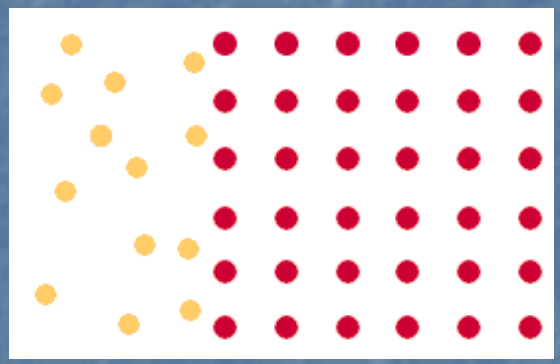

interstitial diffusion

Nondestructive XSW
"Ångstrøm ruler"

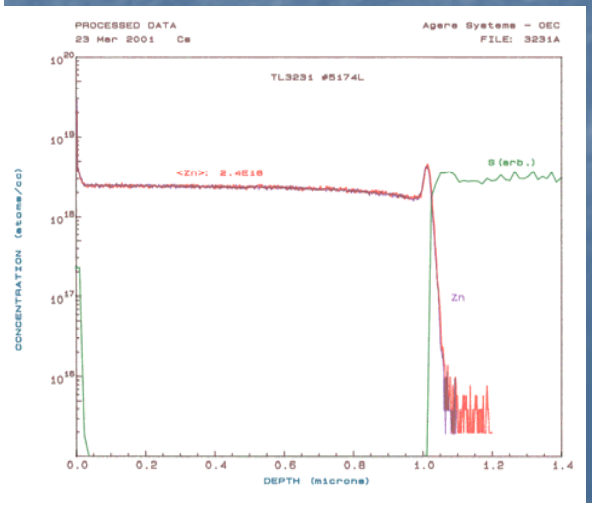

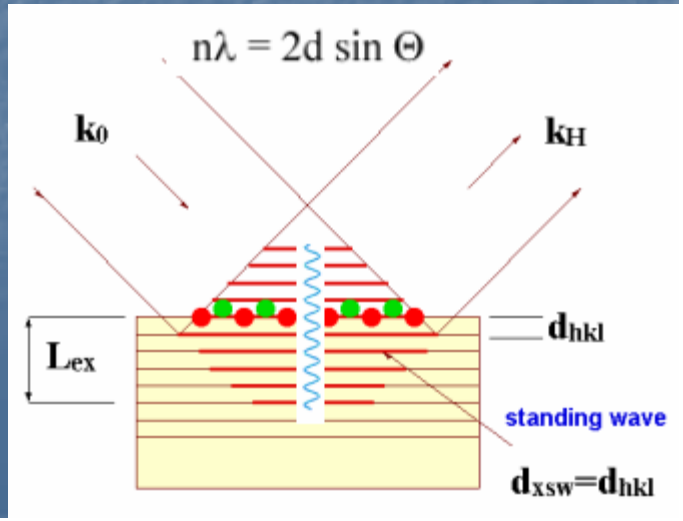

XSW measurements at A2 beamline at CHESS

A2

10 KeV

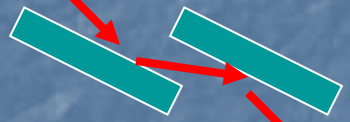

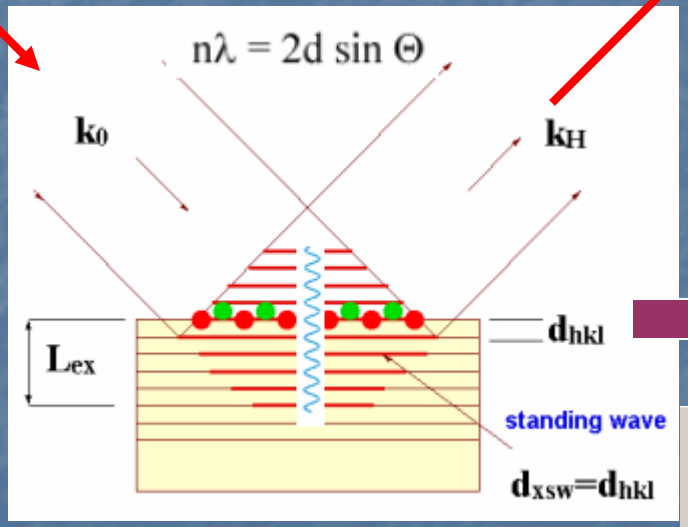

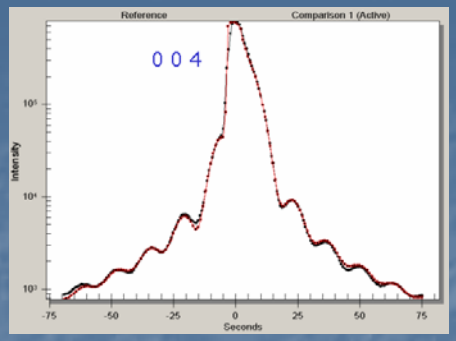

IC

Diffraction Intensity

Fluorescence

XFlash

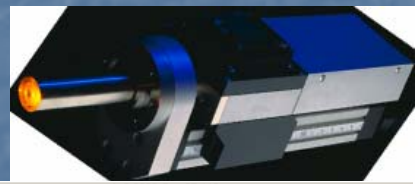

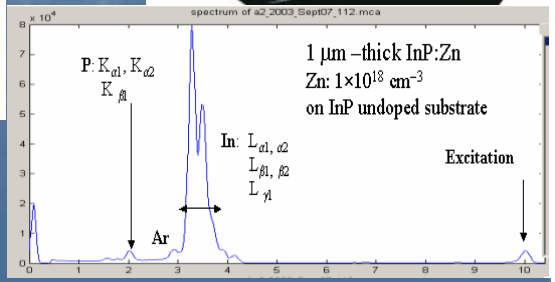

XSW for 0 0 4 reflection; range: 0.02º; 81 points

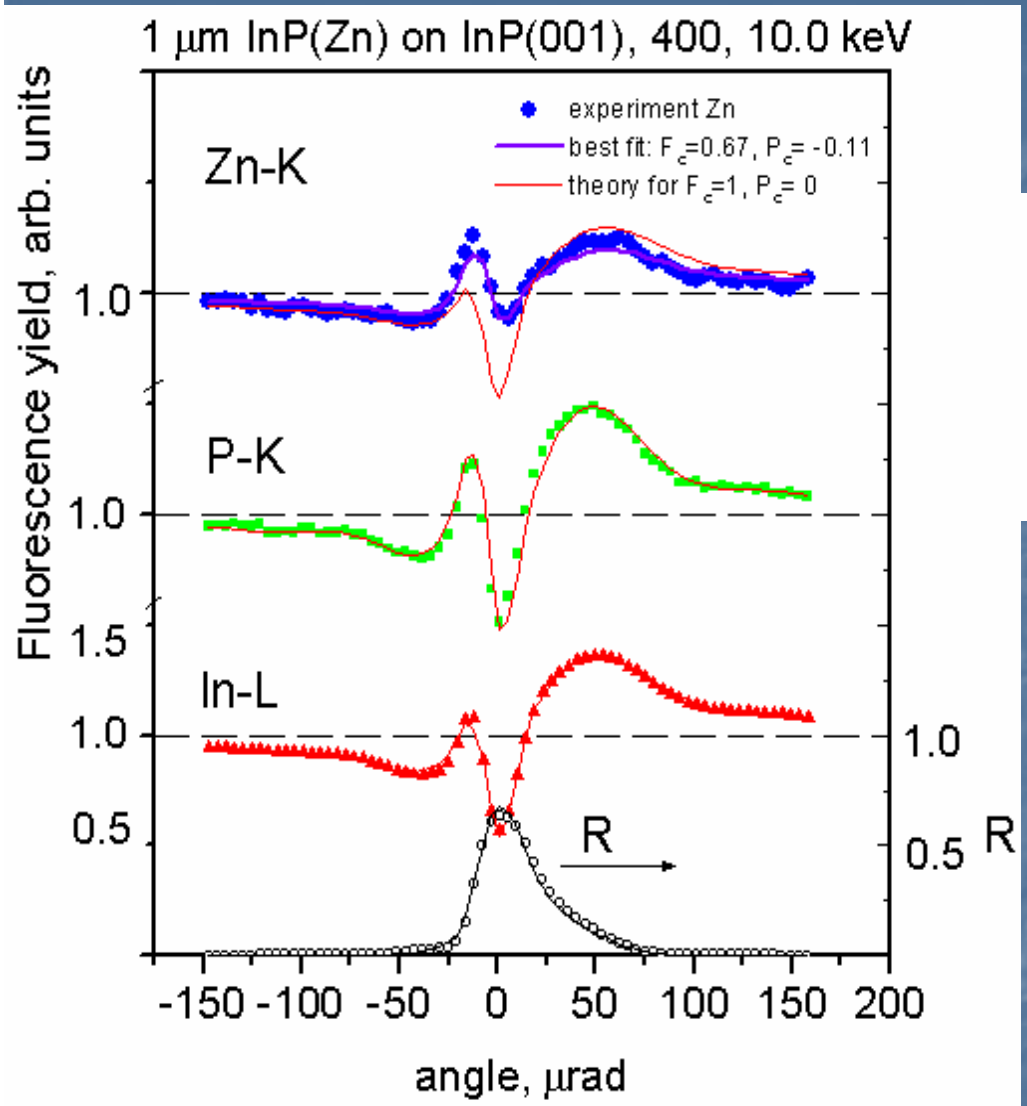

$$P_c = 0.11 \cdot d_{hkl} = 0.11 \cdot a_{InP}/4$$

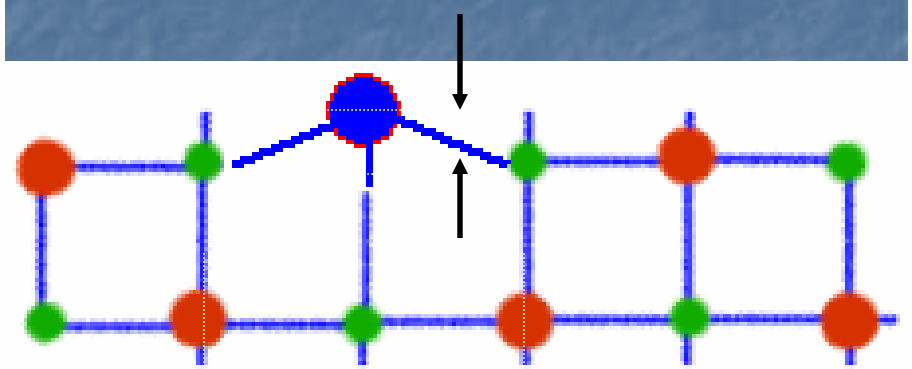

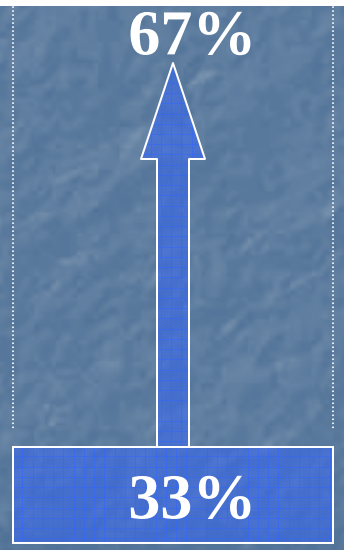

$$F_c = 0.67$$

fit is using the dynamical diffraction theory in layered crystal structures.

Effect of RTA on Zn incorporation
XSW for 0 0 4 reflections

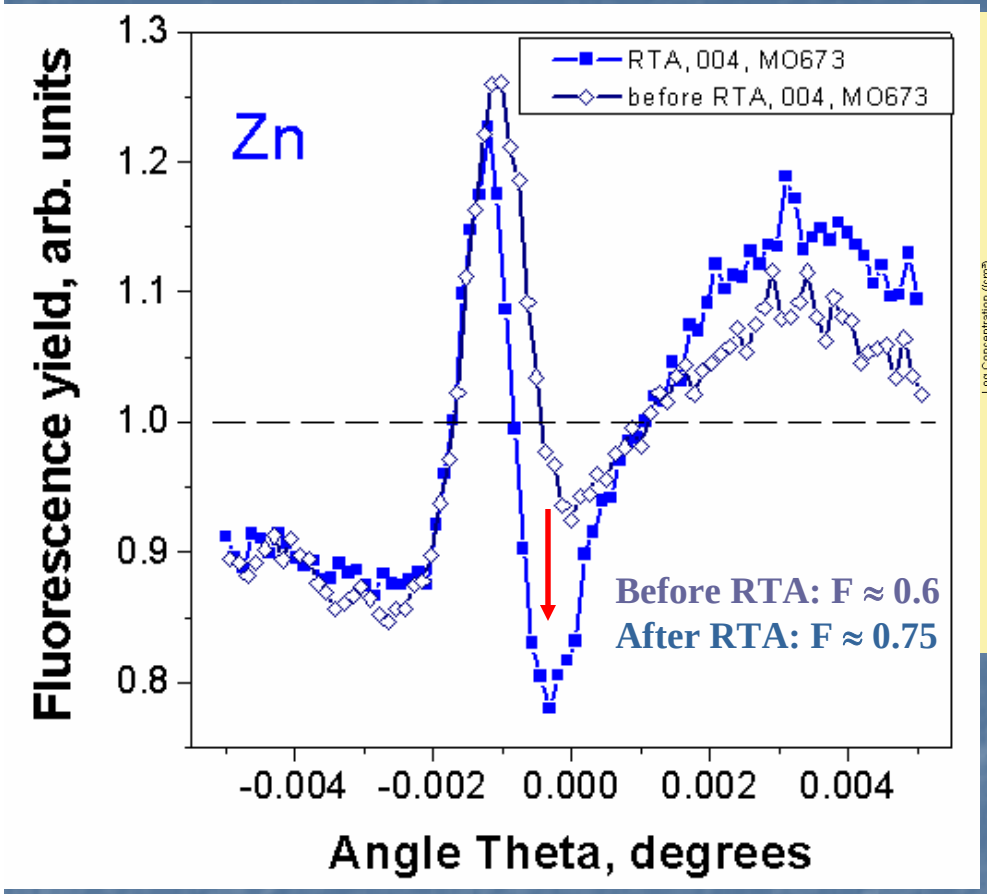

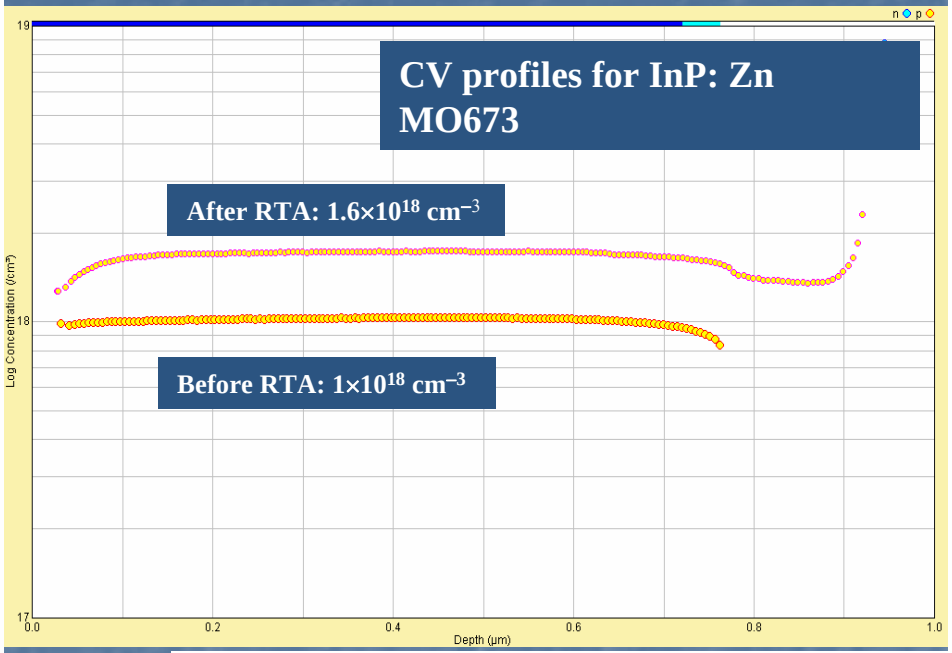

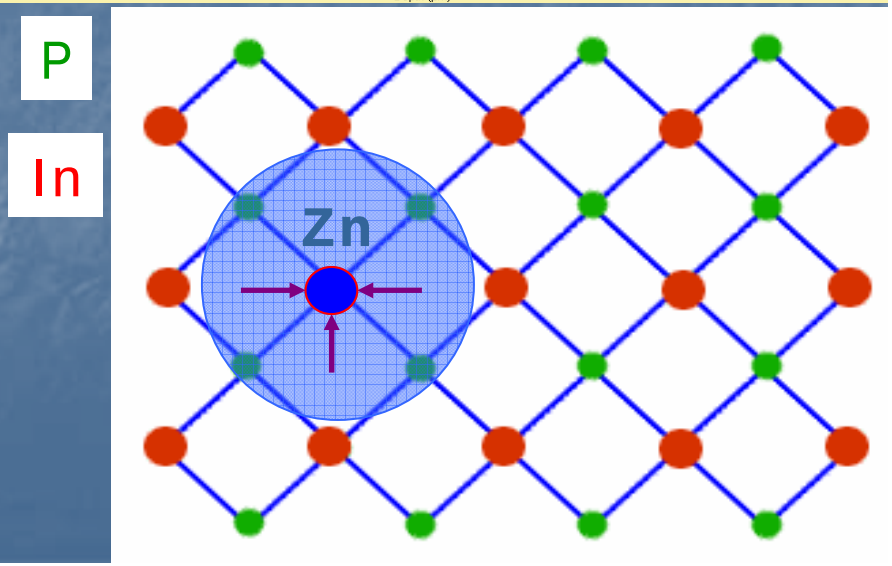

RTA – Rapid Thermal Annealing

Summary for XSW part

- **Using a combination of XSW technique, SIMS, and "CV" we have studied Zn incorporation and activation in InP epilayers**

Plans for the Future:

- **Zn activation in device structures grown selectively on patterned wafers with sub μm spatial resolution**
- **Other impurities: Mg in GaN**

Summary

- We combined focusing optics and post-focusing optics for high-resolution XRD studies of SAG structures.
- Using micro-beam X-ray diffraction we analyzed strain and composition and thickness enhancement in a variety of MQW SAG structures based on InGaAsP, InGaAlAs, and InGaN/GaN

<u>Plans for the Future:</u> Nitride-based (InGaN, GaBN) and Si-Ge NSAG structures: growth and characterization

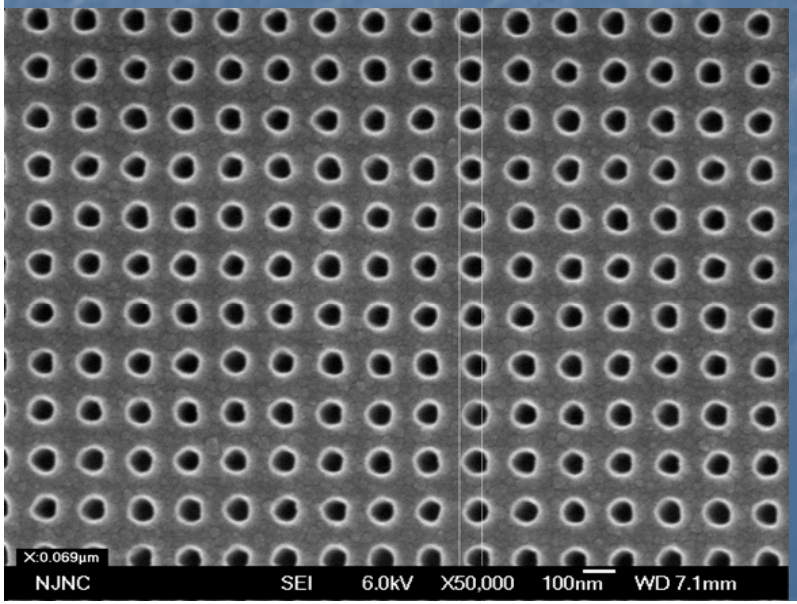

- Strain
- Relaxation
- Composition

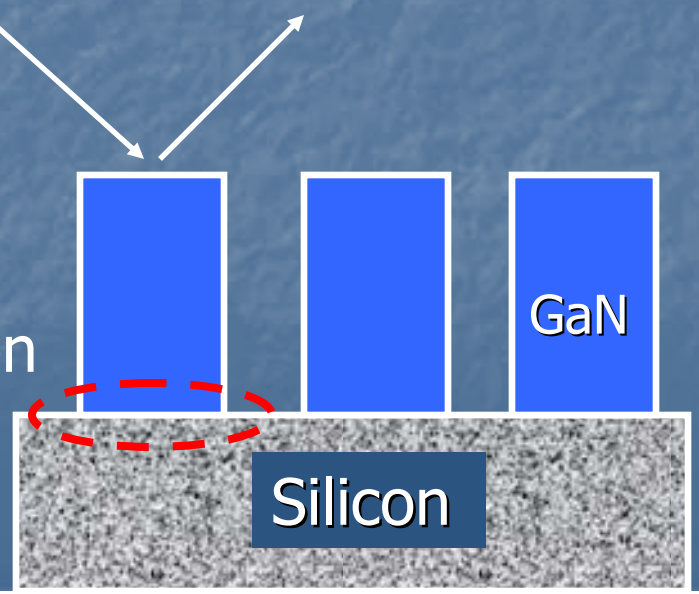

HIGH ANGULAR RESOLUTION BEAMLINE @ ERL

Figure of merit: $N_{ph}/(A \cdot \Delta th)$

APS: 7×106 photons/(240 nm · 350nm · 2arcsec) ≈ 50 photons/(nm^2·arcsec)

Need: 50 photons/(nm2·arcsec)
For RSM's + Real Space mapping and for XSW's

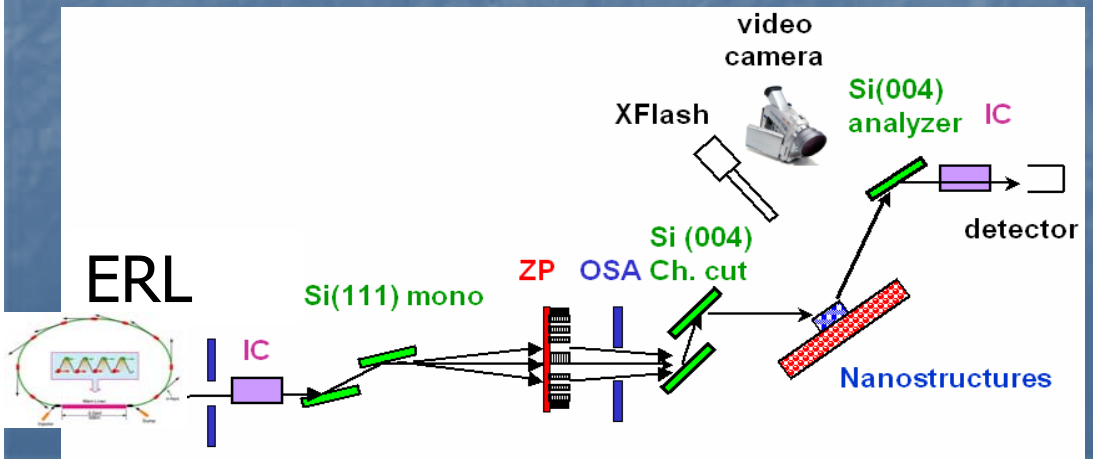

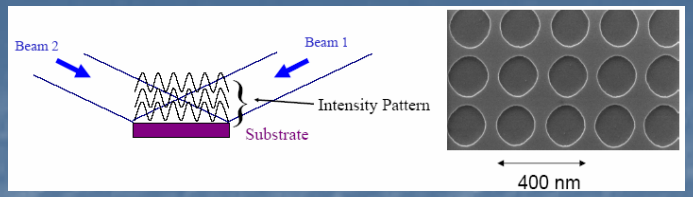

(a) Schematic of two coherent beam interference and (b) SEM micrograph of photoresist patterns produced by the technique of interferrometric lithography. The patterns are formed on a 100 nm-thick layer of thermally grown SiO2 on Si.

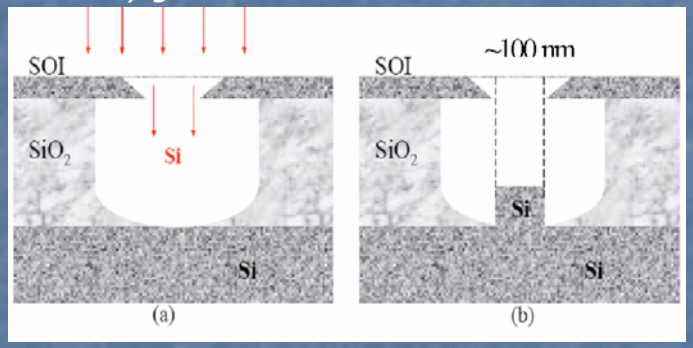

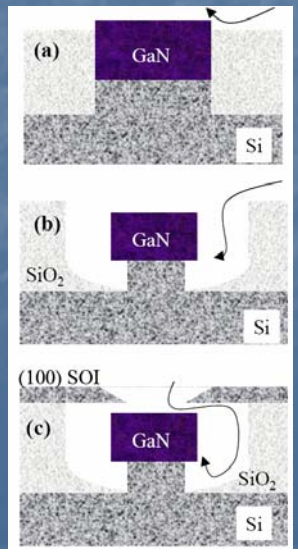

Cross-sectional schematic of MOVPE growth of nitrides on Si nanopillars for different mechanisms of the precursor surface migration: (a) conventional NSAG mask, (b) Si nanopillar with a free-standing sidewalls and (c) SOI mask. Deposition of GaN on the top of the SOI mask is prevented by using in situ chloride-assisted growth.

ERL nanobeams and NSAG structures

Nanometer-Sized ERL X-Ray Beams

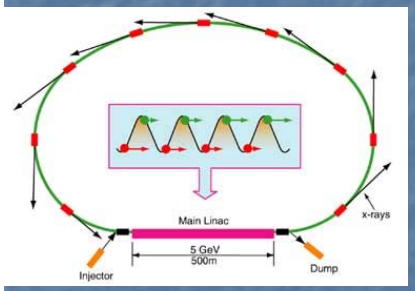

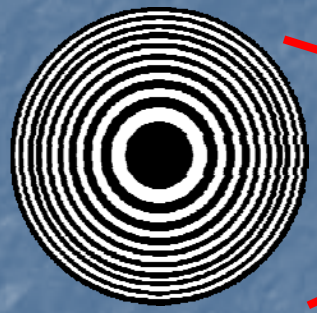

Focusing Devices

Nano science and technology

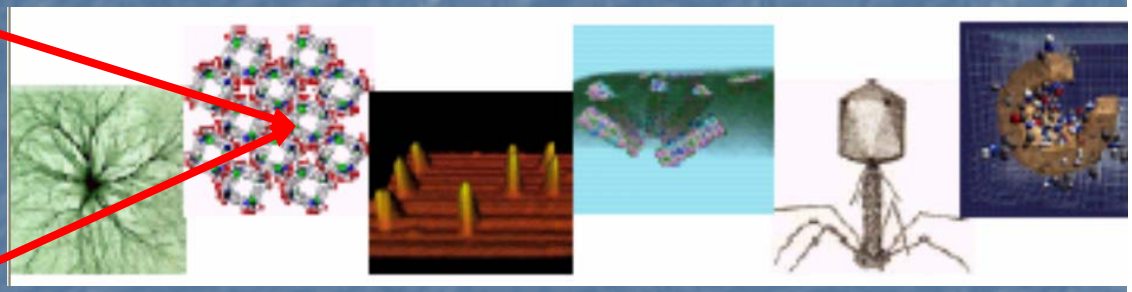

NSAG structures for area detectors based on X-rays → VIS light converters

XSW: basic principles

X-ray Standing Waves

The X-ray standing wave (XSW) technique, inherently an interferometric method, employs the interference field, which is produced by the superposition of an incoming plane and coherently scattered waves, as a probe to measure distances similar to an Å ngstrøm ruler. The technique which only became routinely applicable with highly collimated synchrotron sources will immediately benefit from increases in brilliance: Much smaller samples as well as thin epitaxial layers can be used so that exotic materials can also be investigated; weakly modulated rather than strongly modulated wavefields can be used which widens the application range of the XSW technique tremendously, highly dilute systems can be studied and very short measuring times become possible. Since a single, 100 fs pulse will contain photons it will even be possible to enter the fs time range.

- The standing wave field is generated by the coherent superposition of the incident and diffracted plane waves. In a selected Bragg reflection geometry the wavelength of the incoming X-rays has to match the distance of the diffraction planes of the substrate.
- As a consequence of inelastic scattering processes within the adlayer photoelectrons as well as Auger electrons are produced. Their intensity variation when scanning through the Bragg condition by changing the photon energy is characteristic for the adsorbate site.

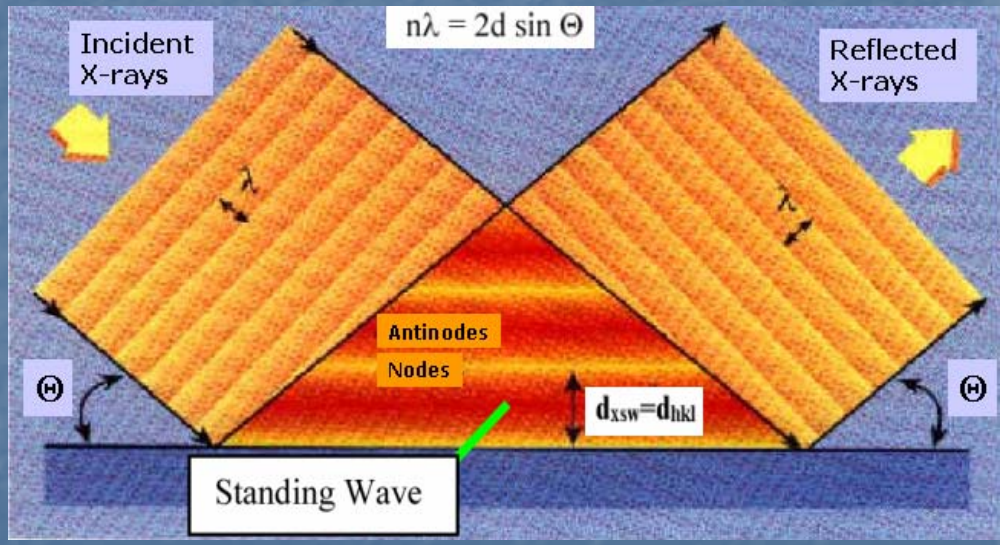

XSW: basic principles

X-ray Standing Waves / Surface Studies.

An XSW measurement of one Fourier component of a monolayer of an adsorbate distribution function takes about 500s (for a strong Bragg reflection) at a second generation SR source with about incident photons. Choosing different reflections usually requires changing the monochromator to realize a non-dispersive crystal setting which is fairly time consuming, since it is crucial to keep the surface clean and stable during the measurements. A thorough analysis of a surface structure by XSW would preferably involve a sizeable number of measurements employing a set of different reflections (H-values) to determine a sufficient set of Fourier components of the system. XSW measurements at third generation sources are just starting. Given the right detector for the photoelectric scattering, measuring times could be cut by a factor of and a large set of H-values could be scanned with a single monochromator (vertical divergence of the source). Already on 3rd generation SR sources the traditional mode of performing XSW measurements will often be abandonned. A single scan of the sample reflection curve can provide enough signal for the XSW analysis within seconds or less. With the divergence of the XFEL is sufficient without additional collimation for practically all XSW measurements (for comparison, FWHM of Si(220) at is about). From this aspect further collimation by a crystal arrangement would hardly be needed. The energy spread of the XFEL which is in the range of would, however, make a monochromator still necessary for many applications. For total reflection XSW or weakly modulated wavefields, which will be discussed below, bandwidth would be sufficient. Measuring times could be reduced by another factor of about , i.e. a monolayer could be measured in about . Piezoelectric devices driven at resonance should make energy scans with a monochromator at a comparable speed possible. These kinds of measuring times fall well into the short time domain which will be discussed later.

XSW: basic principles

X-ray Standing Waves / Extremely Dilute Systems.

Just as the measuring times scale with the brilliance of the sources it scales with the dilution of the system under study. Consequently, extremely dilute systems could be studied with the XFEL. This is a very interesting perspective in the study of impurity diffusion in and on solids or adsorption sites on surfaces in the limit of vanishing adsorbate-adsorbate interactions. A typical question which remains to be answered is whether there is a dominant ionic bond with a different bonding geometry in the adsorption of alkali metals at coverages below 1/100 ML. Diffusion paths of a non-interacting, 2D lattice gas, i. e. a very dilute adsorbate at elevated temperature, could also be analyzed. These are just two examples of systems which cannot be analyzed by diffraction techniques. Just scaling intensities, 1 ppm of a ML (i.e. atoms/)could be analyzed in much less than a second, provided however, given a detection system which can discriminate sufficiently against background signals. Typical ways to enhance surface signals are grazing incidence, which is only applicable in exceptional cases for XSW, and grazing exit fluorescence detection either of which is obtained at the cost of large loss in signal. The latter scheme is possible for 3rd generation sources and perfectly feasible for an X-ray FEL.

The XFEL will deliver between and photons per bunch with a duration of about 100 fs. In principle these are enough photons for a complete XSW measurement - about incident photons are needed for an XSW measurement for one H-value. The proposed bunch spacings are 3 ns (SBLC) and 93 ns (TESLA) and thus offer the possibility of XSW experiments in the fs time domain. The adsorbate would first be sampled by the XSW. A pump pulse from a fast laser in the eV range would then hit the adsorbate covered surface leading to excitation and desorption (in the range if the scheme is to work). Sufficiently fast and powerful pumps are available [23]. The probe, the XSW, is switched on by the XFEL pulse with a desired time delay between 0 and . The total spatial distribution of atoms sampled by the XSW consisting of adsorbed, excited adsorbed and desorbing atoms will thus change with time. Length scales of up to , the interference field spacing are accessible at time scales >100 *fs*. Note that can be varied between fractions of an Å (for Bragg reflection from single crystals) and several hundred Å (for total reflection). To overcome statistical noise (The FEL pulses will also display some intensity fluctuations), a signal averaging technique will have to be used. Several sample-pump-probe cycles have to be run for the same location of the wavefield and this in turn has to be done for several locations of the wavefield.

On a longer time scale (s-ms) the bunches of one bunch train could be used to stroboscopically sample a changing distribution. This could be employed to study e.g. adsorption desorption processes at a solid-electrolyte interface following a step-like change of the applied potential.

Project: Zn diffusion in InP

Mechanism of **Zn** diffusion:

interstitial **Zn** diffuses till it is trapped by **In** vacancy.

vacancy diffusion

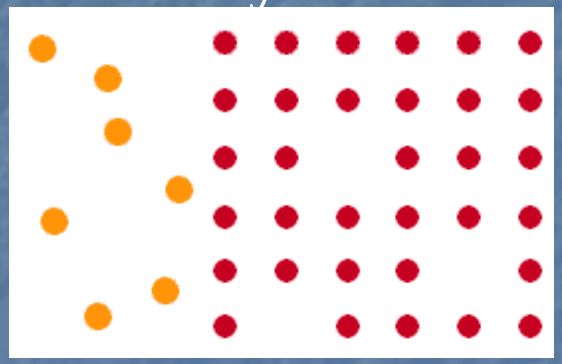

interstitial diffusion

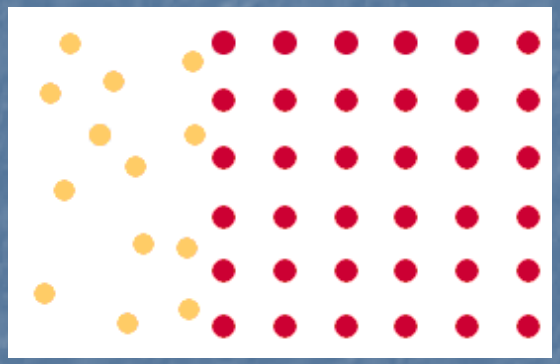

The ease with which an impurity can diffuse through the lattice is reflected in the value of E_A; E_A for vacancy diffusion is in the range 3 - 5 eV, while E_A for interstitial diffusion is between 0.5 - 1.5 eV. Impurities which diffuse through a semiconductor via vacancies diffuse more slowly (slow diffusant) than impurities which diffuse interstitially (fast diffusant).

http://www.elec.gla.ac.uk/groups/sim_centre/courses/diffusion/diff_3.html